

**AUTOMATIC PLASTIC BOTTLE CLASSIFICATION SYSTEM FOR
RECYCLING**

A THESIS IN MECHATRONICS

Presented to the faculty of American University of Sharjah
School of Engineering
in partial fulfilment of
the requirement of the degree

MASTER OF SCIENCE

by
YAHIA TACHWALI
B.S. 2003

Sharjah, UAE
December, 7th, 2005

Automatic Plastic Bottle Classification System for Recycling

by

Yahia Tachwali

We approve the thesis of Yahia Tachwali:

Date of Signature

Dr. Abdul-Rahman Al-Ali
Associate Professor
Thesis Advisor

Dr. Yousef Al-Assaf
Professor
Thesis Co-Advisor

Dr. Khalid Assaleh
Associate Professor
Graduate Committee

Dr. Taleb Hassan Ibrahim
Associate Professor
Graduate Committee

Mr. Abbas Taher
Graduate Committee

Dr. Mohammad Ameen Al-Jarrah
Program Director

Dr. Yousef Al-Assaf
Dean, School of Engineering

Judith Killen
Director, Graduate Studies &
Research

AUTOMATIC PLASTIC BOTTLE CLASSIFICATION SYSTEM FOR RECYCLING

Yahia Tachwali, Candidate for the Master of Sciences Degree

American University of Sharjah, 2005

ABSTRACT

This thesis presents the design, development, implementation and testing of automatic plastic bottles sorting and classification system. The sorting is based on the bottle material chemical composition as well as on the bottle color. Sorted plastic bottles have many industrial applications.

The system has two architectures; one of them is the hardware architecture which consists of a near infrared detection system and a vision system based on a charged coupled device (CCD) camera. The other one is the software architecture which is composed of two classification modules. The first one is based on the near infrared sensor and developed to sort the bottles into three classes based on the bottles' chemical composition, namely Polyethylene Terephthalate containers such as soft drink bottles, soft high-density Polyethylene containers such as milk and juice bottles, and rigid high-density Polyethylene containers such as motor oil and bleach containers. The second stage of classification is based on the CCD camera and developed to separate each near infrared system output class based on bottle color such as clear, green, yellow and gray.

For each stage of classification, appropriate features are extracted to distinguish between the bottles' chemical composition or color. Consequently, various types of classifiers (namely tree classifier and quadratic discriminant function based classifiers) are developed to classify bottles based on composition and color.

The final outcome of this research is a plastic recycling station that can sort and classify plastic bottles based on their chemical composition and color.

CONTENTS

ABSTRACT	iii
TABLES	vii
FIGURES	viii
ABBREVIATIONS	xi
ACKNOWLEDGEMENTS	xii
CHAPTER	
1. INTRODUCTION	1
1.1 The Need for Automatic Plastic Bottles Sorting System	1
1.2 Categories of Plastic Bottles	3
1.3 Literature Survey.....	9
1.4 Challenges and Significance of the Research	16
1.5 Pattern Recognition and Artificial Intelligence Technique.....	17
1.5.1 Feature Extraction	17
1.5.2 Statistical and Non-Parametric Classifiers.....	20
1.6 Thesis Organization	32
2. PLASTIC RESIN CLASSIFICATION USING NIR SPECTROSCOPY	33
2.1 NIR Spectroscopy	33
2.1.1 Theoretical Background.....	33
2.1.2 Comparison Between Infrared Bands	35
2.2 Spectroscopy Hardware Tools	37
2.3 Selection Criteria.....	39
2.4 The Practical Implementation of Near Infrared Spectroscopy.....	40
2.4.1 Introduction	40
2.4.2 Waste Samples Collection.....	40
2.4.3 IR Regions Test.....	42
2.4.4 Preprocessing	56
2.4.5 Feature Extractions.....	59
2.4.6 Classification.....	65

3. COLOR CLASSIFICATION	70
3.1 Color Imaging	70
3.1.1 Theoretical Background.....	70
3.1.2 Imaging Hardware.....	72
3.2 Plastic Bottles Color Classification System Overview	74
3.2.1 The Design Parameters of the Conveyor System.....	76
3.2.2 Vision System	77
3.3 Preprocessing	79
3.3.1 Image Resizing.....	81
3.3.2 Background Foreground Segmentation	82
3.3.3 Object Orientation.....	88
3.4 The Applied Methodology	97
3.4.1 Collecting the Background Images	98
3.4.2 Bottle Detection Algorithm.....	99
3.4.3 Image Resizing.....	100
3.4.4 Bottle Orientation Algorithm	101
3.4.5 Extracting the Top and Bottom Parts of the Bottle	101
3.4.6 Color Features Extraction	101
3.4.7 Classification.....	103
3.5 The Integration of the Plastic and Color Classification Systems.....	111
4. CONCLUSION AND FUTURE WORK	113
4.1 Summary of the Contributions	113
4.1.1 Development and Implementation of a Plastic Bottle Sorting System	113
4.1.2 Implementing Classifier Fusion for Color Classification	114
4.1.3 Integration of Different Classifiers for Multilevel Classification	114
4.1.4 Building a Low-Cost Classifier for Plastic Type Classification	114
4.2 Future Work	115
4.2.1 Morphological algorithms.....	115
4.2.2 K-Mean Clustering.....	117
4.2.3 Tracing Ring	119
4.2.4 Nonlinear Filtering.....	120
4.2.5 Adaptive Monitoring System	121
REFERENCES.....	124
APPENDIX	
A. CHARACTERISTICS OF PLASTIC BOTTLE SAMPLES.....	129
B. CONVEYOR SYSTEM DRAWING.....	134
C. NIR BASED CLASSIFICATION RESULTS	136

D. NIR TEST FINAL REPORT IN DRESDEN, GERMANY	145
VITA	152

TABLES

Table 1-1 Plastic Resins Coding System	5
Table 1-2 Plastic Identification Technologies.....	11
Table 2-1 Advantages and Disadvantages of Near Infrared Spectrum	36
Table 2-2 Advantages and Disadvantages of Mid Infrared Spectrum	36
Table 2-3 Division Ratio of Training and Testing Data	41
Table 2-4 Percentage of Variance Covered by a Number of Principal Components at 900-1700nm	62
Table 2-5 Percentage of Variance Covered by a Number of Principal Components at 1100-2200 nm	63
Table 2-6 Classifier Accuracy Using the Valley Position and Average Value Features in the Range 900-1700nm	66
Table 2-7 Classifier Accuracy Using the Valley Position and Average Value Features in the Range 1100-2200nm	66
Table 2-8 Classifiers Accuracy Using PCA Features in the Range 900-1700nm.....	68
Table 2-9 Classifiers Accuracy Using PCA Features in the Range 1100-2200nm....	68
Table 3-1 The Color Classifier Accuracy for Clear Bottles.....	104
Table 3-2 The Color Classifier Accuracy for Opaque Bottles	107
Table 3-3 Total Classification Accuracy.....	112
Table A-1 Clear Bottles Identity List.....	130
Table A-2 Natural Bottles Identity List	131
Table A-3 Opaque Bottles Identity List	132
Table A-4 Colored Clear Bottles Identity List: Light Blue.....	133
Table A-5 Colored Clear Bottles Identity List: Light Green	133
Table C-1 Error Rates at 900-1700 nm for 60% Training Ratio (PV).....	137
Table C-2 Error Rates at 900-1700 nm for 50% Training Ratio (PV).....	137
Table C-3 Error Rates at 900-1700 nm for 40% Training Ratio (PV).....	137
Table C-4 Error Rates at 1100-2200 nm for 60% Training Ratio (PV).....	138
Table C-5 Error Rates at 1100-2200 nm for 50% Training Ratio (PV).....	138
Table C-6 Error Rates at 1100-2200 nm for 40% Training Ratio (PV).....	138
Table C-7 Classification Accuracy at 900-1700 nm for 60% Training Ratio (PCA)	139
Table C-8 Classification Accuracy at 900-1700 nm for 50% Training Ratio (PCA)	139
Table C-9 Classification Accuracy at 900-1700 nm for 40% Training Ratio (PCA)	139
Table C-10 Classification Accuracy at 1100-2200 nm for 60% Training Ratio (PCA)	140
Table C-11 Classification Accuracy at 1100-2200 nm for 50% Training Ratio (PCA)	140
Table C-12 Classification Accuracy at 1100-2200 nm for 40% Training Ratio (PCA)	140

FIGURES

Figure 1-1 Classification Stages.....	8
Figure 1-2 Pattern Recognition Stages.....	17
Figure 1-3 First Principal Component Line for a Set of Data (x, y)	19
Figure 1-4 Discriminant Function Based Classifier.....	22
Figure 1-5 Quadratic Classifier Flowchart.....	25
Figure 1-6 Linear Classifier Flowchart	26
Figure 1-7 DiagQuadratic Classifier Flowchart.....	27
Figure 1-8 Mahalanobis Classifier Flowchart.....	28
Figure 1-9 Decision Tree Example for the Tree Classifier	29
Figure 2-1 Infrared Spectrum.....	34
Figure 2-2 Emission and Absorption	35
Figure 2-3 Spectrometer Types	38
Figure 2-4 Diode Array Spectroscopy	39
Figure 2-5 Round Robin Method	41
Figure 2-6 The General Hardware Setup for Spectroscopic Measurement	42
Figure 2-7 Dark (Internal Noise) Signal	43
Figure 2-8 Spectrum of the Calibrating White Standard Plate	44
Figure 2-9 Calibration Process.....	44
Figure 2-10 Calibration Effect on the Level of the Spectrum Signal	45
Figure 2-11 Verifying the Effect of External Light on the Spectroscopic Measurements	46
Figure 2-12 The Spectrum Signal of the Conveyor Belt Sample.....	46
Figure 2-13 Effect of Contamination	47
Figure 2-14 Effect of Paper Label.....	47
Figure 2-15 Effect of Plastic Label	48
Figure 2-16 The Hardware Setup Used for Acquiring the Spectrum Signal between 900-1700nm	49
Figure 2-17 Typical Spectrum of a Clear Plastic Bottle	51
Figure 2-18 Typical Spectrum of a Natural Plastic Bottle.....	51
Figure 2-19 Typical Spectrum of an Opaque Plastic Bottle	51
Figure 2-20 Average Level for Spectrum Readings in the Bandwidth 900-1700nm .	52
Figure 2-21 Hardware Setup Used for Acquiring the Spectrum Signal between 1100-2200nm	53
Figure 2-22 Typical Spectrum of a Clear Plastic Bottle	55
Figure 2-23 Typical Spectrum of a Natural Plastic Bottle.....	55
Figure 2-24 Typical Spectrum of an Opaque Plastic Bottle	55
Figure 2-25 Average Level for Spectrum Readings in the Bandwidth 1100-2200nm	56
Figure 2-26 The Spectrum before and after Truncating.....	57
Figure 2-27 Comparing the Filtered Signal with and without Mirroring.....	58
Figure 2-28 Dividing the Spectrum into Six Equally Spaced Regions to Investigate the Positions of Valleys	59
Figure 2-29 Positions of Valleys and Average Level for Different Spectrum Readings for Clear Bottles at the Range of 900-1700nm	60
Figure 2-30 Positions of Valleys and Average Level for Different Spectrum Readings for Natural Bottles at the Range of 900-1700nm	60

Figure 2-31 Positions of Valleys and Average Level for Different Spectrum	
Readings for Opaque Bottles at the Range of 900-1700nm.....	60
Figure 2-32 Positions of Valleys and Average Level for Different Spectrum	
Readings for Clear Bottles at the Range of 1100-2200nm	61
Figure 2-33 Positions of Valleys and Average Level for Different Spectrum	
Readings for Natural Bottles at the Range of 1100-2200nm	61
Figure 2-34 Positions of Valleys and Average Level for Different Spectrum	
Readings for Opaque Bottles at the Range of 1100-2200nm.....	61
Figure 2-35 Feature Space of the First Two Principal Components at the Range of 900-1700nm.....	64
Figure 2-36 Feature Space of the First Two Principal Components at the Range of 1100-2200nm	64
 Figure 3-1 The Color Triangle	71
Figure 3-2 Operation Principle of a CCD Array Detector	72
Figure 3-3 Off-Screen Mode.....	73
Figure 3-4 On-Screen Mode	74
Figure 3-5 Schematic Diagram of the Mechanical System.....	75
Figure 3-6 Basic Component of a Machine Vision System.....	75
Figure 3-7 The Conveyor Belt Motor Driving System	77
Figure 3-8 Frame Time Stamp in Terms of Frame Index	78
Figure 3-9 The Time Difference in Terms of Frame Index	78
Figure 3-10 A Photographic Image of the Automatic Color Sorting System.....	79
Figure 3-11 Interlaced Video Scanning	81
Figure 3-12 The Effect of Interlaced Camera and Removing the Odd Lines and Columns of the Image	82
Figure 3-13 Bottle Image before Processing.....	83
Figure 3-14 Gray Value Histogram.....	84
Figure 3-15 Threshold at Different Levels (a) Threshold at 50. (b) Threshold at 75. (c)Threshold at 100	84
Figure 3-16 Captured Plastic Bottle Image	86
Figure 3-17 Gray Level Image after Tophat Transform	86
Figure 3-18 Thresholded Image after Tophat Transform	87
Figure 3-19 Background Subtraction Algorithm	88
Figure 3-20 Examples of Using Thinning Algorithm to Find the Bottle Orientation.	89
Figure 3-21 Bounding Box Width in Terms of Rotation Angle	90
Figure 3-22 Bounding Box Algorithm to Determine the Bottle Orientation.....	91
Figure 3-23 Flowchart of the Bounding Box Width Algorithm for Plastic Bottle Orientation	93
Figure 3-24 Examples of Bottle Binary Image Rotation	96
Figure 3-25 Flowchart of the Complete Software Classification Module	98
Figure 3-26 Flowchart of the Bottle Detection Algorithm	100
Figure 3-27 Color Feature Extraction for a Plastic Bottle Image	102
Figure 3-28 Feature Space Plotted for the Hue and Saturation Average	102
Figure 3-29 Feature Space Plotted for the Hue and Saturation Variance	103
Figure 3-30 Classifier Fusion.....	104
Figure 3-31 Decision Boundaries of the Quadratic and Tree Classifiers for Hue and Saturation Averages	105
Figure 3-32 Decision Boundaries of the Quadratic and Tree Classifiers for Hue and Saturation Variance	106

Figure 3-33 Image Processing Procedures for Bottles Fitted in a Single Frame	112
Figure 3-34 Image Processing Procedures for Bottles Fitted in a Two Frame	112
Figure 3-35 Integrated System Overview	112
Figure 4-1 Segmentation Steps Using Morphological Algorithms.....	115
Figure 4-2 Segmenting Water Bottles Using Morphological Operations.....	116
Figure 4-3 Segmenting HDPE Bottles Using Morphological Operations	116
Figure 4-4 K-Mean Clustering Algorithm Flowchart	118
Figure 4-5 Segmenting Plastic Bottles Colors Using K-Means Clustering	119
Figure 4-6 Extracting Tracing Ring from Plastic Bottle Images	120
Figure 4-7 The Result of the Kuwahara Filtering on the Plastic Bottle Images	121
Figure 4-8 Background Updating Algorithm.....	123
Figure B-1 Conveyor System Drawing.....	135
Figure C-1 Error Rate Using 60% Training Ratio	141
Figure C-2 Error Rate Using 50% Training Ratio	141
Figure C-3 Error Rate Using 40% Training Ratio	142
Figure C-4 Accuracy as a Function to Training Data Ratio for [1P1V]	143
Figure C-5 Accuracy as a Function to Training Data Ratio for [1P3V]	143
Figure C-6 Accuracy as a Function to Training Data Ratio for [3P1V]	144
Figure C-7 Accuracy as a Function to Training Data Ratio for [3P3V]	144

ABBREVIATIONS

CCD	Charge Coupled Device
DFBC	Discriminant Function Based Classifier
HDPE	High Density Polyethylene
LDPE	Low Density Polyethylene
MIR	Mid Infra Red
NIR	Near Infra Red
PET	Polyethylene Terephthalate
PP	Polypropylene
PPM	Part Per Million
PS	Polystyrene
PVC	Polyvinyl Chloride
RPM	Rotation Per Minute

ACKNOWLEDGEMENTS

First of all, I would like to thank my parents for their support and care, thanks to my brothers, especially Basil, for their help on this work.

I express my deep sense of gratitude to my thesis advisor, Dr. Abdul-Rahman Al-Ali, for his excellent guidance, invaluable suggestions, and encouragement during my study in the Mechatronics Master Program. Great thanks to my co-advisor Dr. Yousef Al-Assaf for all his time and technical support. Dr. Abdul-Rahman Al-Ali and Dr. Yousef Al-Assaf were supporting me not only in the working times but also in the “free times”.

I am also thankful to Aqua Engineering Company, especially Mr. Abbas Taher, for supporting and funding this work and being a part of my committee. Thanks to the Graduate Studies Department for funding my trip to Germany. I can not forget to thank Sentronic Company in Germany for its help and support, and for using Sentronic equipment to collect near infrared measurements as well as creating an ideal environment for my work in Germany. Special thanks to Katrin Glatzer for all her time and help during my stay in Germany.

I wish to thank also Dr. Mohammed Al-Jarrah for granting me the opportunity to be a part of the Mechatronics Master Program, and for his advice and support.

I am very grateful to Dr. Khalid Al-Saleh for his time, technical advice in image processing and for all the knowledge I gained from his classes in pattern recognition. I really learned a lot from him.

Thanks to Dr. Taleb Hassan Ibrahim for his time and willingness to be on my committee.

An ideal atmosphere has been created to work in the Industrial Control Lab by various people and facilities, thanks for allowing me to work in such a wonderful lab.

I would also like to thank all my colleagues in the Mechatronics Lab, Mahmood Hadi, Fadi Saleem and Mohammed Al-Jarrah, for all the great moments we have spent together. Special thanks to Mohammed Mehdi Hassan, Behrooz Mozaffari and Ihab Abu Younis. I wish to acknowledge all the friends who had provided a wonderful company. I thank every person who is directly or indirectly involved in helping me out in any way.

CHAPTER

1. INTRODUCTION

1.1 The Need for Automatic Plastic Bottles Sorting System

Every day, tons of waste is generated, thus causing a major problem to various cities and their municipal authorities due to the shortage of landfill to dump such waste. In addition, the toxic hazard materials among the waste cause some health problems and damage to the environment. For local regions, a huge amount of money is spent for recycling waste. According to Engineer Hamdan Al-Shaer, manager of Dubai Environment Department, Dubai has spent 7.25 million AED in 2004 on waste management and 39 million AED is the expected recycling expense for the year 2005 due to the plan of landfill expansion and recycling infrastructure [1]. Therefore, the environmental protection and waste management issues have come to the forefront of public awareness. Many modern cities have established studies, built Material Recycling Facilities (MRF) and addressed the economical impact of the recycling industry [2-4].

Plastic bottles are a major part of the municipal waste. They have special importance due to their low density to volume ratio. In other words, these types of waste consume a large volume in the landfill. Moreover, they are chemically stable since they are non-biodegradable materials (i.e. the biodegradation process is very slow). This means that plastic waste will be visible for months or years, and waste will sit in landfill sites for years without degrading [5]. Therefore, plastic bottles can cause a serious environmental problem.

One way to address this problem is to recycle the plastic waste material and reuse it. Recycling is becoming an important issue with the shortage of the landfill and environmental pollutions as well as its economical impact. The efficiency and

quality of the recycling process depends highly on the purity and accuracy of the sorted raw materials. Many studies have been conducted for detecting and sorting different materials such as metal, glass, paper and plastics in order to sort them out and prepare them to be recycled [6-11]. Some studies also integrated the output of the automatic plastic sorting system to produce gas and energy [12].

The sorting stage is the essential part of the recycling process and therefore the need for an automated sorting system can be considered as a natural result of the growing needs for high throughput rate and accuracy. Manual sorting of material can be applied and may achieve good accuracy, but at the expense of throughput and cost of production especially when we are talking about a large scale recycling. Moreover, in some cases such as in plastic recycling where standards exist for labeling plastic components and are intended to be read by human dismantlers, these labels may be incorrect. For example, a company may change the resin type used for an injection molded component, but may not change the mold used, and hence, the molded in plastic identification will be incorrect for the newer components [11].

In order to overcome the shortcomings of manual sorting, an automatic sorting system should be developed. However, automating the process contains many challenges to be addressed due to its random nature.

Various studies from different countries showed the efficiency and cost reduction achieved by using automated recycling facilities [13-15].

1.2 Categories of Plastic Bottles

Plastic bottles can be classified into different categories based on its chemical resin, transparency and/or color. The classification categories should be marketable and within the requirement of plastic recycling industries. The following is a brief description of the plastic bottles categories.

Chemical resin-based categories

There are seven plastic types based on their chemical composition. They vary in transparency and strength as well as other characteristics. The plastic types can be one of the following [16]:

- a. Polyethylene Terephthalate (PET No. 1) Containers.

These plastic containers commonly are used for beverages such as mineral water and soda beverages. These items are identified as always being transparent and usually green or clear in color.

- b. High Density Polyethylene (HDPE No. 2) Containers.

These plastic containers can be rigid or soft. Rigid HDPE containers are generally opaque and solid in color, such as oil containers, household cleaning solution bottles, base cups of large beverage bottles, etc. Soft HDPE containers are generally semi-transparent and white colored, such as juice and milk bottles.

- c. Polyvinyl Chloride (PVC No. 3) Containers.

They contain transparent, translucent, or opaque (colored usually high gloss) bottles. Typical products are salad dressing, salad and vegetable oil, floor polish, mouthwash, and some translucent pharmaceutical bottles.

- d. Low Density Polyethylene (LDPE No. 4).

Film plastics used for such purposes as agricultural covering, grocery bags, food industry wrap, dry cleaning bags, etc. The actual film is thin and flexible, opaque or clear, and has a very low weight to volume ratio.

e. Polypropylene (PP No. 5).

Plastics used in the following products: battery cases, medical containers, oil additive containers, some dairy tubs, cereal box liners, bottle labels and caps, rope and strapping, combs, snack wraps, and bags.

f. Polystyrene (PS No. 6).

Plastic containers used in yogurt cups and tubs, cookie and muffin trays, clear carry-out containers, and vitamin bottles. Expanded or foamed polystyrene, are used in meat and produce trays, egg cartons, and carry-out (clamshell) containers.

g. Other Plastics (Other No. 7).

All plastic products made of other than the six most common listed above. Examples are: plastics made of multiple resins in layers, such as microwavable serving ware, "brick pack" juice boxes, water coolers bottles, and squeezable bottles used for ketchup, condiments, jellies, and syrups.

Most of the plastic bottles have a figure inside a triangular recycling symbol that is printed at the bottom of the bottle. This figure refers to the type of the plastic. Table 1-1 illustrates this recycling symbol code as well as the description, applications and the products made of the recycled version of the plastic type [17].

Table 1-1 Plastic Resins Coding System

Codes	Descriptions	Properties	Packaging Applications	Recycled Products
	Polyethylene Terephthalate (PET, PETE). PET is clear, tough, and has good gas and moisture barrier properties. Commonly used in soft drink bottles and many injection molded consumer product containers. Other applications include strapping and both food and non-food containers. Cleaned, recycled PET flakes and pellets are in great demand for spinning fiber for carpet yarns, producing fiberfill and geo-textiles. Nickname: Polyester.	Clarity, strength, toughness, barrier to gas and moisture, resistance to heat	Plastic soft drink, water, sports drink, beer, mouthwash, catsup and salad dressing bottles. Peanut butter, pickle, jelly and jam jars. Ovenable film and ovenable prepared food trays.	Fiber, tote bags, clothing, film and sheet, food and beverage containers, carpet, strapping, fleece wear, luggage and bottles.
	High Density Polyethylene (HDPE). HDPE is used to make bottles for milk, juice, water and laundry products. Unpigmented bottles are translucent, have good barrier properties and stiffness, and are well suited to packaging products with a short shelf life such as milk. Because HDPE has good chemical resistance, it is used for packaging many household and industrial chemicals such as detergents and bleach. Pigmented HDPE bottles have better stress crack resistance than unpigmented HDPE bottles.	Stiffness, strength, toughness, resistance to chemicals and moisture, permeability to gas, ease of processing, and ease of forming.	Milk, water, juice, cosmetic, shampoo, dish and laundry detergent bottles; yogurt and margarine tubs; cereal box liners; grocery, trash and retail bags.	Liquid laundry detergent, shampoo, conditioner and motor oil bottles; pipe, buckets, crates, flower pots, garden edging, film and sheet, recycling bins, benches, dog houses, plastic lumber, floor tiles, picnic tables, fencing.
	Vinyl (Polyvinyl Chloride or PVC): In addition to its stable physical properties, PVC has excellent chemical resistance, good weatherability, flow characteristics and stable electrical properties. The diverse slate of vinyl products can be broadly divided into rigid and flexible materials. Bottles and packaging sheet are major rigid markets, but it is also widely used in the construction market for such applications as pipes and fittings, siding, carpet backing and windows. Flexible vinyl is used in wire and cable insulation, film and sheet, floor coverings synthetic leather products, coatings, blood bags, medical tubing and many other applications.	Versatility, clarity, ease of blending, strength, toughness, resistance to grease, oil and chemicals.	Clear food and non-food packaging, medical tubing, wire and cable insulation, film and sheet, construction products such as pipes, fittings, siding, floor tiles, carpet backing and window frames..	Packaging, loose-leaf binders, decking, paneling, gutters, mud flaps, film and sheet, floor tiles and mats, resilient flooring, cassette trays, electrical boxes, cables, traffic cones, garden hose, mobile home skirting.

(Table Continues)

 4 LDPE	Low Density Polyethylene (LDPE). Used predominately in film applications due to its toughness, flexibility and relative transparency, making it popular for use in applications where heat sealing is necessary. LDPE is also used to manufacture some flexible lids and bottles and it is used in wire and cable applications	Ease of processing, strength, toughness, flexibility, ease of sealing, barrier to moisture.	Dry cleaning, bread and frozen food bags, squeezable bottles, e.g. honey, mustard.	Shipping envelopes, garbage can liners, floor tile, furniture, film and sheet, compost bins, paneling, trash cans, landscape timber, lumber
 5 PP	Polypropylene (PP). Polypropylene has good chemical resistance, is strong, and has a high melting point making it good for hot-fill liquids. PP is found in flexible and rigid packaging to fibers and large molded parts for automotive and consumer products.	Strength, toughness, resistance to heat, chemicals, grease and oil, versatile, barrier to moisture.	Catsup bottles, yogurt containers and margarine tubs, medicine bottles	Automobile battery cases, signal lights, battery cables, brooms, brushes, ice scrapers, oil funnels, bicycle racks, rakes, bins, pallets, sheeting, trays.
 6 PS	Polystyrene (PS). Polystyrene is a versatile plastic that can be rigid or foamed. General purpose polystyrene is clear, hard and brittle. It has a relatively low melting point. Typical applications include protective packaging, containers, lids, cups, bottles and trays.	Versatility, insulation, clarity, easily formed	Compact disc jackets, food service applications, grocery store meat trays, egg cartons, aspirin bottles, cups, plates, cutlery.	Thermometers, light switch plates, thermal insulation, egg cartons, vents, desk trays, rulers, license plate frames, foam packing, foam plates, cups, utensils
 7 OTHER	Other. Use of this code indicates that the package in question is made with a resin other than the six listed above, or is made of more than one resin listed above, and used in a multi-layer combination.	Dependent on resin or combination of resins	Three and five gallon reusable water bottles, some citrus juice and catsup bottles.	Bottles, plastic lumber applications.

Other recycling industries require getting the plastic waste sorted by transparency. It has been shown that the degree of light transmission through a sample provides information regarding polymer type [8]. Moreover, transparency testing in practice can be processed much faster than analysis which allows for a higher throughput. Therefore, sorting plastic bottles based on the transparency can be effective in terms of classification speed but with lower classification accuracy comparing with chemical resin analysis. Color sorting is also required to avoid recycling plastics from different colors so that it is possible to produce a one color recycled plastic. The sorting of transparency and color is the focus of this research.

In this research, plastic bottles have been classified through two stages:

First stage: Transparency classification

- Clear Plastic that includes Polyethylene Terephthalate (PET). PET is clear, tough, and has good gas and moisture barrier properties. It is commonly used in soft drink bottles, mineral water, and many injections molded consumer product containers.
- Natural Plastic: Polypropylene (PP) and high density Polyethylene (HDPE) containers that are not rigid, single color. This type of plastic is used to make bottles for milk, juice, and laundry products.
- Opaque Plastic: High density Polyethylene (HDPE) containers that are rigid and mixed colors, opaque polyvinyl chloride (PVC) containers and opaque polystyrene (PS) container. Virtually no light passes through, whereas in translucent, light is diffused and the material cannot be seen through as it is seen in transparent ones.

It can be noticed that the most common plastic bottles are labeled with a #1 (polyethylene terephthalate - PET) and #2 (high-density polyethylene - HDPE).[18]. Therefore we focus on these two chemical types that can be divided into three different transparency categories. Moreover, while the recycling industry has experienced significant market challenges due to price fluctuations, the recovery of polyethylene terephthalate (PET) and high-density polyethylene (HDPE) is still being carried out in numerous large scale operations throughout the world [10].

Second stage: Color classification

The clear and opaque plastic bottles will be sorted into different colors while the natural plastic bottles do not require color classification since they appear in white color only. We have focused on limited number of color categories. However, the same classification methodology can be developed to classify more colors. Figure 1-1 shows the categories of classification used in this thesis.

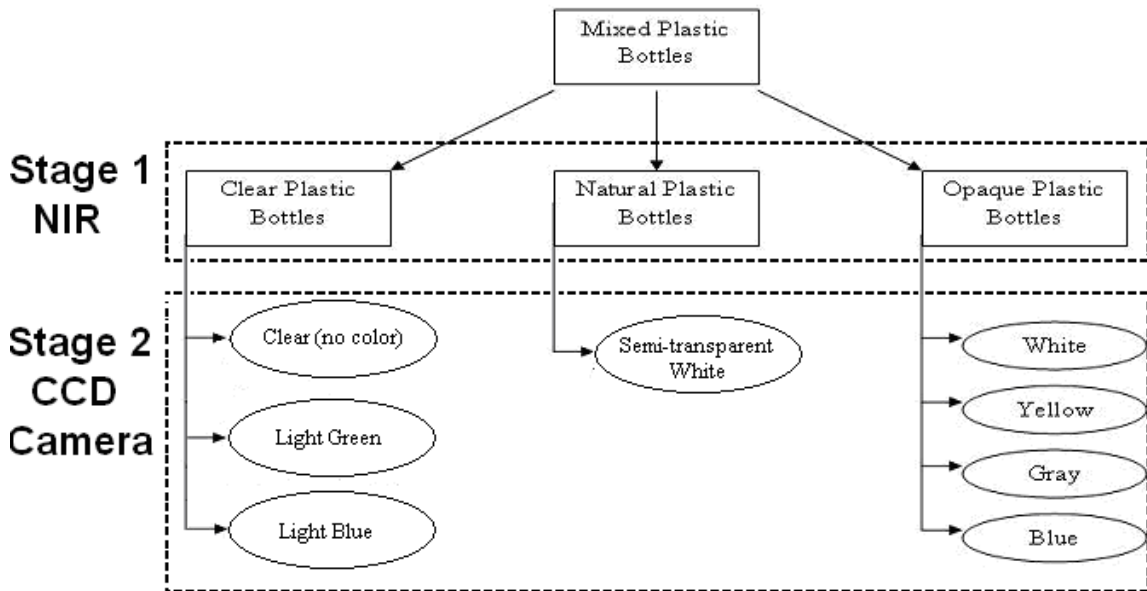


Figure 1-1 Classification Stages

1.3 Literature Survey

Although plastic bottles contribute only a small amount of the municipal wastes disposed in the landfills, they have a market value, and recycling them saves energy and resources. Plastic bottles recycling is currently conducted for a wide range of plastic types. Therefore, it requires the plastic bottles to be sorted into different categories as mentioned before to be ready for recycling.

The identification of plastics before the recycling process is a critical operation in order to avoid contamination of plastic batches to be recycled. There are different techniques to identify the plastic, and they vary according to the categories that can be identified such as transparency or chemical resin.

To identify the plastic transparency, there are some techniques that are based on light transmission and reflection using different types of photodiodes and LEDs. Such techniques can provide measurements that can be processed faster. However, light transmission is not possible through most plastic parts from durable goods. Coatings, particular metallic ones, also interfere with most types of light analysis techniques [8].

On the other hand, plenty of techniques are available to identify the chemical resin of plastic. Simple techniques such as burning smoke color and smell, as well as water sink test can identify plastics [5]. But, for automatic sorting systems there are different techniques that differ whether the identification is to a polymer material between non-polymer materials or between different polymer types described in appendix A. Actually, resin classification is a critical operation since mixing some of them can cause a serious problem. For example, PVC has been a particularly significant impediment to PET recycling. PET and PVC can sometimes be impossible to separate with the human eye. When PET contaminated with PVC is melted, hydrochloric acid is formed, which corrodes the metal parts of the processing machines. As little as 50 parts per million parts (ppm) of PVC can contaminate an entire load of PET and result in the load being unmarketable.

The resin identification can be carried out using chemical methods [5] by applying chemical reactions to separate different polymer types, or by using mechanical methods based on their density such as air and water classification [1,8,19,20], or using electromagnetic identification technology by measuring the

electromagnetic spectrum absorption ratio. Different plastics differ in their light absorption ratio in the electromagnetic spectrum coming from different sources such as x-ray, laser and near infrared light (NIR) [19,20]. Electromagnetic technology is the only plastic-from-plastic identification technology that was found in wide use in the plastic recycling industry. The theory of operation of each of these identification methods is similar, but they vary in the capabilities [11] .Table 1-2 shows the difference between various electromagnetic sensing systems that can be used to identify different types of polymer and their limitations [11].

Another resin identification technology is based on electrostatic separation by using a system to attract or repulse different plastics according to their charge, which causes different plastics to make different movements. Polymers can be sorted by the difference of the melting point; it is normally used to sort two polymers by means of a hot conveyor belt or a hot roll working on a conveyor belt where a mono-layer of flakes is laying down. One kind will stick while the other falls down by gravity.

Marking all containers with an invisible ink that is readily detectable was also one of the methods proposed for identifying plastic [20]. This method is developed by Continental Container Corporation, or even molecular marker in other researches. Using marker can help in speeding up color, resin sorting. However, it is costly and requires lots of modifications in the currently installed plastic producing and recycling systems.

Table 1-2 Plastic Identification Technologies

FT-IR	<ul style="list-style-type: none"> • FT-IR stands for Fourier Transform – Infrared. • FT-IR has greater discriminative power than FT-NIR and Xray techniques. • FT-IR is very sensitive to the condition of the surface being identified. Because most consumer plastics carry different types of commercial labeling, it is often not possible to obtain any surface IR spectral measurement reliably. • Problems may arise with stickers, lacquers, contaminations, etc. on the surface of the plastic products. • The IR spectra have to be recorded from “clean” surfaces. • FT-IR has difficulty identifying very thin plastic such as that used for plastic bags, and cannot identify blown polystyrene (PS).
FT-NIR	<ul style="list-style-type: none"> • Uses near infrared light. • Unlike FT-IR, the FT-NIR reflection technique cannot identify black materials. • Can be used only on transparent items. • Can NOT sort PVC from PET bottles and flakes.
FT-Raman	<ul style="list-style-type: none"> • FT-Raman uses a YAG laser. • FT-Raman has no difficulty identifying very thin plastic such as plastic bags. • FT-Raman is able to identify rough surfaces and powders, can accommodate almost any shape, color, and surface condition, and is at least 50 times faster than FT-IR. • FT-Raman cannot identify black or darkly-colored surfaces. • Laser spectral analysis penetrates the surface and measure emission spectrum which depends upon heat capacity and thermal conductivity • Color doesn't matter. • Not largely used because response time is pretty long.
X-Ray	<ul style="list-style-type: none"> • The use of X-ray techniques is restricted to specific problems, like the separation of PVC and PET (plastic bottles).

(Table Continues)

Polarized Light	<ul style="list-style-type: none"> Used to check difference of crystallinity Sort PVC from PET bottles or anyway a mixture of two components. The limit is bottles need to be lined up one by one therefore production rate will be pretty low.
UV Light	<ul style="list-style-type: none"> Used to separate polymers that exhibit different UV absorption or UV induced fluorescence. To human eyes, PET will stay clear while PVC turns black. Very common way to manually sort bottles.
Photoacoustics Nd:YAG laser	<ul style="list-style-type: none"> Very little damage occurs on the plastic surface due to small energy input. Different thickness, forms and surface structures do not play any role in identifying plastics. Printing and different additives also do not play any role.

In this thesis we use the NIR spectroscopy to identify the type of plastic bottles. Probably the most significant advantage of using NIR spectroscopy is the speed of identification. To be more specific, NIR scanning is much faster than FTIR [10]. Because of the great scanning speed of the spectroscopic instrument, many readings of one sample can be taken in short periods of time. This allows multiple checks to ensure proper identification. A second advantage is the lack of specimen preparation. Labels, or other obstructions like dirt, do not interfere with readings. Another advantage of this system is that color does not interfere with proper resin identification. Except for black, the readings are independent of the color of the resin. Black is a strong absorber in the near-infrared region, and scanning of black plastics results in a featureless spectrum. However, studies have provided a solution to overcome this limitation in mid infrared range using an acousto-optical tunable filter spectrometer [29]. Although part of mid infrared region (2.5–20 mm) suffers from noise generated by the thermal background, it has been shown that the restriction to the wavelength region between 2.5 and 4 mm is sufficient for a reliable distinction of the major types of (blackened) plastics.

A few different models of spectroscopic units are in commercial use today. These include Magnetic Separation System's BottleSort system and Automation Industrial Control's Poly-Sort system [20].

To add more value to the sorted plastic bottles based on chemical resin type, clear and opaque bottles can be sorted into different colors [21]. Color identification is

performed using different technologies, mainly by using machine vision utilizing charged coupled device (CCD) cameras [22] or array of LED's [23].

In our research, machine vision using CCD camera was chosen for color identification, although this will increase the capital cost of our system, but using a camera will provide a wide infrastructure for future work to expand the capability of this system as well as it helps in adding more intelligence to the system due to the additional information that it can provide.

Although different identification technologies are available, analyzing the signal outputs is not straightforward and requires processing and complex feature analysis in order to identify the plastic whether in terms of resin or color. For plastic resin identification using near infrared technology, research has been conducted on identifying plastic materials from non-plastic material or identifying different plastic types using IR spectroscopy, or imaging and examining different classifiers and preprocessing techniques. Outcomes and results varied according to the hardware setup and measurement technology in addition to the classification techniques. Early studies have presented the application of classical classification techniques based on linear discriminant analysis (LDA) and partial least squares (PLS) [24]. In spite of the simplicity of these techniques, there was a need to take into account the nonlinear behavior of the spectral data in the near infrared region. For this purpose a work using near infrared imaging and multilayer feed forward artificial neural network (MLF-ANN) has been presented and examined under different environmental conditions to test the robustness of the process. This showed a success rate of 80% separation between plastic and non-plastic materials with some experimental parameter to be stabilized [25]. However the neural network in this study was treated as a black box due to the shortage of a general accepted way to interpret the calculated classification model generated by neural networks. Other studies utilized neural networks to analyze the signals received from sensor fusion to perform material classifications through the information crossover between the magnetic and infrared signals [26]. However, representative training data is essential for any classifier model design. Statistical test techniques or Kennard-Stone algorithm can be used for samples selection to improve the quality of the training data [27].

Other methods counted on the preprocessing techniques and performed the classification with basic techniques, such as applying wavelets transform on the NIR spectrum and constructing a quaternion number from the wavelets coefficients [28],

then classifying the plastic by measuring the Euclidean distance of the quaternion number. This technique can be used in low quality spectra but showed a classification limitation at some types of plastics.

The studies indicated above were performed in the near infrared range. However, the mid infra-red range also was used to identify the black colored plastic [29].

On the other hand, the color identification using machine vision contains many problems that were addressed in the literature, such as optimal color space selection based on the application and the surrounding environment, foreground-background extraction, color segmentation and non-uniform illuminated image binarizations. These problems exist in the application of plastic bottle color sorting; therefore it is required to investigate different algorithms and to verify the efficiency of adapting them in our application. For color space selection, many studies examined the pros and cons of different color spaces and evaluated their stability in representing color in the existence of some external noises such as lighting variation. It has been found that HSV (Hue Saturation, Value) performs better than both other color spaces in normal (i.e. no noise) as well as noisy conditions and suggestions have been provided that HSV could be a superior color space compared to RGB (Red, Green, Blue) for color analysis [30,31]. Although most of the cameras available provide images in RGB spaces, and the transformation to the HSV space is nonlinear and requires additional computation time, it is still applicable for real time applications [32].

One of the critical problems in our application is to isolate the plastic bottle from conveyor belt image, or in other words, foreground-background extraction. This problem can be found in different applications and is addressed intensively in the literature. The extraction of the background can be done by color clustering or segmentation [33-37], or sometimes estimating the background to be removed by providing a statistical model [38]. However the segmentation algorithms proposed are iterative or sometimes require heavy computations which make them not appropriate for real time applications. A faster method is by using thresholding techniques that can be locally adaptive [39], and can utilize some artificial intelligence techniques [40]. Some studies also provided thresholding methods in the HSV color space [41]. Thresholding techniques are good for foreground extraction but for most of the studies reviewed a posterior processing is required to filter the image from small

background portions that may survive from the thresholding process. It was found that the most proper method for real time application is to record the background image (conveyor belt), then subtract them from the acquired image at the exact position of the conveyor belt [42]. However, to guarantee the stability of this method in case of external noise such as light or background color variations, an adaptive background image update was proposed [42], where records of the background images are updated according to the frequency of the color appearance at each pixel position. As a result, keeping records of the background images may require more hardware resources in terms of memory capacity, but it will boost the foreground – background extraction process as well as providing an infrastructure for building adaptive system to accommodate process conditions variations such as light and background color variations.

The earlier work in providing an automatic plastic bottle sorting solution was focusing on the plastic chemical composition classification or color classification. This thesis presents a study on integrating the color and chemical type classification in one classification system unit and explores the outcomes of implementing classifiers fusion as well as an interlock between the two classification systems.

1.4 Challenges and Significance of the Research

Plastic bottle sorting is a very random process, since bottles with different sizes come to the classification area in different orientations and shapes, and may be crashed and deformed. Bottles are being compressed and crashed in the collection stage to save volume where the collection cost is based on the volume (container) while the cost of the sorted material is based on the weight. On the other hand, this practice will complicate the automatic sorting and classification problem.

In addition to the above, labels with different sizes and colors as well as having different handles and caps design make the classification more challenging.

Therefore it is required to have a complex and intelligent algorithm that can address these difficulties and be able to classify the bottles regardless of their orientation, shape and existence of label.

Although they are commercially available recycling systems [20], conducting a research using artificial intelligence and sensor fusion technique will improve efficiency and performance to existing plastic recycling system and overcome various limitations such as accuracy, throughput, and cost. Commercial systems can sort plastic bottles based on color and chemical resin using near infrared and X-ray sensors, but the cost of these systems is not less than 50,000 US Dollars with a throughput of 500 kg/hour which is equivalent to 3 bottles per second [20]. Moreover, the maximum number of categories that commercial system can identify is limited (not more than 5)[20].

The importance and motivations of this research are:

- The environmental and financial impact of this application in the region by reducing the amount of material going to the landfill and providing an economical industry.
- Integrate different sensor types to build a classification system that is able to sort plastic bottles in terms of color, transparency and chemical resin at once, which adds more value to the output of the sorting system and enhance its operation cost.
- Examining different classifiers on the NIR readings and proving the feasibility of using a new classification technique in this application which is the quadratic classifier and decision trees as well as the fusion of these classifiers.

1.5 Pattern Recognition and Artificial Intelligence Technique

Pattern recognition (PR) techniques categorize objects based upon some measurements made on those objects. The measurements are multidimensional, they could be an actual pattern of intensities in an image, or a set of measurements of completely unrelated physical properties. Feature extraction techniques define the rules that govern proper separable parameters between different classes, see Figure 1-2.

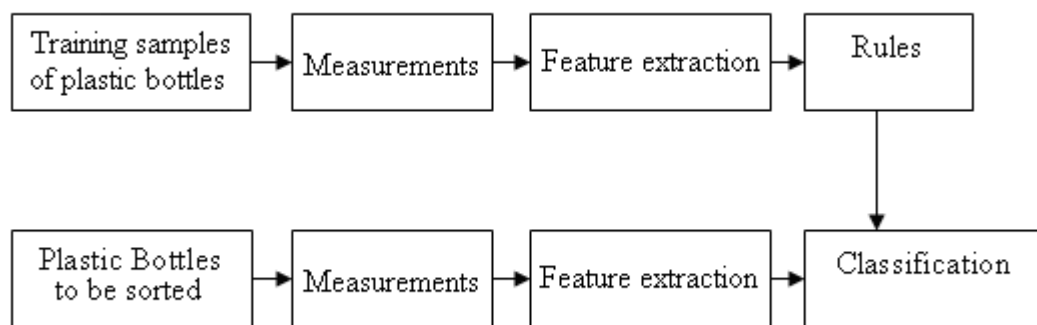


Figure 1-2 Pattern Recognition Stages

1.5.1 Feature Extraction

Introduction

The main purpose of feature extraction is to represent the data in a reduced number of dimensions. There are many reasons behind the dimension reductions, one of them being to ease the analysis and improve the classification through more stable representation. Other reasons include removing redundancy or irrelevant information that can reduce the classification performance.

This research proposes two methods to reduce the dimensionality of a given set of measurements:

- To identify variables contributing in the classification task, thus the task is to seek ‘d’ features (d should be determined) out of ‘ p ’ measurements ($d < p$).
- To find a transformation from p measurements to a lower dimensional feature space. This transformation can be linear or nonlinear combination of the original variables. In this thesis, principal component analysis was used.

Feature extraction using principal component analysis

Feature extraction is the transformation of the original data with all the variables to a data set with a reduced number of variables. So it is using all the measurements or variables and projects them to a smaller dimensional domain. Actually there are several reasons to perform feature extraction:

1. To reduce the bandwidth of the input data.
2. To provide a relevant set of features for a classifier to improve the classification performance.
3. To reduce redundancy.
4. To produce a low dimensional representation (ideally in two dimensions) with minimum loss of information so that the data can be visualized better.

The purpose of principal component analysis is to derive variables that are linear combinations of the orthogonal variables and are uncorrelated. Geometrically, it can be thought of as a rotation of axes of the original data coordinated to a new set of orthogonal axes that are ordered in terms of the amount of variation of the original data they account for.

If we consider a set of data (x, y) where the variable x is an input variable and y is a dependant variable on x , and we wish to estimate the value of y given x , $E[y|x]$, then the best regression line of y on x ($y = mx + c$) is the line for which the sum of the squared distances of points from the line is a minimum. Principal component analysis thus produces the best single line with the minimum sum of the squares of the perpendicular distances from the sample points (x, y) to the line, The variable defined by the line of the best fit is the first principal component as shown in Figure 1-3, while the second component is the variable defined by the line that is orthogonal with the first.

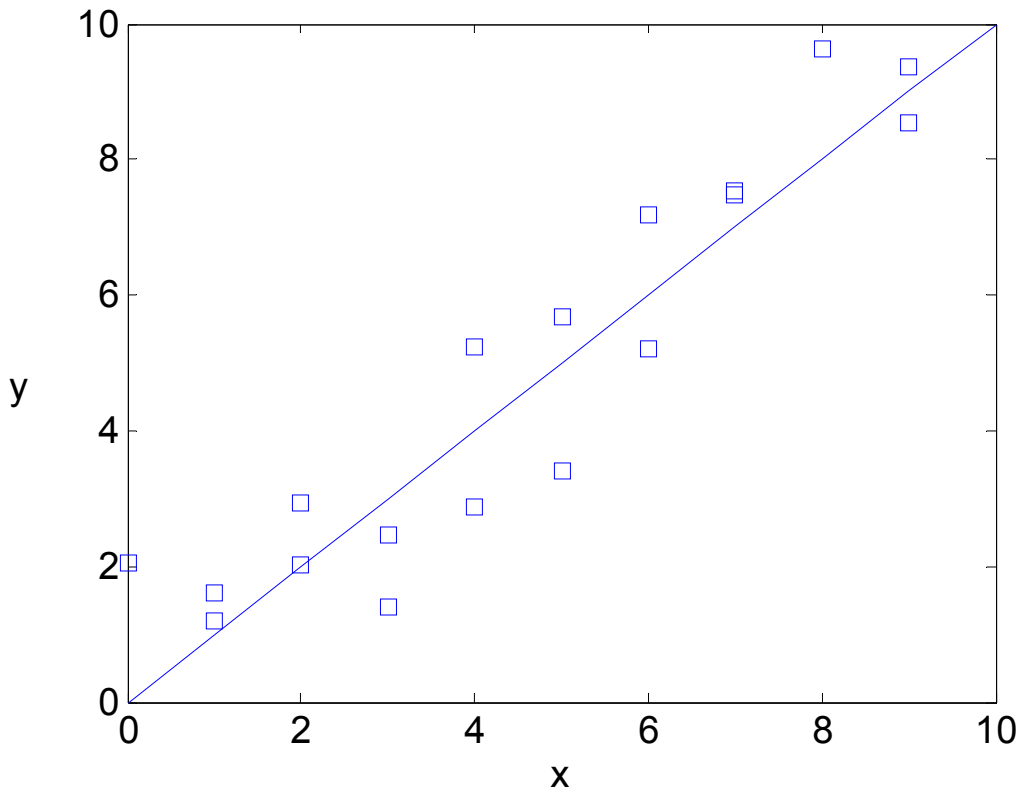


Figure 1-3 First Principal Component Line for a Set of Data (x, y)

In general, principal components analysis produces an orthogonal coordinate system in which the axes are ordered in terms of the amount of variance in the original data for which the corresponding principal components account, and the variances are the principal values.

Looking at the covariance matrix of data $\mathbf{K} = E[(\mathbf{x} - \bar{\mathbf{x}})^T(\mathbf{x} - \bar{\mathbf{x}})]$, we see the variances of each dimension along the main diagonal and the covariances as the off-diagonal terms. If the matrix is diagonal, the variables are independent and in this case we can represent the data with the least square error by choosing the variables with the greatest variances. However if the matrix is not diagonal then it can be diagonalized by the transformation with the matrix composed of its eigenvectors. The resulting matrix has the variances along the directions of the eigenvectors as its main diagonal. Then the features we wish to use are the eigenvectors themselves as a weighted sum of all measurements.

The covariance matrix sums up the variation in the data; its eigenvectors show the primary directions of the variance and the associated eigenvalues give the magnitude of the variance along those axes. The eigenvectors of the covariance

matrix K are often referred to as the "principal axes" or "principal components" of the variance in the data. So Principal Component Analysis uses eigenvector analysis of K to find the best reduced-dimensional representation.

1.5.2 Statistical and Non-Parametric Classifiers

Introduction

In this thesis, we examined two main types of classifiers:

- Discriminant function based classifiers (DFBC)

The DFBC are Bayes rule based classifiers where the class-conditional densities are not known and they should be learned from the available training patterns. The form of the class-conditional densities in these classifiers are assumed to be a multivariate Gaussian, but some of the parameters of the densities (e.g., mean vectors and covariance matrices) are unknown, and can be estimated from the training data. They come in 4 main shapes [43]:

- Linear: It fits a multivariate normal density to each group with a pooled estimate of covariance.
- Quadratic: It fits also a multivariate normal density but it makes an estimation of the covariance matrix for each classification group.
- DiagQuadratic: Same as 'quadratic', except that the covariance matrices are assumed to be diagonal.
- Mahalanobis: It also uses different covariance estimation for each classification group but uses Mahalanobis distances instead of fitting a normal density.

- Decision trees

A decision tree is a set of simple rules, used to perform a classification or regression operations [12]. Decision trees do not require any assumptions about the distribution of the measurements in each group.

Discriminant function based classifiers

In discriminant analysis-based approach, the class conditional density function is estimated using Bayes' rule. One approach is to assume a simple parametric model for the density functions such as multivariate normal distribution. Then, the parameters of the assumed model are estimated using the available training set [44]. Let us assume that the conditional property of a certain feature giving the class or, in other words, the likelihood is based on the normal distribution:

$$p(\mathbf{x} | \omega_i) = \frac{1}{2\pi^{\frac{p}{2}} |\Sigma_i|^{\frac{1}{2}}} \exp\left\{-\frac{1}{2}(\mathbf{x} - \boldsymbol{\mu}_i)^T \boldsymbol{\Sigma}_i^{-1} (\mathbf{x} - \boldsymbol{\mu}_i)\right\} \quad (1.1)$$

Where,

\mathbf{x} Feature vector $\mathbf{x} = (x_1, \dots, x_p)^T$

ω_i Label for class i.

p the dimension of feature vector

$\boldsymbol{\Sigma}_i$ Sample covariance matrix for class i.

$\boldsymbol{\mu}_i$ Mean of feature vector in class i.

Classification is achieved by assigning a pattern to a class for which the posterior probability $p(\omega_i | \mathbf{x})$ is the greatest or equivalently $\log(p(\omega_i | \mathbf{x}))$ is the greatest. Using Bayes' rule and the normal assumption for the conditional densities above, we can obtain the posterior as follows:

The posterior probability is defined as:

$$\text{posterior} = \frac{\text{likelihood} \times \text{prior}}{\text{evidence}}$$

$$p(\omega_i | \mathbf{x}) = \frac{p(\mathbf{x} | \omega_i)P(\omega_i)}{p(\mathbf{x})} \Rightarrow$$

$$\log(p(\omega_i | \mathbf{x})) = \log(p(\mathbf{x} | \omega_i)) + \log(P(\omega_i)) - \log(p(\mathbf{x}))$$

$$= -\frac{1}{2}(\mathbf{x} - \boldsymbol{\mu}_i)^T \boldsymbol{\Sigma}_i^{-1} (\mathbf{x} - \boldsymbol{\mu}_i) - \frac{1}{2}\log(|\boldsymbol{\Sigma}_i|) - \frac{p}{2}\log(2\pi) + \log(p(\omega_i)) - \log(p(\mathbf{x}))$$

Since $p(x)$ is independent of the classes, we can remove the constant terms from the previous equation giving the discriminant rule: assign x to ω_i if $g_i > g_j$ for all $j \neq i$, where

$$g_i(x) = \log(p(\omega_i)) - \frac{1}{2} \log(|\Sigma_i|) - \frac{1}{2}(x - \mu_i)^T \Sigma_i^{-1} (x - \mu_i) \quad (1.2)$$

Hereby, classifying a pattern x on the basis of the values of $g_i(x)$, $i=1,\dots,C$ gives the normal based quadratic discriminant function. See Figure 1-4.

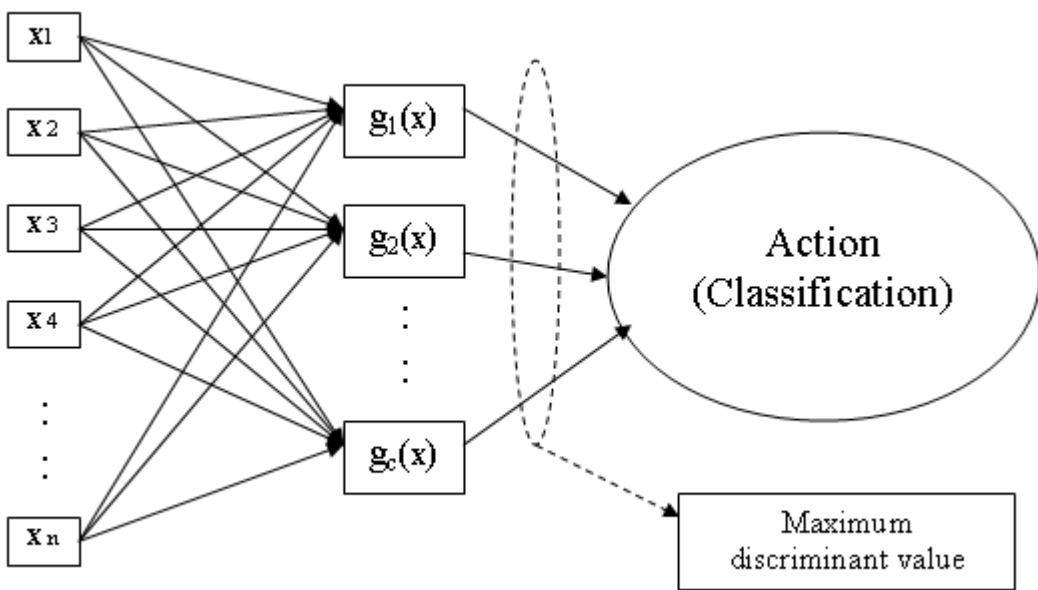


Figure 1-4 Discriminant Function Based Classifier

In equation (1.2) we need to obtain μ_i and Σ_i . These parameters can be estimated from the training set, and this is why this method is called estimative approach in the sense that we use an estimate of a parameter (for example θ_i) based on the samples D_i in a class conditional density of a known form (Normal in our case), thus we take :

$$p(x|\omega_i) = p(x|\hat{\theta}_i)$$

where $\hat{\theta}_i$ is the estimate of the parameter θ_i based on the sample.

The estimation of the mean and covariance is performed so that the likelihood function $L(x_1, \dots, x_n | \theta)$ is maximized. And the maximum likelihood estimate of these parameters for a class i composed of n samples will be:

- $\hat{\mu}_i = \frac{1}{n_i} \sum_{r=1}^n z_{ir} \mathbf{x}_r$ where $z_{ir} = 1$ if $\mathbf{x}_r \in class i$, 0 otherwise.
- $\hat{\Sigma}_i = \frac{1}{n-1} \sum_{j=1}^n z_{ij} (\mathbf{x}_j - \hat{\mu}_i)(\mathbf{x}_j - \hat{\mu}_i)^T$

So the Gausian classifier or the Quadratic discrimination rule becomes: assign \mathbf{x} to ω_i if $g_i > g_j$ for all $j \neq i$, where $g_i(\mathbf{x})$ is calculated by equation (1.2).

That is the general case, problems occurred when any of the matrices $\hat{\Sigma}_i$ is singular. In this case, it is possible sometimes to do simplification assumptions to go around the singularity problem as well as using the pseudo inverse matrix. There are several simplified alternatives commonly employed. We have used in this thesis three simplified forms of the quadratic classifiers, which are Linear, DiagQuadratic, and Mahalanobis Classifier.

In this thesis, we will try all these classifiers to classify the data rather than using one of them as alternative solution in case of having singular $\hat{\Sigma}_i$. In this case we solve the problem of singularity by adding a white noise on the training data with negligible values compared to the absolute numbers of training data, and this showed in many cases better results than the commonly used alternative forms.

Moreover, calculating the density $p(\omega_i | \mathbf{x})$ involves finding the inverse of the covariance matrix Σ_i , but inverting a potentially large matrix explicitly is usually not a good idea in terms of computational time as well as the complexity of having Σ_i nearly singular [45]. One of the good methods to go around this is through the QR decomposition of the centered data matrix bearing in mind that the centering is different for each class. Since Q is orthonormal, then $\hat{\Sigma} = R^T \times R$.

The following classifier flowcharts show the algorithms used in the quadratic classifier and for the other three alternative forms assuming that:

- \mathbf{X}_{train} [$n \times d$ matrix] : is the training data

$$\mathbf{X}_{train} = \begin{bmatrix} \mathbf{x}_{train_1} \\ \mathbf{x}_{train_2} \\ \vdots \\ \mathbf{x}_{train_c} \end{bmatrix}$$

- \mathbf{x}_{train_i} [$n_i \times d$ matrix] is the training data for class i.
- \mathbf{X} [$m \times d$ matrix] : is the testing data.

Where n is the number of training samples, n_i is the number of samples for a class I , m is the number of the testing samples, c is the number of classes and d is the pattern dimension.

Quadratic Classifier

The flowchart below (See Figure 1-5) illustrates the algorithm used to find the discriminant function $g(x)$ described in equation (1.2) without any simplification assumptions. The covariance matrix for each class can be an arbitrary Σ_i , class dependant and non-diagonal, so the decision boundaries (or surfaces) become more complex.

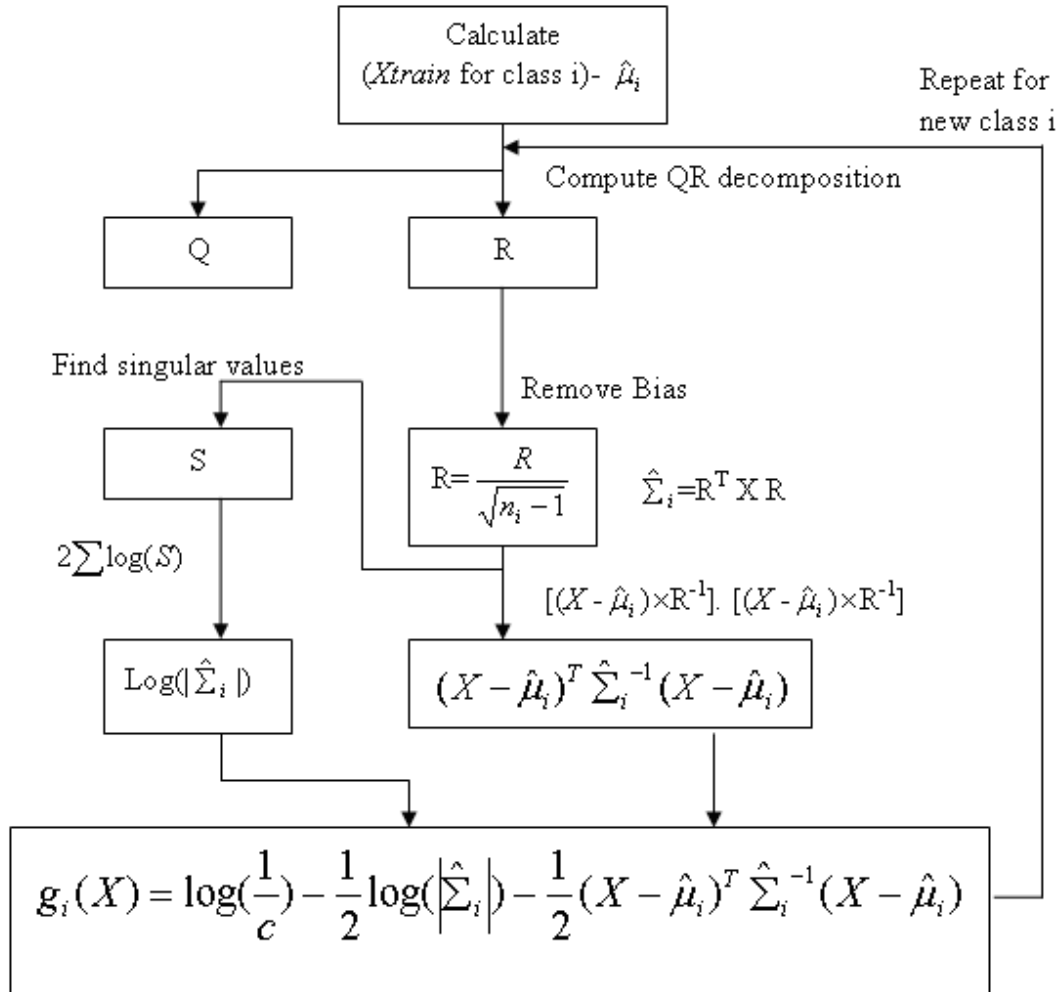


Figure 1-5 Quadratic Classifier Flowchart

Linear Classifier

In this classifier, it is assumed that the class covariance matrices are the same $\Sigma_i = \Sigma$.

In the training data was taken as a whole set without considering the label for each sample and the covariance for the whole training data was computed through QR decomposition. For each discriminant function $g_i(x)$ the same covariance matrix will be applied, and as a result the decision boundaries will be a straight lines since it can be simplified into a line equation [44]. Figure 1-6 illustrates the calculation steps of the linear classifier.

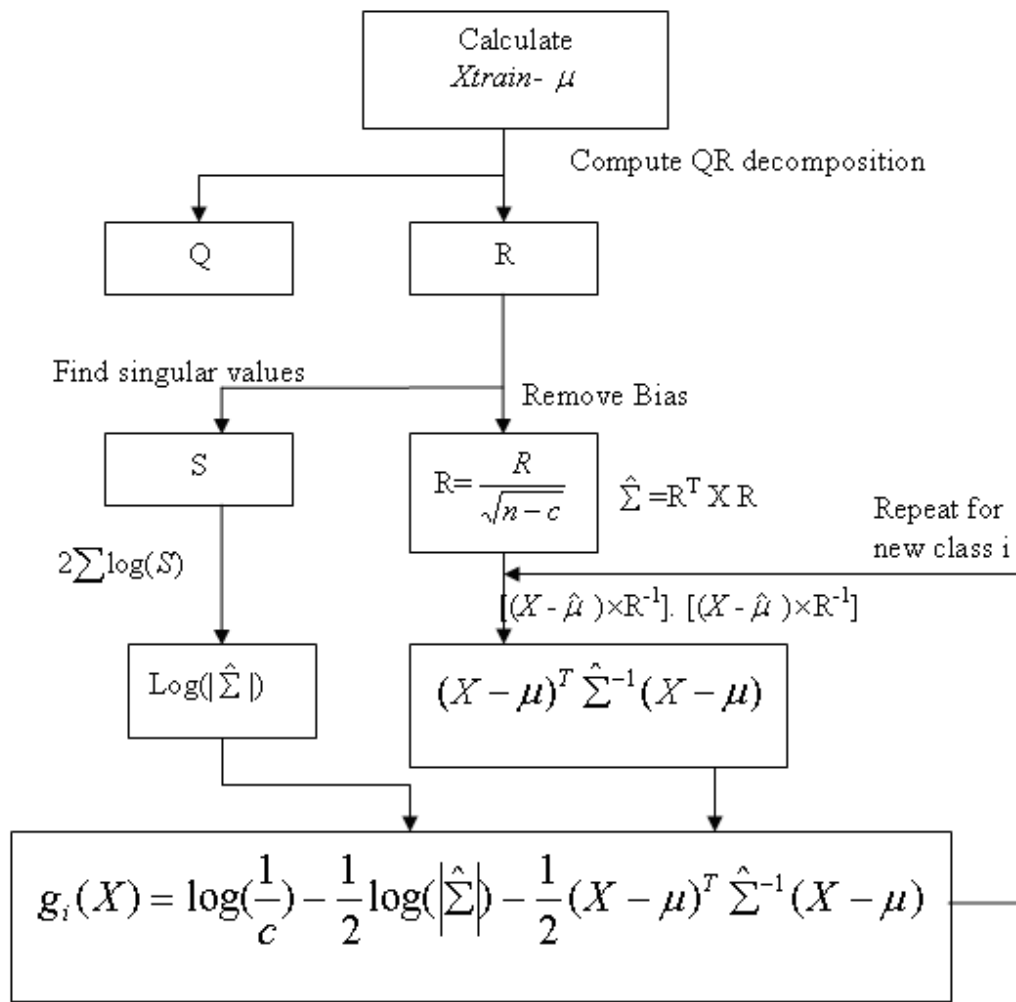


Figure 1-6 Linear Classifier Flowchart

DiagQuadratic Classifier

Here it is assumed that the covariance matrix is diagonal Σ_i , but the covariance matrix is estimated for each class. So it is assuming that the features used are not correlated and therefore it will not use the diagonal components only in the covariance matrix. Figure 1-7 illustrates the calculation steps of the DiagQuadratic classifier.

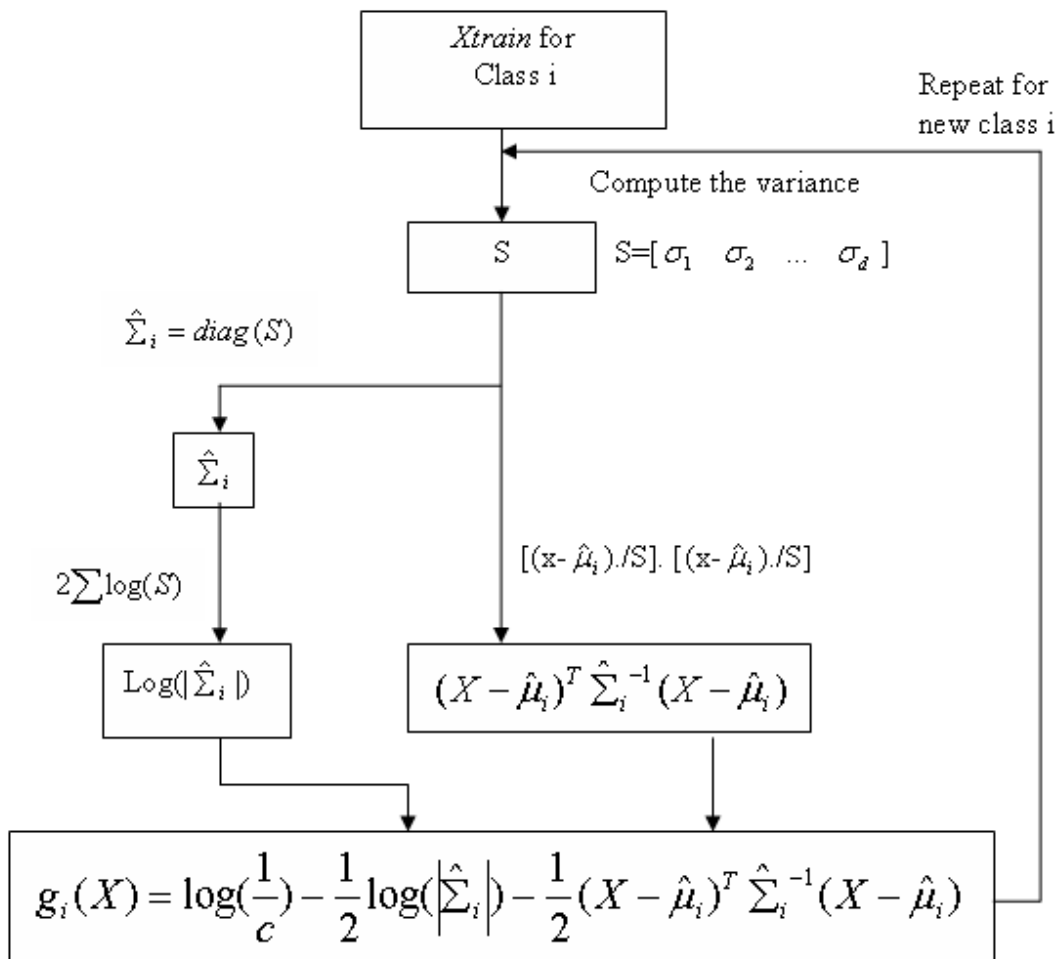


Figure 1-7 Diag Quadratic Classifier Flowchart

Mahalanobis Classifier

It is based on calculating the Mahalanobis distance between the samples and training data [46]. It assumes that $\log(1/c)$ is equal for all the classes which means that the training samples for all the classes have the same size, and therefore it will not cause any difference between the calculated g_i for different classes as shown in Figure 1-8.

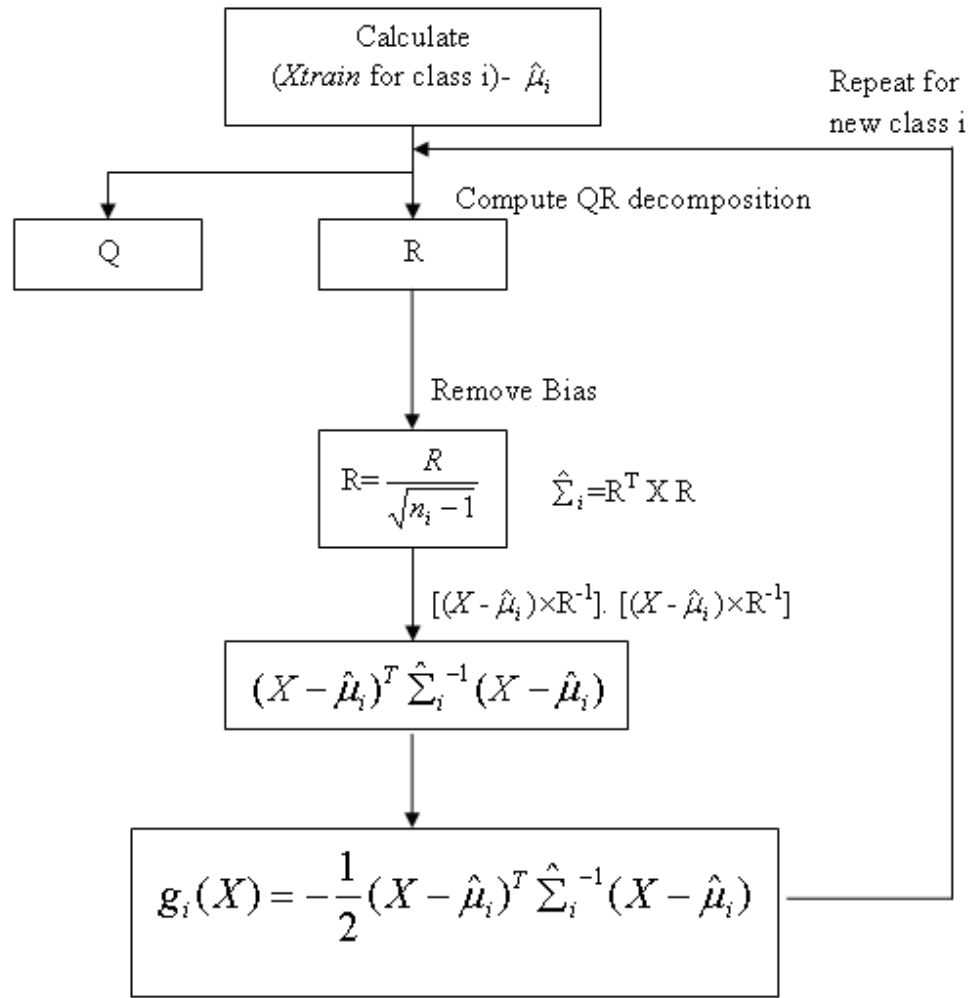


Figure 1-8 Mahalanobis Classifier Flowchart

Decision Tree Classifier

Tree classifier is a special type of nonparametric classifiers which can be described as a sequence of questions that can be answered as yes or no (in other words, it is a binary recursive partitioning), plus a set of fitted target values (class labels). Each question asks whether a predictor satisfies a given condition. Predictors can be continuous or discrete.

Depending on the answers to one question, you either proceed to another question or arrive at a fitted response value.

During classification, just those features which are under consideration at each level are needed for the test pattern under consideration. So, feature selection is implicitly built-in.

The most commonly used decision tree classifiers are binary in nature and use a single feature at each node, resulting in decision boundaries that are parallel to the feature axes. However, the main advantage of the tree classifier is its speed, since it is possible to interpret the decision rule in terms of individual features. Therefore a testing sample (feature vector) can be classified directly by a series of simple comparison operations.

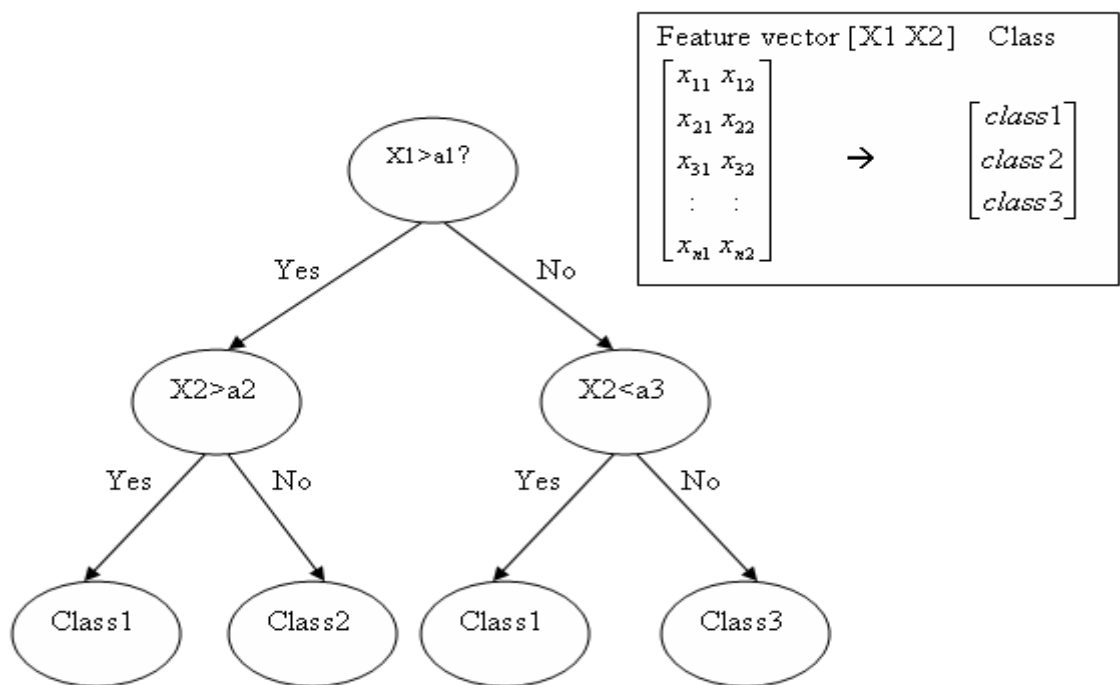


Figure 1-9 Decision Tree Example for the Tree Classifier

Figure 1-9 shows a typical tree which is capable to classify a 2 dimensional feature vector into one of three classes (class1 class2 class3). Assuming that the optimum structure had to be of three levels as shown in Figure 1-9, the classification procedure for sample k of n samples of feature vectors is done as follows:

- At first level it will compare the first feature component x_{k1} with a threshold a_1 .
- The result of the comparison will lead the feature vector to the next node at the next level.
- Successive comparison operations are performed until it reaches the end of the tree where a class will be assigned to it.

The construction process starts with a training set consisting of pre-classified records. "Pre-classified" means that the target field has a known class or label. The goal is to build a tree that distinguishes among the classes. For simplicity, assume that there are only two target classes (+,-) in a set of samples S and that each split is binary partitioning. The splitting criterion easily generalizes to multiple classes, and any multi-way partitioning can be achieved through repeated binary splits. To choose the best splitter at a node, the algorithm considers each feature component in turn. In essence, each feature component is sorted. Then, every possible split is tried and considered, and the best split is the one which produces the largest decrease in diversity of the classification label within each partition (this is just another way of saying "the increase in homogeneity") which can be measured by the gain of information:

$$Gain = Entropy(S) - \sum_{v \in Values(A)} \frac{|S_v|}{|S|} Entropy(S_v)$$

(1.3)

$$Entropy(S) = \sum_C -\left(\frac{n_{bc}}{n_b}\right) \log_2 \left(\frac{n_{bc}}{n_b}\right)$$

(1.4)

Where,

n_b the number of instances in branch b.

n_{bc} the number of instances in branch b of class c. $n_{bc} \leq n_b$

n_t the total number of instances in all branches.

A the feature component to be examine at the corresponding node.

S_v the subset of S that satisfies the rule at the corresponding node for a value=v.

S the size of the feature vector.

This gain is calculated for each feature component and the final choice is the one that achieves the maximum gain of information.

The process is continued at the next node and, in this manner, a full tree is generated until no more useful splits can be found.

It is obvious that decision trees can be easily overtrained (i.e. it is "explaining" random elements of the training data that are not likely to be features of the larger population of data) and the resulting tree at this level can become meaningless and often harmful for predicting unknown labels. Pruning the tree is the process of removing such leaves and branches to improve the performance of the decision tree when it moves from the training data (where the classification is known) to real-world applications (where the classification is unknown -- it is what you are trying to predict). The tree-building algorithm makes the best split at the root node where there are the largest number of records and, hence, a lot of information. Each subsequent split has a smaller and less representative population with which to work. Towards the end, idiosyncrasies of training records at a particular node display patterns that are peculiar only to those records. These patterns can become meaningless and sometimes harmful for prediction if you try to extend rules based on them to larger populations.

Pruning methods solve this problem. They let the tree grow to maximum size, and then remove smaller branches that fail to generalize. Since the tree is grown from the training data set, when it has reached full structure, it usually suffers from overfitting. This results in poor performance on real life data. Therefore, it has to be pruned using the validation data set.

1.6 Thesis Organization

The thesis is divided into two main topics. The first topic is covered in chapter two which is the plastic bottle classification based on chemical type using near infrared spectroscopy. It contains an introduction to the near infrared spectroscopy for plastic identification, and then the practical implementation of the plastic bottle classification is presented using two different hardware setups. Two different methods of feature extraction and five classifiers are presented. At the end of this chapter, there is a summary of the work.

The second topic is covered in chapter three which is the plastic bottle classification based on color using machine vision. It contains a brief introduction about different machine vision components. It explains different algorithms that have been tested before finding the last classification algorithm. Then, it explains in details the color classification algorithm implemented and the integration with the plastic type classifier and summarizes the results at the end of the chapter.

Chapter four is the overall thesis summary. The contributions in this thesis are listed in this chapter as well as the future work to upgrade the automatic plastic bottle sorting system

CHAPTER

2. PLASTIC RESIN CLASSIFICATION USING NIR SPECTROSCOPY

2.1 NIR Spectroscopy

2.1.1 Theoretical Background

Infrared (IR) radiation refers broadly to that part of the electromagnetic spectrum between the visible and microwave region. Normally, band positions in IR spectra are presented as wavenumbers (\bar{v}) whose unit is the reciprocal centimeter (cm^{-1}); this unit is proportional to the energy of the vibration and normally modern instruments are linear in reciprocal centimeters. Wavelength (λ) was used in the older literature in units of micrometers. Wavenumbers are reciprocally related to wavelength as follows:

$$\text{cm}^{-1} = \frac{10^4}{\lambda(\mu\text{m})} = \frac{1}{\lambda(\text{cm})} \quad (2.1)$$

Near infrared spectrum spans the $833 \text{ nm} - 10^6 \text{ nm}$ ($12000 \text{ cm}^{-1} - 10 \text{ cm}^{-1}$). Typically, the IR region in terms of wavelength or frequency is divided into three regions [47]:

- Near : $833 - 2500 \text{ nm}$ or $12000 - 4000 \text{ cm}^{-1}$
- Middle : $2500 - 50000 \text{ nm}$ or $4000 - 200 \text{ cm}^{-1}$
- Far : $50000 - 10^6 \text{ nm}$ or $200 - 10 \text{ cm}^{-1}$

Figure 2-1 shows the infrared bands:

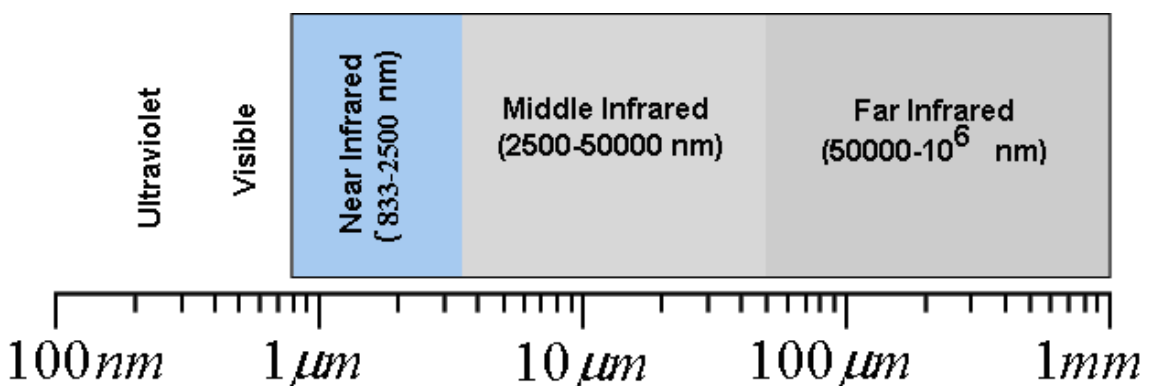


Figure 2-1 Infrared Spectrum

Infrared spectroscopy is normally applied for qualitative analysis, which is basically to identify materials (especially organic ones) using comparative method between a referenced spectrum of a known material and the tested one. Although the infrared light is not energetic enough to break molecular bounds, but it will excite specific vibrational modes in large complex molecules to higher energy levels. This can be used in return to identify specific organic molecules since each has its unique fingerprint in the IR spectra.

When a light beam of NIR falls on a plastic bottle, part of the incident radiation is reflected off the surface as regular reflectance. The remaining radiation transmits through the surface, encounters small interfaces in the cellular structure, and scatters in all directions. Some of the radiation will be scattered back to the surface and leave the plastic bottle in the vicinity of the point of incidence. The remaining scattered light diffuses deeper into the plastic. As the NIR light travels through the plastic, a certain amount is absorbed by various constituents of the plastic. The absorption varies with the constituents. The absorbed energy is transformed into other forms of energy. Part of the absorbed radiation may be transformed into other forms of radiation. Thus, the radiation that leaves the surface of the plastic may consist of regular reflectance, body reflectance, transmittance, and emissions. The characteristics of the radiation that leave the surface of the plastic depend on the chemical properties of the plastic and the incident radiation. Thus, determining transmittance and absorption characteristics of plastic can provide information related to the resin type.

The energy absorption by transparent materials in any portion of the electromagnetic spectrum causes atoms or molecules to pass a state of low energy to a

higher energy, these energy states can be in different shapes (electronic, vibrational, spin ...etc) and this happens only when the energy of a photon matches the energy gap between a pair of initial and final states. In the interaction of radiation with matter, if there is no pair of energy states such that the photon energy can elevate the system from the lower to the upper state, then the matter will be transparent to that radiation with that frequency. Figure 2-2 illustrates the concepts of emission and absorption:

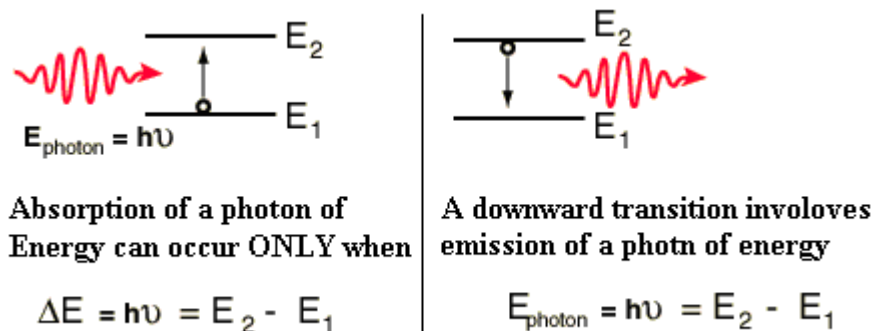


Figure 2-2 Emission and Absorption

The excitation process here is quantized, only selected frequencies of energy in this process are absorbed representing the energy difference between the excited and initial states, and these frequencies are dependant on the masses of the atoms, the force constants of the bonds and the geometry of the atoms. Therefore, every type of bond has a natural frequency of vibration, and the same bond in different compounds has a slightly different frequency of vibration. In organic molecules with polar covalent bonds and dipole moments, the infrared radiation absorbed is converted into energy of molecular rotation and vibration. Infrared spectroscopy is concerned only with the vibrational spectrum causing stretching and bending effects on the bonds.

2.1.2 Comparison Between Infrared Bands

In order to choose the spectrum band that is appropriate for plastic bottles identification for recycling application, a brief comparison between the characteristics of Mid infrared and NIR infrared is performed, since the Far infrared instrumentations are currently not available for industrial applications [48].

Near Infrared

This band excites the overtone vibration and combination vibrations, and has the following advantages and disadvantages that are listed in Table 2-1.

Table 2-1 Advantages and Disadvantages of Near Infrared Spectrum

Advantages	Disadvantages
<ul style="list-style-type: none"> • Accessible with technology derived from telecommunications systems. • Established, proven and industrially accepted method. • Instrumentations are available. • Weak water absorption. 	<ul style="list-style-type: none"> • Absorption bands are broader and less structured than mid-IR. • Less sensitive than mid-IR. • Reduced capability to distinguish different analyses exclusively by their spectral characteristics, application of chemometrics* almost required

*Chemometrics is the combination of mathematics, statistics and computer science to reach information from chemical data.

Mid Infrared

This band excites the fundamental transition between the ground state of a vibrational mode and its first excited state, and has the following advantages and disadvantages that are listed in Table 2-2.

Table 2-2 Advantages and Disadvantages of Mid Infrared Spectrum

Advantages	Disadvantages
<ul style="list-style-type: none"> • Higher absorption coefficients. • Well structured specially in the fingerprint region ($1200\text{-}400\text{ cm}^{-1}$). • More sensitive and selective than NIR. 	<ul style="list-style-type: none"> • Strong absorption of water. • Limited instrumentations.

Moreover NIR spectrophotometer can be assembled with optical components employed for UV-Visible instruments. This fact imparts a lower cost to the NIR instrument when compared with the mid-infrared (MIR) spectrophotometer.

From this comparison, it was clearly noticed that the NIR range is more applicable for waste plastic identification due to its lower sensitivity to water, in addition to its availability.

2.2 Spectroscopy Hardware Tools

Classification of NIR instruments based on the technology employed

Spectrophotometry is the measurement of the absorption of specific frequencies of light. Starting with a bright, broad frequency light source, and passing it through a prism or reflecting it off a diffraction grating breaks the light into its component frequencies. This dispersed light is passed through a narrow slit to get a particular frequency. The prism or grating can be rotated to take a measurement at a different frequency and thereby determine the absorption as a function of frequency.

- The IR spectrometer uses IR light to excite vibrational modes in complex molecules. These absorption spectra provide a quick positive ID for complex organic molecules.
- The most common application of IR spectra is a comparative analysis of the spectra of an unknown compound with the spectra of suspects. An IR spectrum might be considered analogous to a fingerprint of an individual. Supposedly, there are no two individuals with the same set of fingerprints.

There are five technologies used in NIR process spectrometers. They differ in operating principle, range of application, robustness, speed and price. There are:

1. Filter spectrometer, based on optical (interference) filters.
2. Scanning grating monochromator spectrometer.
3. Photodiode array spectrometer with InGaAs (IndiumGallium Arsenide)-detector.
4. FT (Fourier-Transform)-NIR spectrometer.
5. AOTF (acousto-optical tunable filter) spectrometer, based on internal crystals.

NIR probes are available for measurements in transmission mode and in diffuse reflectance mode. It is more practical for industry to use the reflectance mode where a single transducer coupled to one side of the test piece serves as both transmitter and receiver (pulse/echo mode).

Figure 2-3 shows the different types of spectrometers available of IR spectroscopy.

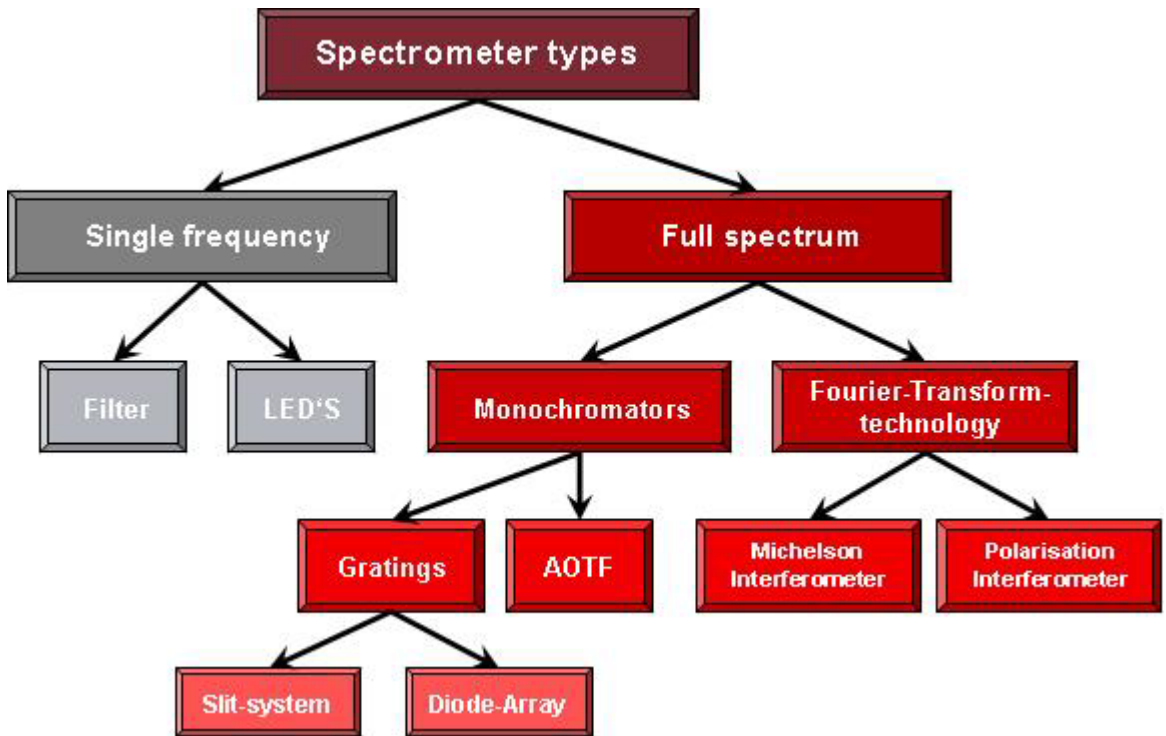


Figure 2-3 Spectrometer Types

The most frequently employed detectors for the NIR spectral region are based on silicon, PbS and InGaAs photoconductive materials. In particular, InGaAs photoconductive materials possess a very high detectivity and a very high response speed. Together with high powered radiation sources (a tungsten coil or a halogen lamp is employed by the majority of manufacturers) these detectors can impart a very high signal-to-noise ratio for NIR measurements. This fact partially compensates for the lower intensities of NIR absorption bands. They are used also in the diode array spectrometers which are dispersive optic based instruments.

Dispersive instruments based on diffraction gratings were employed in the early days of NIR spectroscopy and were responsible for the research initially developed to consolidate NIR spectroscopy as an analytical tool. The instruments based on grating monochromators present the advantage of a relatively low cost when compared with other scanning instruments employing modern technologies. The main disadvantages of dispersive instruments are the slow scan speed and the lack of wavelength precision, which deteriorates for long term operation due to mechanically driven mechanism fatigue. This can be a negative regarding maintenance of

multivariate models. Also, the presence of moving parts limits the use of dispersive instruments in the field and in more aggressive environments.

On the other hand, recent evolution in sensor production technology gives dispersive optics a longer life. That is because it is now possible to construct linear arrays of PbS and InGaAs sensors containing up to 256 independent elements. Placed in the focal plane or concave grating optics, the sensor array allows the scan of an entire spectra in a few milliseconds. Furthermore, as can be observed in Figure 2-4 that no moving parts are present.

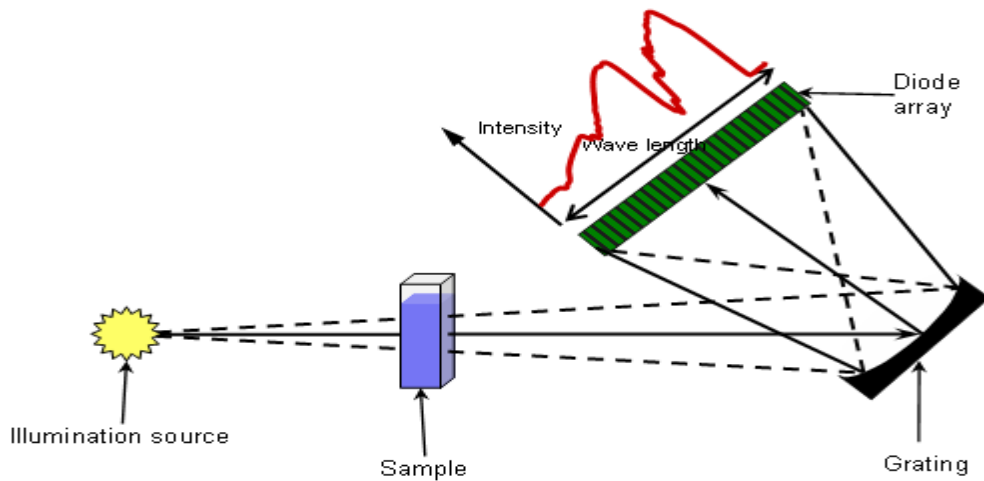


Figure 2-4 Diode Array Spectroscopy

2.3 Selection Criteria

Instrument selection must be guided by the end application. Low cost instruments, based on filters and LEDs, can be sufficient for many dedicated laboratory and routine in field applications. Instruments based on fixed dispersive optics and sensor arrays have proven to be a robust solution when multi-wavelength spectral data for in field applications are required.

Fourier-based and AOTF-based instruments must be the choice when research, wide application spectra and calibration transference are of concern. The AOTF spectrophotometer presents the most rapid random accesses to various wavelengths, which can be useful for certain applications for in-line monitoring, while the Fourier-based instruments show, on average, the best resolution and signal-to-noise ratios.

The use of fiber optic probes is desired, many modern applications are based on their intensive use due to their noise immunity, in order to facilitate data acquisition routines.

To summarize, the dispersive optic based instrument will be used due to its relatively low cost and the acceptable resolution and accuracy considering our application which does not require a very fine resolution for identifying the plastic resin. 50nm resolution was found to be sufficient in such application.

2.4 The Practical Implementation of Near Infrared Spectroscopy

2.4.1 Introduction

The near infrared spectroscopic identification was performed over two different regions in the NIR spectrum using two different hardware and software setups. The first region is between 900-1700 nm and the second is between 1100 to 2200 nm. Initial tests were conducted to check the effect of environmental conditions on the quality of the measurements. Then the spectral data for plastic bottles was collected, analyzed and classified using the five classifiers described in chapter 1.

2.4.2 Waste Samples Collection

Plastic bottles were collected from different places in Dubai and Sharjah, United Arab Emirates. The samples cover the three different categories (Clear, natural and opaque). 120 samples were used to create the database. The samples composition consists of:

- 30 clear bottles (colored blue or green).
- 30 natural bottles (white).
- 30 opaque bottles (colored).

These bottles were labeled by a code and listed with a brief description of the condition [normal or compressed, wet or dry, clean or dirty] and color for each bottle.

The code was used to name the corresponding NIR spectrometer readings files. Appendix A contains the list of all bottles. This data for each category was divided into training and testing data for classifier design with three different ratios (see Table 2-3).

Table 2-3 Division Ratio of Training and Testing Data

	Training data ratio of total data	Testing data ratio of total data
	[%]	[%]
Division 1	60	40
Division 2	50	50
Division 3	40	60

For each arrangement ratio, the different bottles for training and testing were chosen using Round Robin method in which a window that covers a specified ratio of the data is used to select the training data while the rest of the data is for testing, and then this window moves along the data by a step of 5 samples for 6 times. The following Figure 2-5 illustrates the method of arranging the data for one of the previous categories into 60% training and 40% testing.

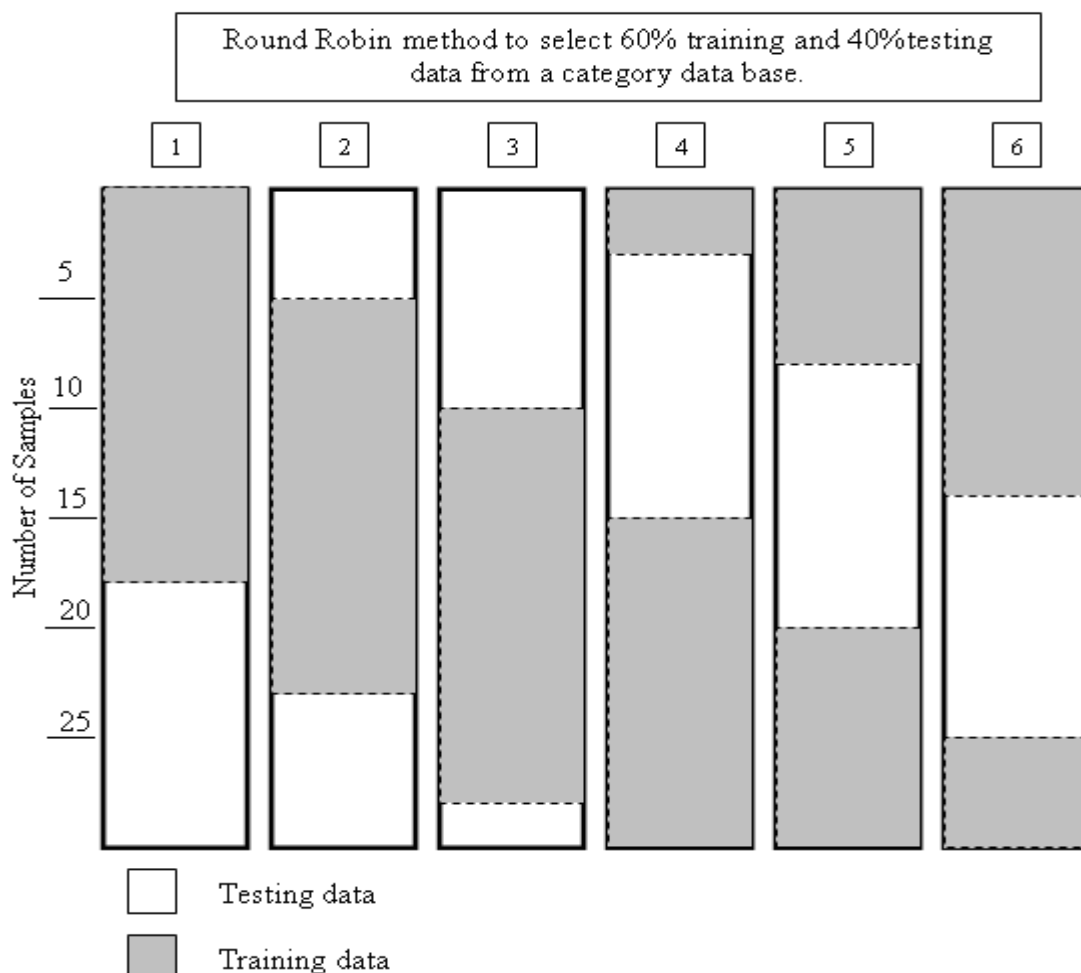


Figure 2-5 Round Robin Method

2.4.3 IR Regions Test

Multiple tests have been performed to verify the functionality of the spectrometer. Appendix D contains the completer test report on different spectrometers performed in Sentronic® Company, Dresden-Germany.

Initial testing for environmental effects on readings

The general hardware setup for spectroscopic measurement is illustrated in Figure 2-6. The probe or the measurement head in the setup direct the light to the spectrometer where it is analyzed using array of detectors, the resulting spectrum is transferred to the computer connected to the spectrometer by an Ethernet cable. Some initial procedures have been performed to verify the functionality of the spectrometer and examining different environmental effect of the measurement process.

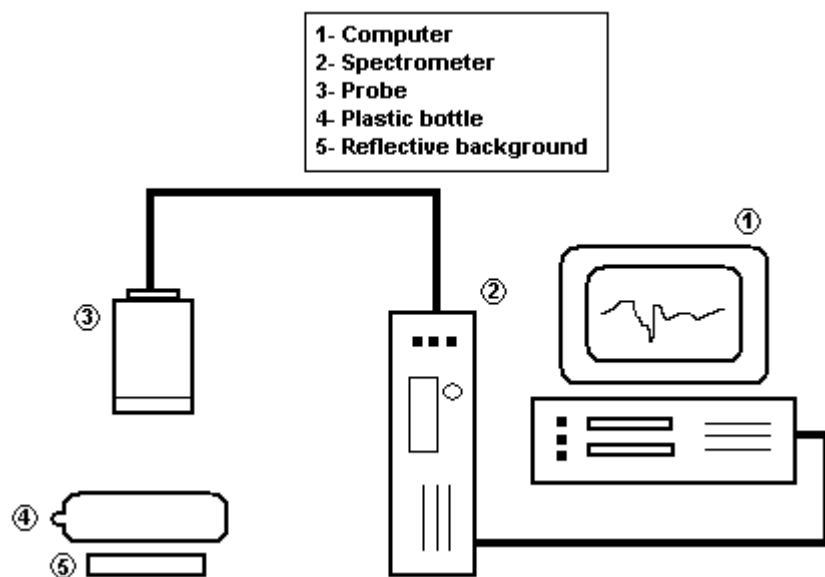


Figure 2-6 The General Hardware Setup for Spectroscopic Measurement

The calibration procedure and internal noise compensation

The calibration procedure consists of 2 steps:

- Dark light (Internal noise) compensation

The dark light or sometimes referred to as stray light is the light radiation of false wavelengths, which strikes a pixel of the detector array and it is caused by the imperfections of the gratin, dust or errors in other optical elements. This

parameter impacts the accuracy of the spectrometer measurements. To accommodate this effect, the NIR spectrum is first acquired when the infrared source is shutdown (Halogen Lamp). Hence, only the internal noise and other external wavelengths will be recorded and they will be subtracted from the acquired spectrum in the normal operation. Noise level was very small and Figure 2-7 shows an internal noise of the spectrometer, the spectrum is the raw data out of 65536 for a 16bit ADC and it is not in the reflectance mode (%).

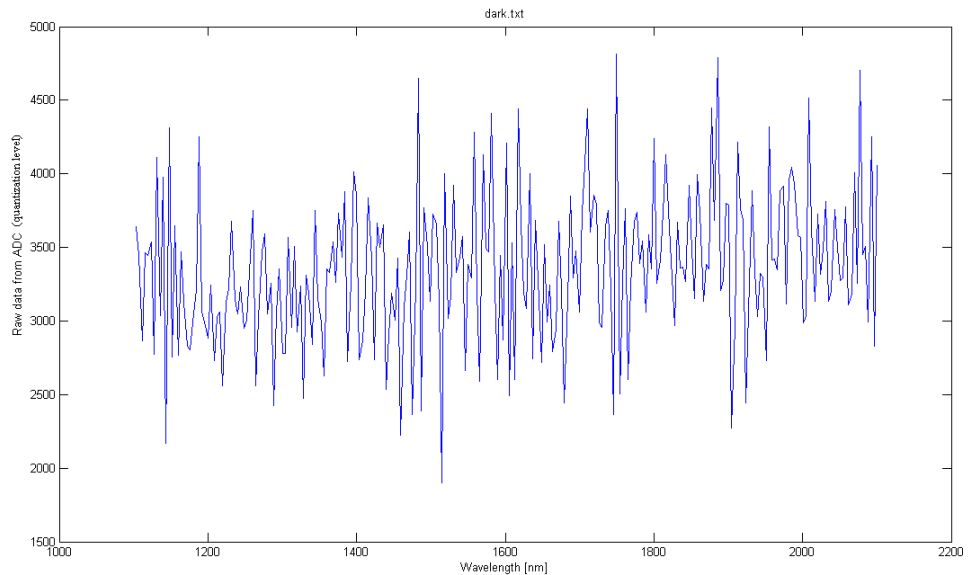


Figure 2-7 Dark (Internal Noise) Signal

- Spectrometer calibration

Calibration is performed by using a standard white plate that provides a maximum reflectance of the IR waves back to the probe. This procedure is used also to compensate the nonlinearity in the spectrometer as shown in Figure 2-8 where the sensitivity varies along the spectrometer range. The spectrum is the raw data out of 65536 for a 16bit ADC when it is not in the reflectance mode (%). Part of the initial calibration procedure is to find the proper integration time of the system which is the time required by the analog to digital converter in the spectrometer to formulate the acquired signal. This time actually is the bottle neck of the acquiring procedure since the communication and processing time in PC is negligible comparing to the integration time. The integration time can affect the quality of the signal, and need to be adjusted when the distance between the probe and the background is changed. The best setting for the integration time [49] is found by

stimulating the full dynamics of the system using the standard white plate to reach a level between 2/3 and full scale.

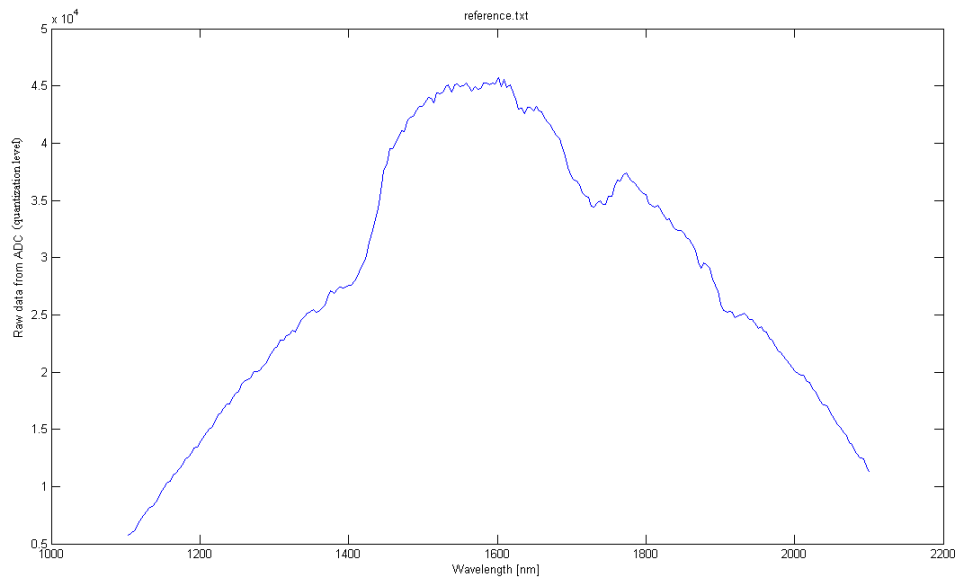


Figure 2-8 Spectrum of the Calibrating White Standard Plate

The calibration procedure was performed in regular bases every one hour during acquiring NIR data for plastic bottles. Figure 2-9 shows the hardware setup during the calibration, where the standard white plate is used.

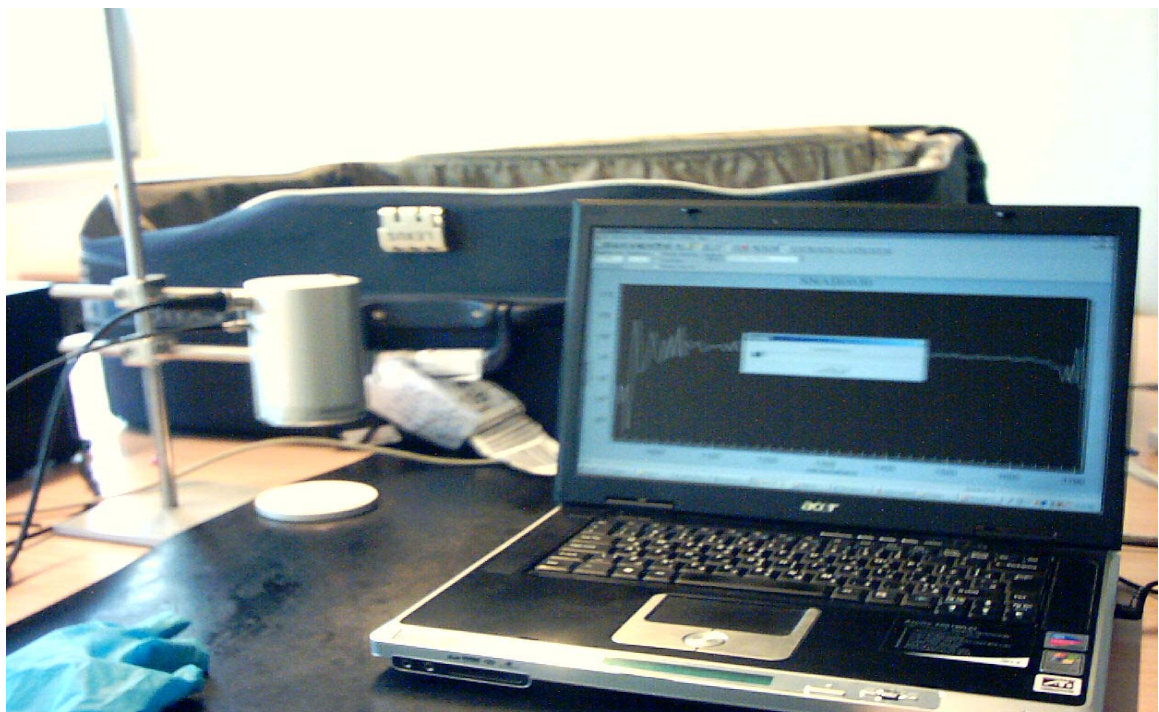


Figure 2-9 Calibration Process

In Figure 2-10, it can be seen the importance of calibration to lift the level of a signal and have better resolution.

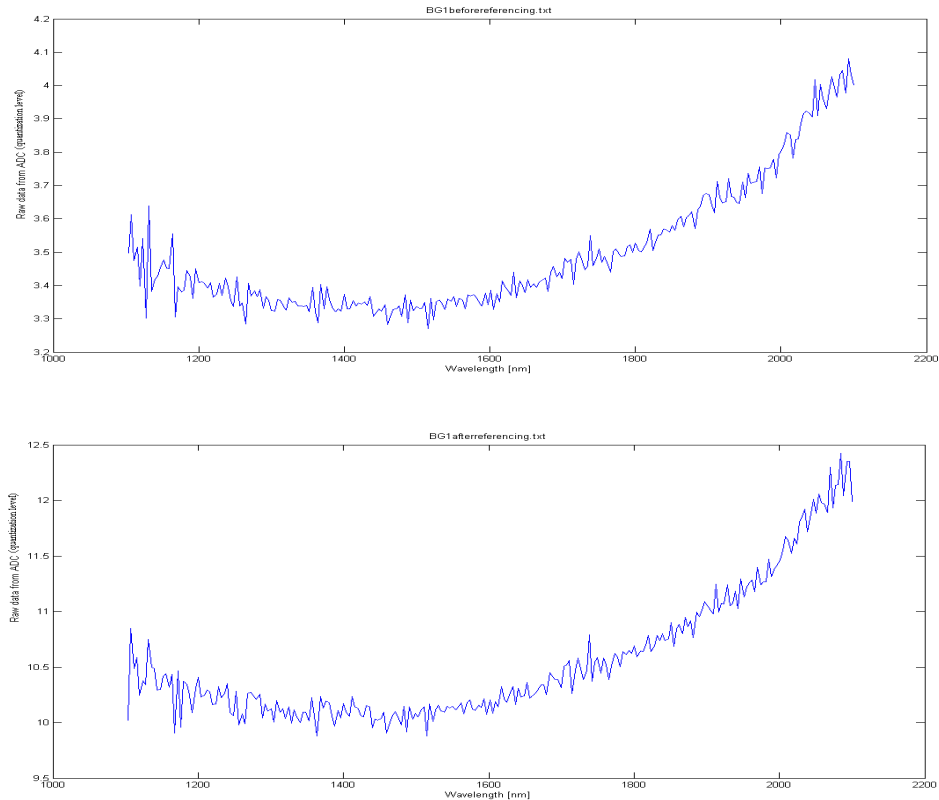


Figure 2-10 Calibration Effect on the Level of the Spectrum Signal

The light effect

The test was performed on 4 different bottles (one from each category) and the spectrum was recorded under day light and another one in a dark room, see Figure 2-11. There was no noticeable effect on the readings which means that the lighting is not an essential parameter in the calibration procedure.



Figure 2-11 Verifying the Effect of External Light on the Spectroscopic Measurements

The background effect

A piece of the rubber material used to manufacture the conveyor belt was used as the background of the measurements in order to simulate the environment of the sensor if mounted in the conveyor system. The results showed that the rubber absorb a large amount of the spectral power and reflects only less than 4% of the incident light. However, this percentage can be enhanced to 10% after calibration and of course it can be enhanced much better with a proper choice of a reflective background material that can provide a reflection quality close to the calibration standard white plate. Figure 2-12 shows the spectrum of the background in the reflectance mode.

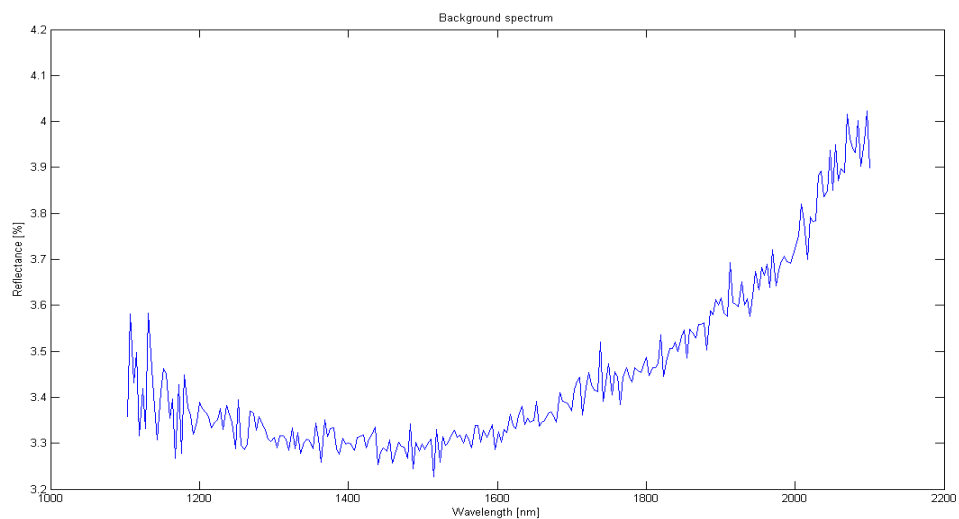


Figure 2-12 The Spectrum Signal of the Conveyor Belt Sample

The probe height effect

The probe distance from the tested bottle has a direct effect on the level of the spectrum signal during the calibration of the system. An optimum distance is specified for the probe used with the system since each probe type has a built in halogen lamp that functions as an infrared source. Also, the power of this lamp varies from probe type to another. The deviation from this distance will affect the power level of the signal and not the shape of it.

The contamination effect

By checking different contamination types, we found that the dry contamination on the plastic bottle does not harm the quality of NIR signal. However, the existence of paper label deforms the signal while a very thin plastic label does not. Figures 2-13, 2-14, 2-15 show the effect of the label and contamination.

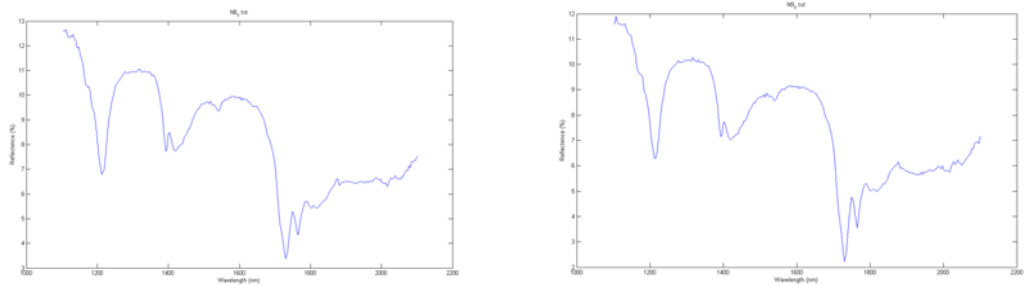


Figure 2-13 Effect of Contamination

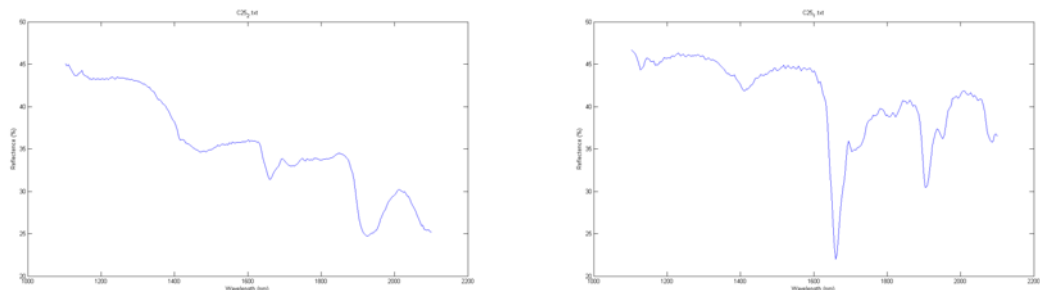


Figure 2-14 Effect of Paper Label

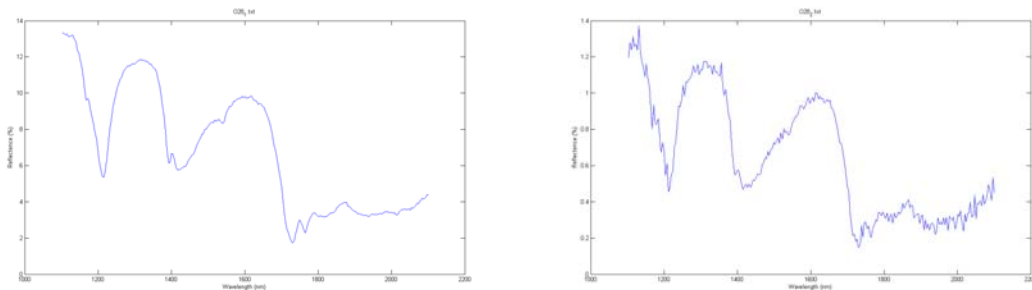


Figure 2-15 Effect of Plastic Label

The integration time effect (speed test)

As mentioned before, the integration time is the bottle neck of the spectrum acquisition. To verify the effect of the integration time on the acquisition speed, the following test was performed.

Procedure

- Initially the sampling time was 40 msec which is the optimum setting for the hardware setup available since it provides a full range signal.
- Trace logging was performed for 2 minutes with zero sampling time interval using the system clock to generate the time interval between logged files.
- After 2 minutes time period elapsed, the data files (18KB each) stored in the hard disk along one complete minute were counted.
- The number of readings possible for one average size bottle was determined..
- The procedure was repeated for an integration time of 25 msec.

Results

- For 40 msec
 - Number of files found during one minute: 531 files.
 - Approximately 3 different spectrum readings can be achieved for an average bottle length of 30 cm moving in a speed of 1m/sec.
- For 25 msec
 - Number of files found during one minute: 652 files.
 - Complete 3 different spectrum readings can be achieved for an average bottle length of 30 cm moving in a speed of 1m/sec.

Plastic spectroscopy at bandwidth 900-1700nm

The spectrum data has been collected for the 120 plastic bottle samples in the range of 900-1700nm using a spectrometer setup described in the following section in

order to find the important features in the signals for different categories (Clear, Natural, Opaque).

Hardware setup and settings

The following was the hardware and software setup used for the measurements:

- Hardware: GetSpec NIR1.7-128TTS + Sentrohead 50/35
- Software: Spec32 [SNAB0030 (Serial Number of the Spectrometer)].
- Reference: Sentrohead White Standard placed over the conveyor.
- Head height level: 80 mm between the head and the conveyor belt sample.
- Integration time: 450 msec – 100 msec.
- Number of integration: 1
- Dark Setup: Dark Spectrum Subtraction in manual mode.
- Sample Setup: Measurement type is Reflection in percentage and for the reference in counts.
- Detector temperature control set point was -20°C.

The following Figure 2-16 shows the hardware setup.



2-16 The Hardware Setup Used for Acquiring the Spectrum Signal between 900-1700nm

Collecting spectrum database for plastic bottles at 900-1700 nm

Spectrum acquisition was performed for 450 msec integration time and referencing was taken periodically in approximately 30 minutes bases. Then the acquisition was repeated for 100 msec integration time due to the saturation occurring in some spectral measurements.

The acquisition was performed three times for each plastic bottle sample. In other words, each bottle has 3 spectrum readings (one at the top, at the bottom and next to the label if exist). These readings were saved in text files and named in the format of “Xn_m.txt” where,

- X can be (C for Clear, N for Natural, or O for Opaque),
- n is the sample number between 1 to 30 for each category,
- m is a number between 1 and 3 since each sample has 3 readings from three different places at the bottle as mentioned before.

Figures 2-17, 2-18, 2-19 are typical results for the following categories: (clear, natural, and opaque).

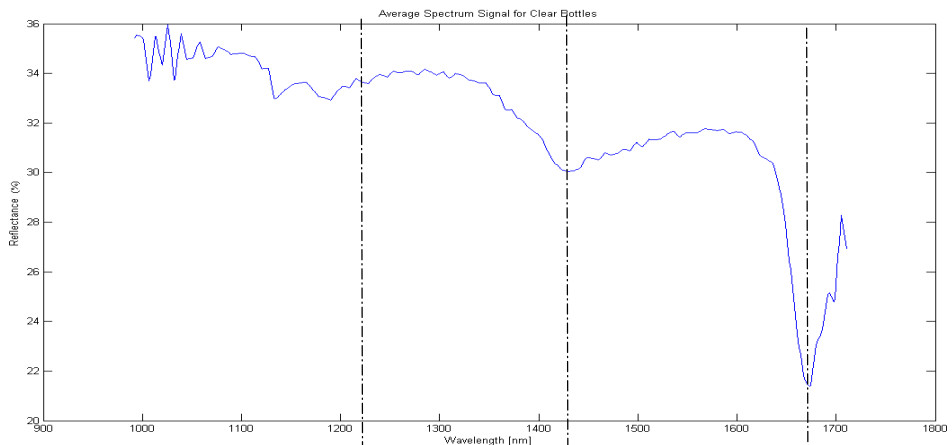


Figure 2-17 Typical Spectrum of a Clear Plastic Bottle

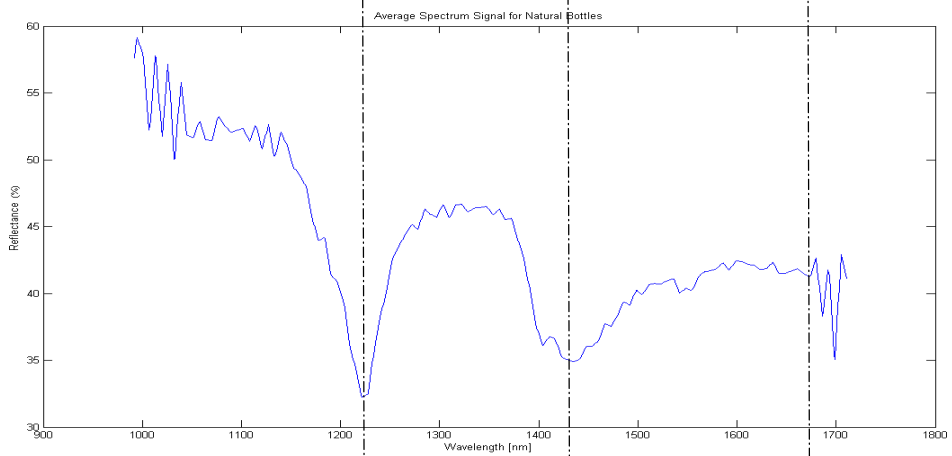


Figure 2-18 Typical Spectrum of a Natural Plastic Bottle

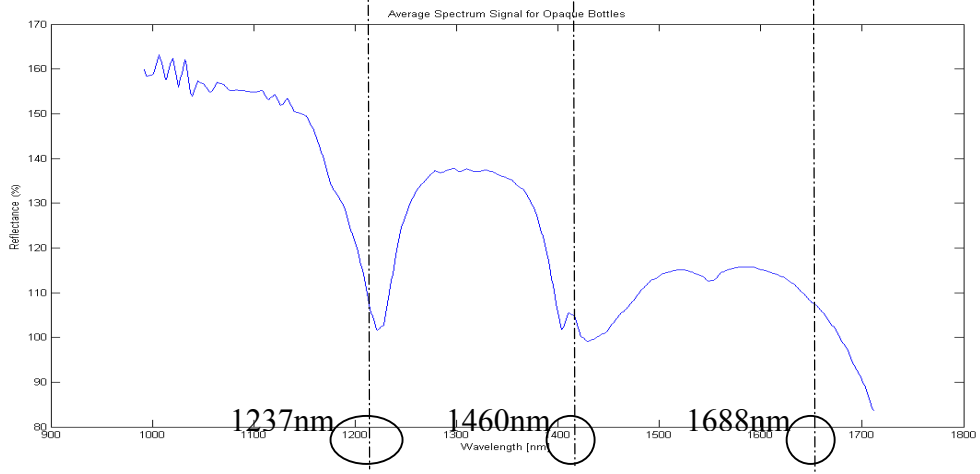


Figure 2-19 Typical Spectrum of an Opaque Plastic Bottle

It can be realized from the figures that the clear plastic bottle spectrum has a valley at around 1688 nm while the natural and opaque bottles have two main valleys at 1237 nm and 1460 nm. Actually these valleys present the chemical type of the plastic. As mentioned before, most of the clear plastic bottles are made of PET, while the natural and opaque are made of HDPE. This explains the similarity between the natural and opaque signals. However, to get indication about the transparency, it is clear that the transparent (clear) plastic bottles will allow more light to pass through compared to natural and opaque ones, which means that the reflectance spectrum of clear bottles has lower level than the case for natural and opaque. Figure 2-20 shows the average level for each sample. The average level shown is the average of the three readings taken.

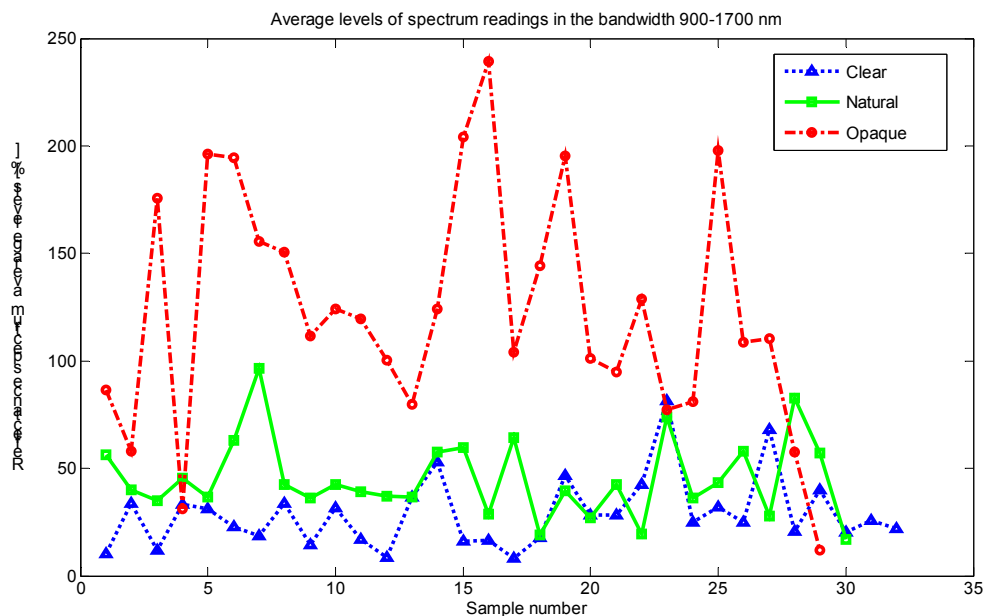


Figure 2-20 Average Level for Spectrum Readings in the Bandwidth 900-1700nm

Plastic spectroscopy at bandwidth 1100-2200nm

The spectrum data has been collected for the 120 plastic bottle samples in the range of 1100-2200nm using a spectrometer setup described in the following section in order to find the important features in the signals for different categories (Clear, Natural, Opaque).

Hardware setup and settings

- Hardware: Polytec PSS NIR2.1+ Sentohead (NIR100)
- Software: Polytech: PSS Device Driver ActiveX Demo.
- Reference: Sentohead White Standard placed over the conveyor.
- Head height level: 135 mm between the head and the conveyor belt sample.
- Integration time: 30msec
- Number of integrations: 10
- Dark Setup: Dark Spectrum Subtraction in manual mode.
- Sample Setup: Measurement type is Reflection in percentage and for the reference in counts.

The following Figure 2-21 shows the hardware setup.

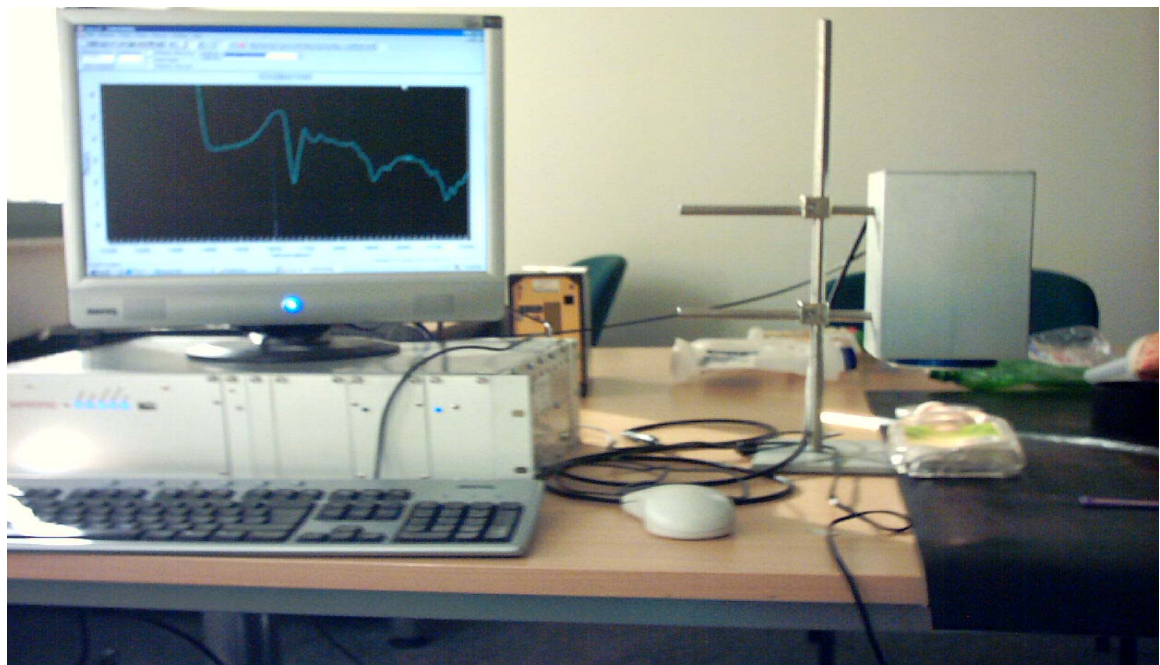


Figure 2-21 Hardware Setup Used for Acquiring the Spectrum Signal between 1100-2200nm

Collecting spectrum database for plastic bottles at 1100-2200 nm

Spectrum acquisition was performed for 30 msec integration time and referencing was taken periodically in approximately 30 minutes bases.

The acquisition was performed three times for each plastic bottle sample. In other words, each bottle has 3 spectrum readings (one at the top part, at the bottom

and next to the label if exist). These readings were arranged in text files and named in the format of “Xn_m.txt” where,

- X can be (C for Clear, N for Natural, or O for Opaque),
- n is the sample number between 1 to 30 for each category,
- m is a number between 1 and 3 since each sample has 3 readings from three different places at the bottle as mentioned before.

Figures 2-22, 2-23, 2-24 are the typical results for the following categories: (clear, natural, and opaque).

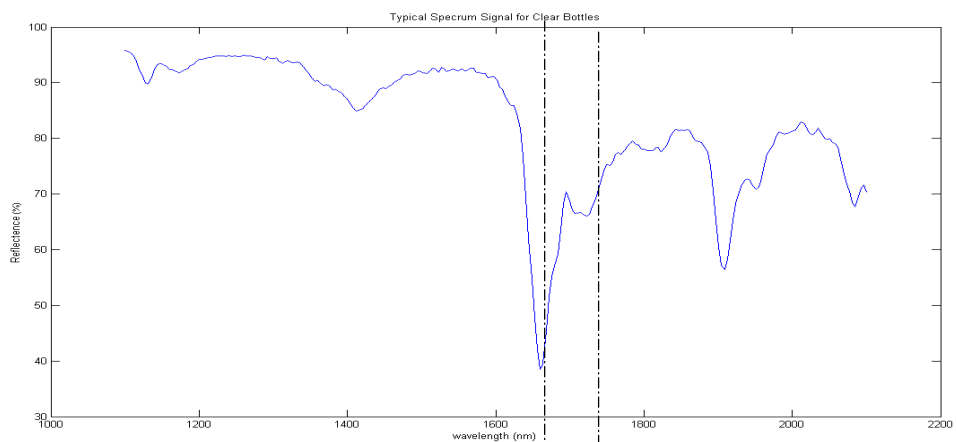


Figure 2-22 Typical Spectrum of a Clear Plastic Bottle

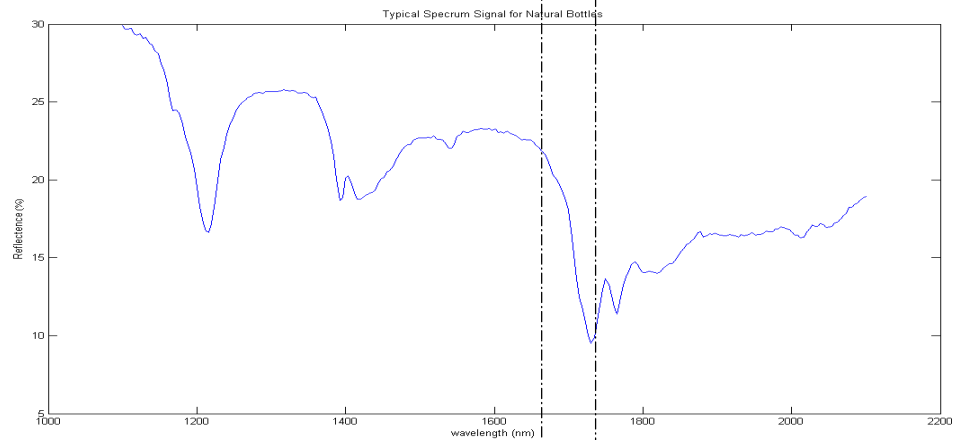


Figure 2-23 Typical Spectrum of a Natural Plastic Bottle

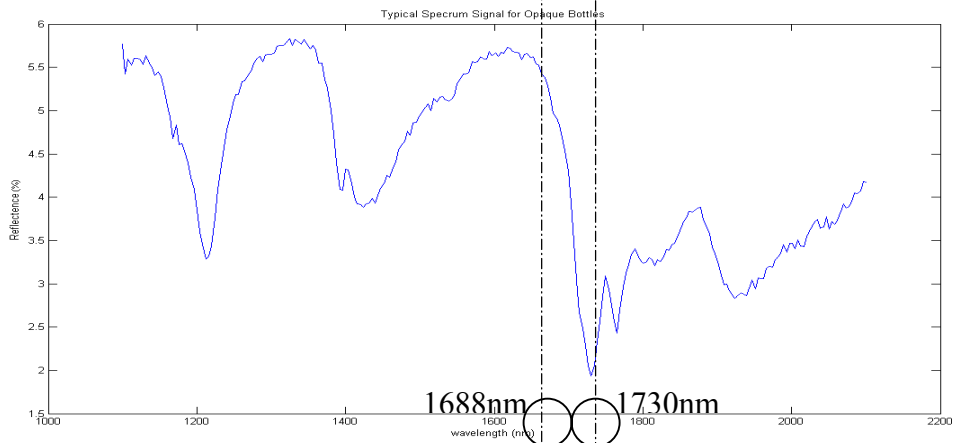


Figure 2-24 Typical Spectrum of an Opaque Plastic Bottle

It can be realized from the figures that the clear plastic bottle spectrum has a valley at around 1688 nm while the natural and opaque bottles have a main valley at 1730nm. As the valleys are an indication for the chemical type of plastic, the average value of the spectrum is an indication of transparency. However, the separability

using this feature was not clear as shown in Figure 2-25. This is due to the relatively small integration time used in this setup. After acquiring all the spectrum data, the average level was obtained for each sample by averaging the three average levels for each of the three readings per sample.

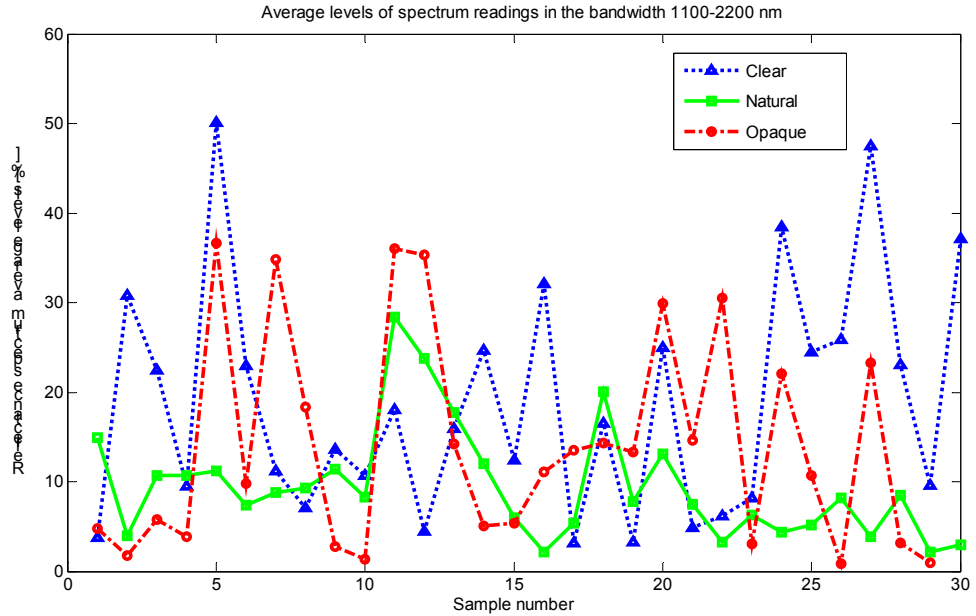


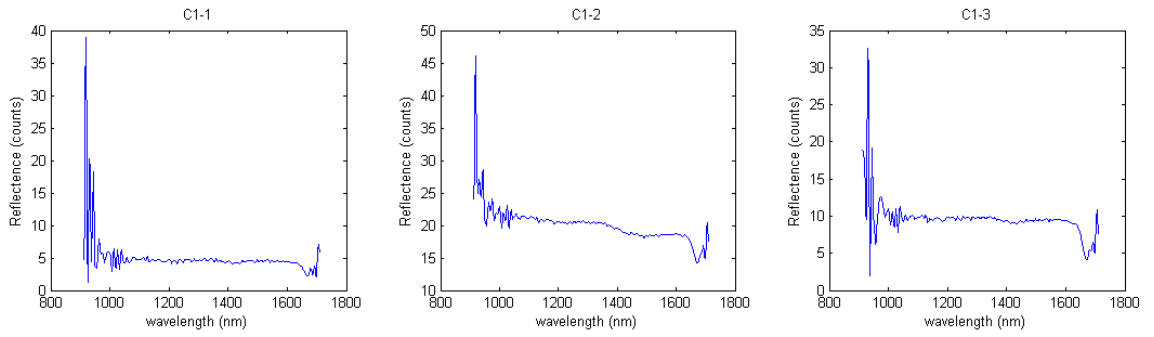
Figure 2-25 Average Level for Spectrum Readings in the Bandwidth 1100-2200nm

2.4.4 Preprocessing

- Step1: Signal truncation at boundaries

This is done due to the low accuracy of the spectrometer at the boundaries of its bandwidth; therefore the signal tends to be very noisy and heavily affects the feature extraction. Since no representative information was observed at the beginning of the region (900 nm-1000 nm), this part was discarded from the spectrum. In Figure 2-26, we can see some of the acquired signals and the same signals after truncation.

Before Truncation



After Truncation

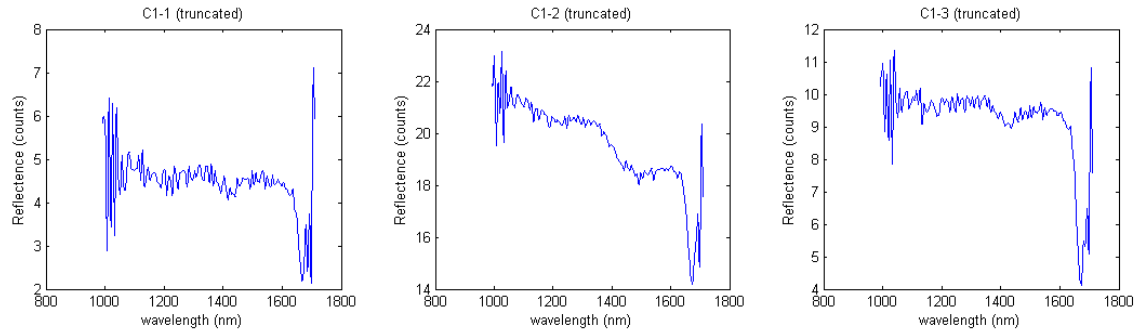


Figure 2-26 The Spectrum before and after Truncating

- Step 2: Filtering the signal

In order to remove unreliable and misleading noise in the signal, a low pass filter was applied to the spectrum taking into consideration mirroring the signal on both sides to avoid the boundaries effect during the convolution procedure. The low pass filtering is implemented by passing an averaging window over the whole signal. The width of the averaging window is around 5% of the signal length. Figure 2-27 shows the mirroring effect on the signal filtering.

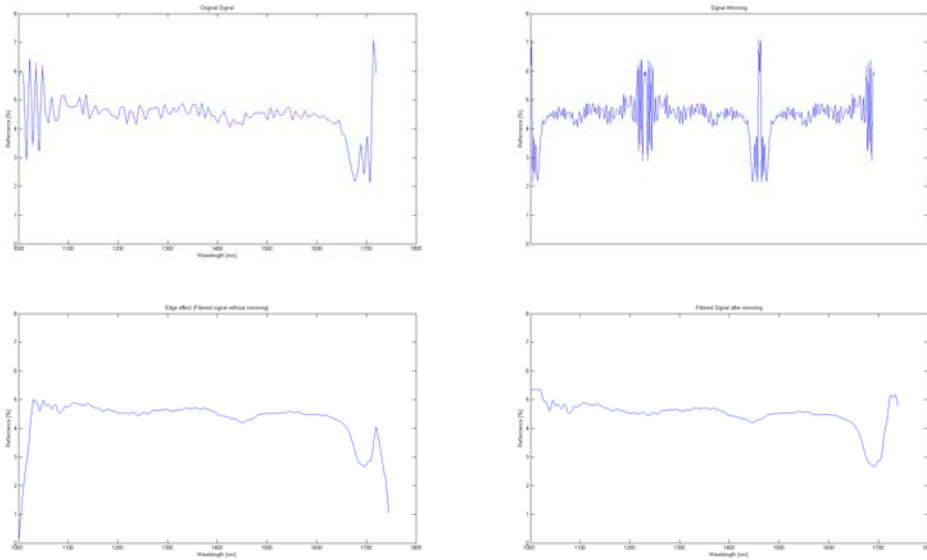


Figure 2-27 Comparing the Filtered Signal with and without Mirroring

- Dividing the spectrum

From different spectrum reading observations, it was clear that the representative information in the signal is spread in the spectrum and can be found along the truncated spectrum. By trial and error, it was found that dividing the spectrum into six equally spaced regions is sufficient to extract reliable features of the spectrum signal for the region between 900-1700 nm and four regions for 1100-2200 nm. So to find the first two global minimum points at a spectrum, we extract the minimum point at each of the sub-regions and satisfy the condition that this point is not at the boundaries of the region because if it is so there is no real valley at this corresponding region, and the region has a slope without valleys. Figure 2-28 explains the idea of this condition. Then we choose the minimum two points between the six or four points. By using this method we can make sure that the valley points will not be connected.

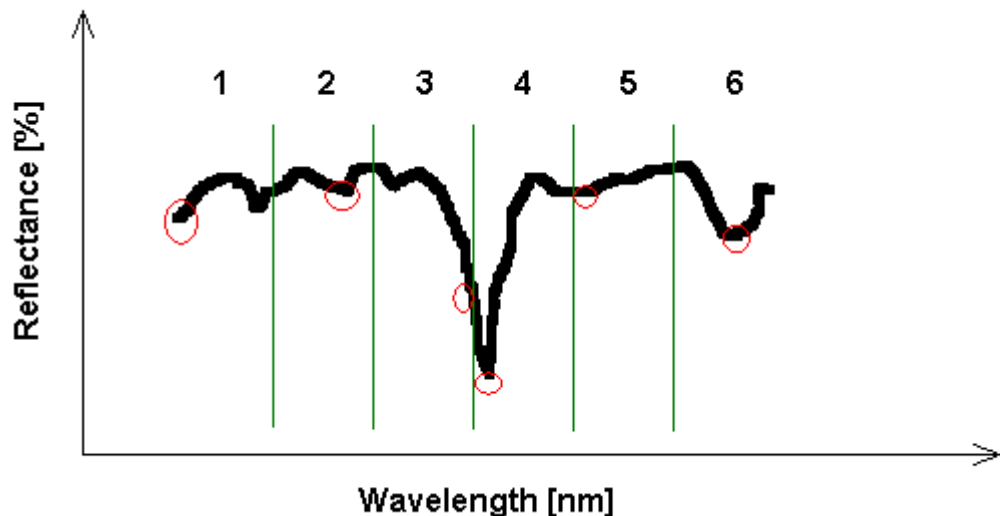


Figure 2-28 Dividing the Spectrum into Six Equally Spaced Regions to Investigate the Positions of Valleys

From this figure, it can be seen that the minimum points at region 4 and 6 respectively will be chosen. Since regions 1, 5 and 3 have minimum values at the boundaries of these regions, they are not considered as minimum points.

2.4.5 Feature Extractions

Two methods were used to generate the features to be used in the classification. The first method is based on the observations described before in the data collection stage using the valleys wavelength positions and average values. The second method is by using principal component analysis.

Average level and valleys positions

In the following Figures 2-29, 2-30, 2-31, 2-32, 2-33, 2-34 the minimum points locations are represented by '*' at the wavelength axis while the average level of the signal is represented by 'o' on the reflectance axis.

- For the spectrum range 900-1700 nm

- Clear plastic bottles

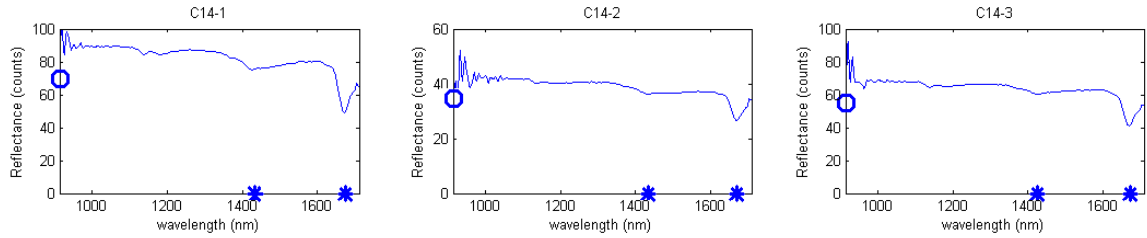


Figure 2-29 Positions of Valleys and Average Level for Different Spectrum Readings for Clear Bottles at the Range of 900-1700nm

- Natural plastic bottles

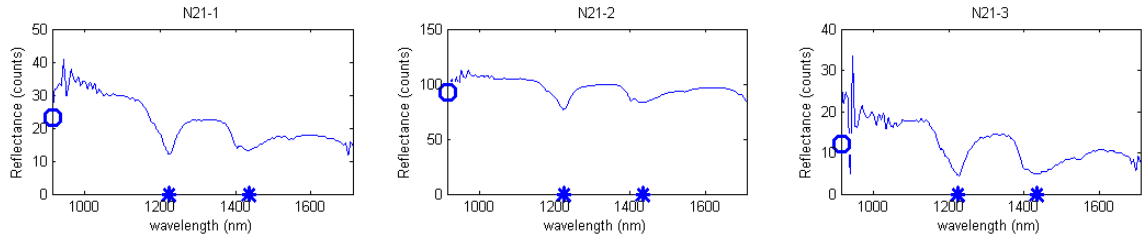


Figure 2-30 Positions of Valleys and Average Level for Different Spectrum Readings for Natural Bottles at the Range of 900-1700nm

- Opaque plastic bottles

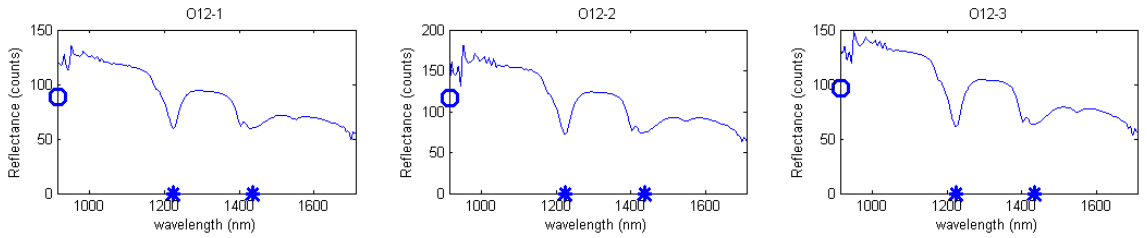


Figure 2-31 Positions of Valleys and Average Level for Different Spectrum Readings for Opaque Bottles at the Range of 900-1700nm

- For the spectrum range 1100-2200 nm

- Clear plastic bottles

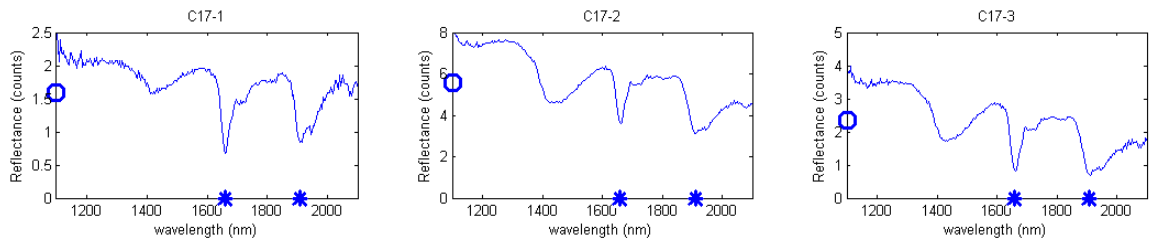


Figure 2-32 Positions of Valleys and Average Level for Different Spectrum Readings for Clear Bottles at the Range of 1100-2200nm

- Natural plastic bottles

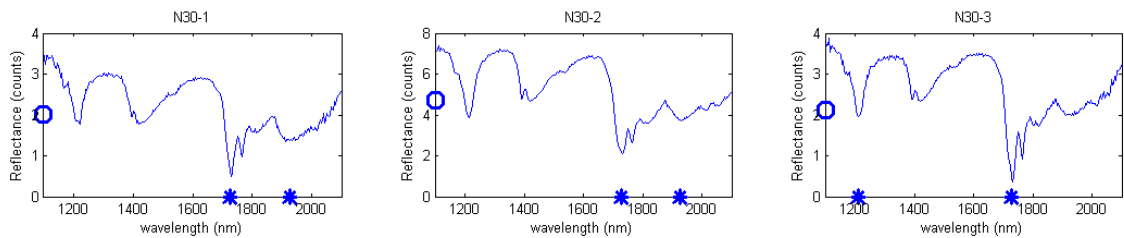


Figure 2-33 Positions of Valleys and Average Level for Different Spectrum Readings for Natural Bottles at the Range of 1100-2200nm

- Opaque plastic bottles

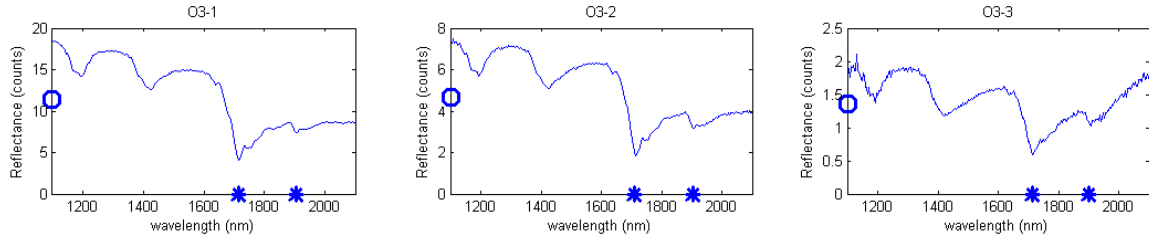


Figure 2-34 Positions of Valleys and Average Level for Different Spectrum Readings for Opaque Bottles at the Range of 1100-2200nm

Principal component feature extraction

It does make sense to filter the data before extracting PCA since removing details will help PCA to provide better representation of the spectrum data.

Before applying the principal component analysis, the three spectrum signals are averaged. Then, principal components are obtained for the raw spectrum data and for the normalized (standardized) data by dividing the spectrum by its variance at each wavelength. Normalizing the data is often preferable when the variables are in different units or when the variance of the different columns is substantial [50]. We compared the results in terms of the percentage of the variance that is accounted for by the sixteen principal components in the bandwidth 900-1700 nm and the first thirteen principal components in the bandwidth 1100-2200. The percentage of the variance is calculated by dividing the variance of each principal component by the summation of the variances of all the principal components. It was shown from the Tables 2-4, 2-5 below that using the first two principal components before standardizing the data will cover more than 99.5% of the variance of spectrum data.

- For the spectrum signals at 900-1700nm

Table 2-4 Percentage of Variance Covered by a Number of Principal Components at 900-1700nm

Number of Principal Components	Accumulative Percentage of Variance Before standardizing	Accumulative Percentage of Variance After Standardizing
1	98.9314	98.8826
2	99.7641	99.6928
3	99.9257	99.9086
4	99.9750	99.9730
5	99.9860	99.9846
6	99.9931	99.9922
7	99.9970	99.9971
8	99.9985	99.9985
9	99.9991	99.9991
10	99.9995	99.9995
11	99.9997	99.9997
12	99.9998	99.9998
13	99.9999	99.9999
14	99.9999	99.9999
15	99.9999	99.9999
16	100.0000	100.0000

- For the spectrum signals at 1100-2200nm

Table 2-5 Percentage of Variance Covered by a Number of Principal Components at 1100-2200 nm

Number of Principal Components	Before standardizing	After Standardizing
1	97.2359	96.8343
2	99.5402	99.4667
3	99.8106	99.7846
4	99.9287	99.9301
5	99.9856	99.9845
6	99.9926	99.9919
7	99.9962	99.9957
8	99.9979	99.9976
9	99.9989	99.9989
10	99.9995	99.9994
11	99.9997	99.9997
12	99.9999	99.9999
13	100.0000	100.0000

A two dimensional feature vector representing the spectrum signal is generated by taking the first two principal components of the signal data. Two principal components are enough to accommodate more than 99.98% of the over all variances in the spectrum data. Moreover, this number (two principal components) is appropriate to visualize the separability of the classes if they are represented by these principal components. A very good separability (almost linear separable classes) was achieved in the spectrum readings in the range 900-1700 nm as shown in Figure 2-35.

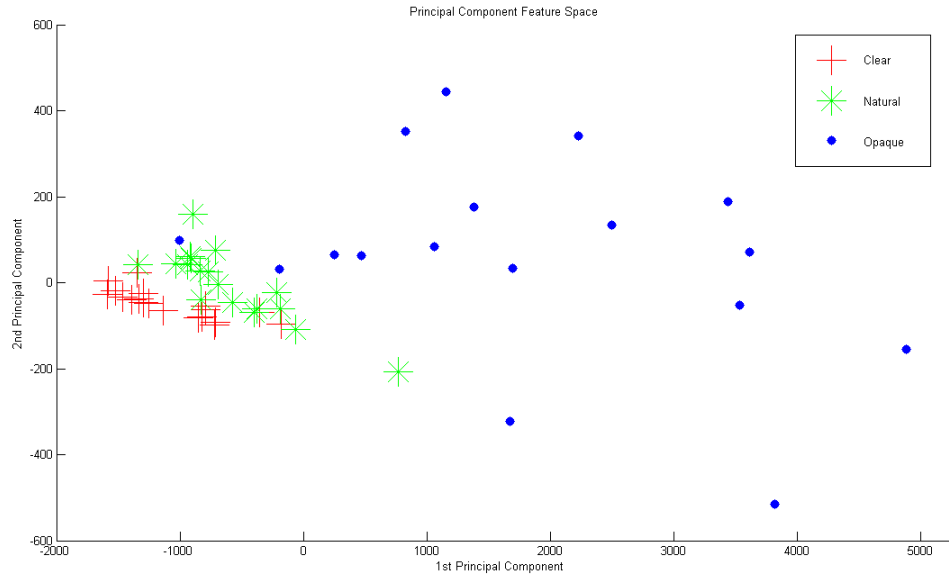


Figure 2-35 Feature Space of the First Two Principal Components at the Range of 900-1700nm

While in the readings of the range 1100-2200 nm, the separability was not as good as in the previous range since it requires a nonlinear decision boundaries to separate the classes as shown in the Figure 2-36 below.

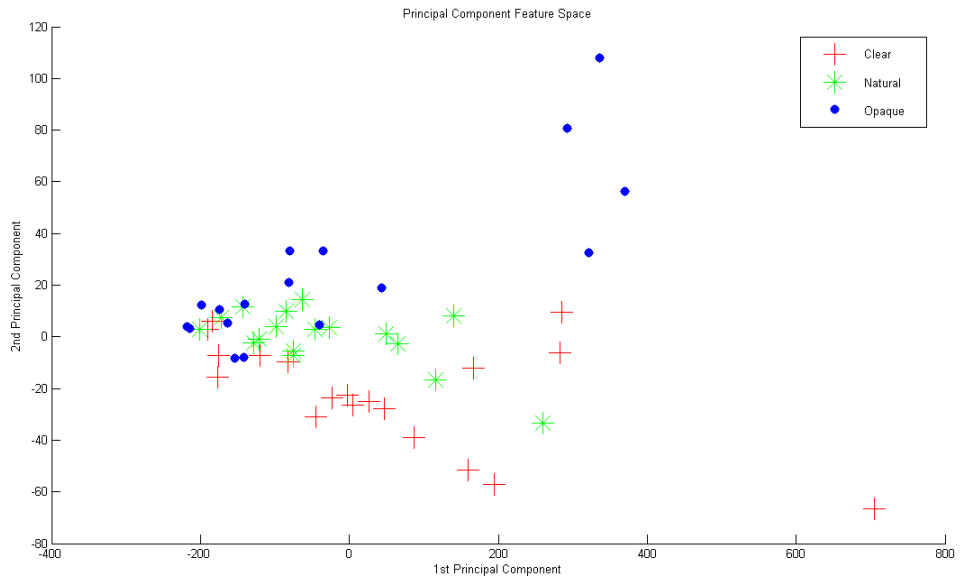


Figure 2-36 Feature Space of the First Two Principal Components at the Range of 1100-2200nm

2.4.6 Classification

The feature vector of the plastic bottle spectrum signal is introduced to the classifier. Both methods for obtaining feature vectors were examined in the classification stage:

- Valleys position + Average spectrum level

Since each plastic bottle has the 3 different spectrum readings, the feature vector was created in 4 different ways [P is a symbol for power level or average level, V is the main valley wavelength position]:

- 1P1V: Taking the average value of the three readings and the most frequent valley wavelength position from the three readings.
- 1P3V: Taking the average value of the three readings and 3 valley wavelength positions from the three readings.
- 3P1V: Taking 3 average values and the most frequent valley wavelength position from the three readings.
- 3P3V: Taking 3 average values and 3 valley wavelength positions from the three readings.

- Principal component analysis

The classification performance was examined for the feature vector of 1, 2, 5 or 10 principal components. In the classification stage, five different classifiers were examined: Discriminant function based classifiers (Linear, Quadratic, DiagQuadratic, Mahalanobis) and Decision Trees.

In the following section we will provide the results of using different feature vectors on the previous classifiers, detailed results are found in the appendix C. The spectrum data used was divided into training and testing data in three different ratios:

- Training data = 60% of total data, Testing data = 40% of total data.
- Training data = 50% of total data, Testing data = 50% of total data.
- Training data = 40% of total data, Testing data = 60% of total data.

For most of the cases, the classifier accuracy was better when training data was covering 60% of total amount of data. Due to the small number of samples per class (30 samples) the Round Robin method described earlier was used to find a generalized measurement for the classifier accuracy.

Using power and valleys positions features

The results showed that the DiagQuadratic classifier had the best classification accuracy with the feature vector of the three average levels of the three readings of each plastic bottle sample and the average wavelength position of the main valley in the three spectrum readings. Table 2-6 is the classification accuracy of the classifiers trained by 60% of the spectrum data available for the range 900-1700nm.

Table 2-6 Classifier Accuracy Using the Valley Position and Average Value Features in the Range 900-1700nm

Classifier	Feature Dimension			
	P1V1	P1V3	P3V1	P3V3
Linear	0.8649	0.8513	0.8514	0.8198
Quadratic	0.9099	0.8378	0.9009	0.8243
Tree	0.8649	0.8378	0.8739	0.8559
Mahalanobis	0.8964	0.8018	0.7838	0.7252
DiagQuadratic	0.9054	0.8649	0.9414	0.8694

While for the range 1100-2200nm, the results showed that the Decision Tree classifier had the best classification accuracy with the feature vector of the three average levels of the three readings of each plastic bottle sample and the average wavelength position of the main valley in the three spectrum readings. The following Table 2-7 is the classification accuracy of the classifiers trained by 60% of the spectrum data available for the range 1100-2200nm.

Table 2-7 Classifier Accuracy Using the Valley Position and Average Value Features in the Range 1100-2200nm

Classifier	Feature Dimension			
	P1V1	P1V3	P3V1	P3V3
Linear	0.4414	0.4370	0.4280	0.4099
Quadratic	0.5315	0.4775	0.4730	0.4730
Tree	0.6306	0.6171	0.7072	0.6622
Mahalanobis	0.5631	0.4595	0.4504	0.3919
DiagQuadratic	0.5360	0.5406	0.4775	0.4910

Evaluating a feature set is measured by its ability to discriminant accurately between classes. This is achieved by defining a class separability measure that is optimized with respect to all possible subsets. Choosing a subset can be done by comparing the accuracy of the classifier for a certain feature subset and comparing the performance for each classifier at each feature subset and then choosing the feature subset and the classifier combination that achieves the highest accuracy, a DiagQuadratic classifier using the four dimensional feature vectors composed of 1

average level of the three spectral readings and the positions of the three global minima in the three spectral readings was found at the end to be the best classifier and feature subsets.

We found that for the valley and power level based feature vectors, the performance of the classifiers in general was better in the bandwidth 900-1700 nm. This can be explained by proper hardware calibration performed at this bandwidth, since the power level features extracted from the spectrometer at 1100-2200 nm were not separable, and this can be related to the small integration time used to construct the spectrum which forced the spectrometer to work in a narrow dynamic range where the data can not be easily separated.

The performance of the Quadratic classifiers in general was very good in terms of output accuracy and especially for DiagQuadratic classifiers. This is due to possible redundancy between feature values by using the global position of minima, which are ideally the same. Therefore, there is a correlation between components in the feature vectors. This correlation may harm the classification process. DiaqQuadratic ignores this effect by just taking into consideration the autocorrelation determined in the diagonal of the covariance matrix only.

Also it can be realized that increasing the dimension of the feature vector will not enhance the classification accuracy, which indicates that some of the features are not independent or they are overlapping in a way that disturbs the process of finding the classification boundaries.

Using PCA features

The results showed that the DiagQuadratic classifier had the best classification accuracy with the feature vector of 10 principal components. The following Table 2-8 is the classification accuracy of the classifiers trained by 60% of the spectrum data available for the range 900-1700nm.

Table 2-8 Classifiers Accuracy Using PCA Features in the Range 900-1700nm

	Principal Components			
	1	2	5	10
Linear	0.66215	0.75675	0.86938	0.84685
Quadratic	0.67115	0.8018	0.86037	0.86937
Tree	0.54503	0.6937	0.81982	0.75675
Mahalanobis	0.68015	0.77928	0.73875	0.7793
DiagQuadratic	0.67115	0.77027	0.9054	0.93692

While in the range of 1100-2200 nm, the results showed that the Quadratic classifier had the best classification accuracy with the feature vector of 10 principal components. The following Table 2-9 is the classification accuracy of the classifiers trained by 60% of the spectrum data available for the range 1100-2200nm.

Table 2-9 Classifiers Accuracy Using PCA Features in the Range 1100-2200nm

	Principal Components			
	1	2	5	10
Linear	0.45047	0.68017	0.76127	0.77477
Quadratic	0.44145	0.7117	0.79728	0.84235
Tree	0.33335	0.68017	0.72522	0.70272
Mahalanobis	0.4189	0.66668	0.72073	0.7928
DiagQuadratic	0.44145	0.67568	0.69822	0.67567

It is again the quadratic classifiers which are doing a good job in classifying principal component features. Although for most of the cases, the more principal components added in the feature vector the higher the accuracy of the classifier. However, this relation was not completely monotonic especially for tree classifiers. This is normal since adding more principal components is equivalent to adding the noises of the spectrum signal which has a small standard deviation.

It is important to mention that the principal component analysis was able to extract some features that can be proposed to the classifier in the range of 1100-2200

which is the region where the features extracted based on visualization were not able to compensate the poor calibration settings.

In conclusion, it is more convenient to choose the bandwidth 900-1700 nm since the classification accuracy for feature vectors extracted by principal component analysis or by power mean and valley wavelength position was better than the accuracy at 1100-2200 nm. However, using the average level and valley wavelength position based feature vectors and DiagQuadratic classifier was found to be the best overall combination for the near infrared plastic bottles spectrum classifiers.

CHAPTER

COLOR CLASSIFICATION

3.1 Color Imaging

3.1.1 Theoretical Background

The need for color classification in automatic plastic bottle sorting is increasing since plastic bottle manufacturers are also gearing up to take advantage of the marketing edge inherent in using a spectrum of colors. Moreover, there is a trend to introduce a new set of colors into plastic bottles [22]. While the wider color choice is good for plastic bottle marketers, it poses new challenges and increases costs to plastic bottle recycling.

To handle this widening array of color, it is required to come up with an intelligent machine vision based system that is capable of learning new sets of colors that appear in different surfaces (opaque, transparent or semi transparent) and identify them. In this context color representation is a critical issue in designing a color classification system. In fact, humans perceive colors by a combination of three primary colors (Red, Green, and Blue), but as this perception may differ between humans [51], it is required to convert the usual RGB signals that are generated by traditional CCD cameras into HSI (hue, saturation, intensity) domain before assessing the color of the plastic bottle to employ the hue parameter which is independent of the intensity parameter as the latter is bound to be particularly sensitive to lighting variation as well as other reasons that have been mentioned in the literature survey.

The intensity I refers to the total light intensity and is defined by:

$$I = \frac{R + G + B}{3} \quad (3.1)$$

Hue H is a measure of the underlying color, and saturation S is a measurement of the degree to which it is not diluted by white light (S is zero for white light). S is given by the simple formula:

$$S = 1 - \frac{3 \min(R, G, B)}{R + G + B} \quad (3.2)$$

It can be seen that S does not express color but it measures the proportion of color and differentiation from white.

Hue is defined as an angle of rotation about the central white point W in the color triangle [52] see Figure 3-1. It is the angle between the pure red direction defined by the vector R-W and the direction of the color C in question defined by the vector C-W. As a result, H can be described by $\cos(H)$ which depends on the dot product $(C-W) \cdot (R-W)$:

$$H = \cos^{-1} \left(\frac{\frac{1}{2}[(R-G)+(R-B)]}{\sqrt{[(R-G)^2 + (R-B)(G-B)]^{1/2}}} \right) \quad (3.3)$$

Or 2π minus this value if $B > G$ [52]

When checking for the color of a plastic bottle, the hue is the most important parameter for color measurements. A rigorous check on the color can be achieved by constructing the hue distribution and comparing it with the hue distribution of a suitable training set. The most straightforward way to carry out the comparison is to compute the mean and the standard deviation of the two distributions to be compared and to perform discriminant analysis assuming normal distribution functions as described in chapter 1.

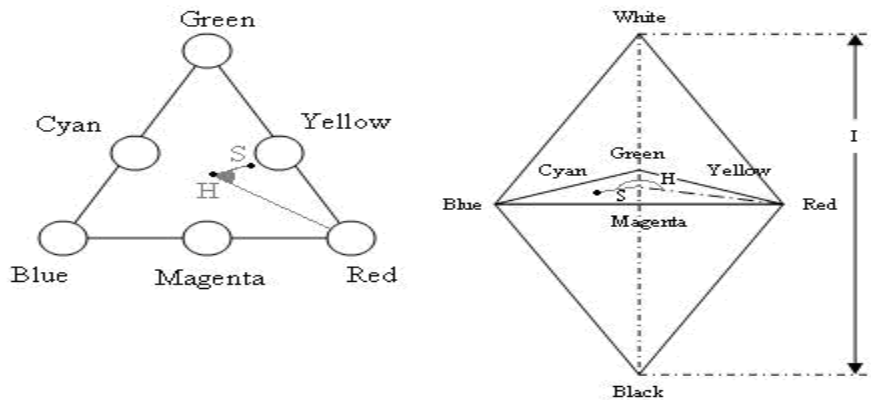


Figure 3-1 The Color Triangle

3.1.2 Imaging Hardware

CCD camera

Charged Coupled Devices are array detectors with metal-oxide capacitors (photogates). During the illumination by the spectrum focal line a charge (electron – hole pairs) is produced and stored under the gate. The pixel is the building block for the CCD imager, a rectangular array of pixels on which an image of the scene is focused. The read out of the array is proceeded by a charge transfer by means of varying gate potentials according to special clock schemes. The charges of the pixels are transferred simultaneously to the shift register(s), followed by a sequential transfer to the output section, where the charge is converted into a proportional voltage, see Figure 3-2 [49]. The node doing this is first set to a reference level (clamp level) and afterwards to the signal level. The difference is used as the final signal. This technique is called Correlated Double Sampling (CDS) and allows a significant reduction of the system noise.

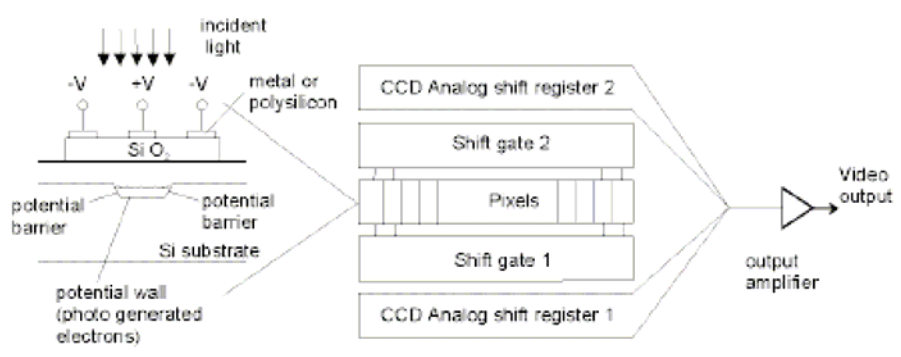


Figure 3-2 Operation Principle of a CCD Array Detector

The signal coming from each pixel is a time-varying video signal. Timing information for the vertical and horizontal positions and the sensor value combine to form the video signal.

For standard analog cameras, the lines of the CCD are interlaced to increase the perceived image update rate. This means that the odd-numbered rows (the odd field) are scanned first. Then the even-numbered fields (the even field) are scanned. The two fields make up one frame. Electronic Industries Association (EIA) RS-170 and NTSC cameras update at 30 frames/s with a resolution of 640 columns \times 480 rows.

Analog cameras are low in cost and easy to interface with standard analog acquisition devices [53].

Frame Grabber

The frame grabber was designed around a Video Scaling Processor that provides image transfer using PCI Direct Memory Access (DMA) transfers. This PCI bus mastering device can transfer the image data directly to the system or display memory in real time, leaving the CPU free to run other tasks.

The frame grabber uses the PCI bus for real-time transfer of video to system memory. The PCI bus has a theoretical data transfer rate that is fast enough for real-time transfer of video data; however, actual performance depends on such factors as CPU, memory caching, interaction among cards, operating system, bus implementation, motherboard chip-set, and BIOS version. There are two capturing modes available in the frame grabber which are off-screen mode and on-screen mode. The following explains the concepts for each mode.

Off-Screen capture

With off-screen capture, the video is first transferred to the system memory. Then, it is sent to the VGA display memory (see Figure 3-3). The refresh rate varies depending upon the VGA card used, the size of capture window, and the color bit depth selected. The video frame rate should be between 5 and 15 frames per second, depending on your system configuration. This mode is provided to be used by any VGA cards.

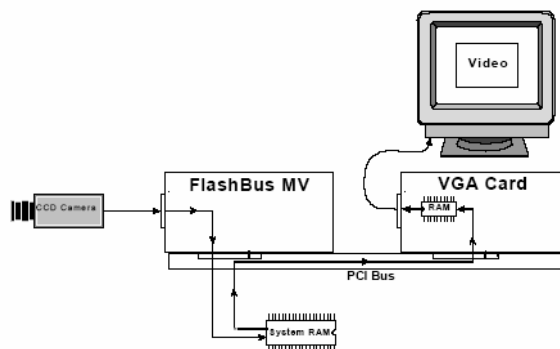


Figure 3-3 Off-Screen Mode

On-Screen capture

With On-screen capture, video is transferred directly to display memory (see Figure 3-4). Achieving full throughput performance requires the use of a high-performance display card. This is the best method for displaying full-resolution, 30-frames-persecond video on your VGA monitor.

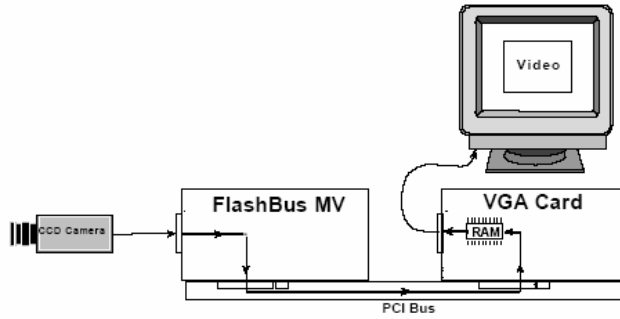


Figure 3-4 On-Screen Mode

3.2 Plastic Bottles Color Classification System Overview

The automatic plastic bottle color sorting system consists of two main parts:

- The mechanical part

In the practical plant situation, plastic bottles from domestic wastes are carried away by conveyor belt drives and the inspection system operates on the plastic bottle images grabbed in motion. The mechanical system is represented by the conveyor system which is basically a rubber belt driven by an AC motor with a gearbox. The motor speed is controlled by a frequency inverter; this system transmits the inspected bottle through the inspection chamber installed at the middle of the system, the box was built to isolate the inspected bottle from external lighting and provide a fixed lighting for the testing area by lamps mounted at the top of the box. The lamps surround the CCD camera which is mounted at the middle of the box roof.

The system prototype is designed to identify the bottle color on the fly without stopping the motor for inspection. Therefore the speed of the motor was determined to provide a range of linear speed. Figure 3-5 shows a schematic diagram of the system.

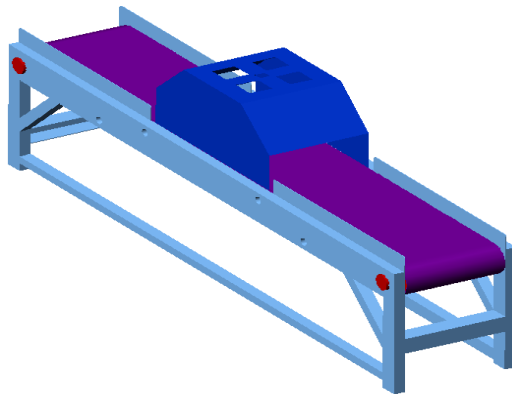


Figure 3-5 Schematic Diagram of the Mechanical System

- The vision system

The vision system has the task of grabbing the images of the plastic bottles, processing the acquired images, extract color features and classify the color of the bottle. The vision system consists of the CCD camera with RGB adapter, the frame grabber, illumination unit, a computing and display unit.

The CCD camera provides analog signals which are the responses of the CCD pixels to the three different wavelength ranges (Red, Green, and Blue (RGB)). These signals are received by the RGB adapter and transformed to an analog NTSC TV signal; this type of signal was standardized by the National Television System Committee. The TV signal is acquired by the frame grabber which will sample, digitize and quantize the image multi-spectral signal to get a digital colored image. The image is analyzed by the processing unit which executes the algorithms for color classification. Figure 3-6 shows the basic component of a machine vision system.

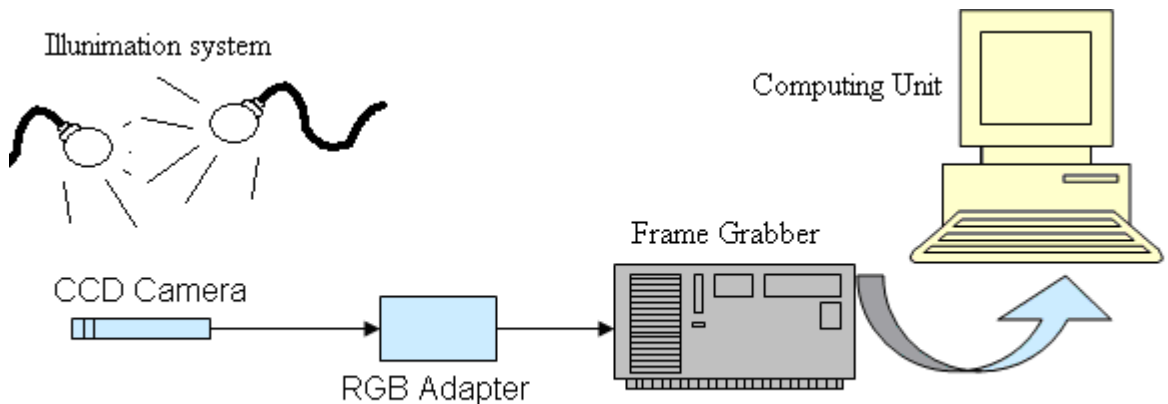


Figure 3-6 Basic Component of a Machine Vision System

3.2.1 The Design Parameters of the Conveyor System

A prototype model of the automatic color sorting system was developed at American University of Sharjah. The mechanical part is a simple conveyor system, consisting of a black colored conveyor belt with a width of 50 cm and a total length of 600 cm rotating around two cylinders and their centers are separated by a distance of 300 cm. The detailed dimensions of the system can be found in appendix B. The conveyor belt is rotated by means of a 0.25 kW AC motor with a nominal speed of 850 rpm at 50Hz.

The transmission speed of the conveyor belt required for the prototype system is to achieve a variable speed from 0.3 to 1 m/s.

In order to control the speed of the AC motor, a variable frequency inverter was obtained. The operation dynamic range of the frequency inverter is from 0-240 HZ.

To calculate the transmission speed of the conveyor belt rotating around a cylinder of 17.18 cm diameter at 50 Hz, provided that the thickness of the conveyor belt is ignored in the speed calculations:

$$\begin{aligned}\text{Transmission speed} &= \text{Rotational speed} \times \text{the radius of the cylinder} \\ &= 850 [\text{rpm}] \times 2\pi \times (17.18/2)[\text{cm}] = 7.64 \text{ m/sec}\end{aligned}$$

It can be seen that the speed is much higher than the requirements. Driving the motor at very low speeds for a long time is not preferable because at this speed the cooling fan of the motor looses its effectiveness and the motor temperature will increase significantly. A better solution is to add a worm gearbox to the motor in order to reduce the rotational speed output. A gear ratio of 20 was chosen to bring the speed into the range of 0.3-1 sec.

After adding the gearbox, the transmission speed becomes $7.64 / 20 = 0.38$ m/sec.

So to achieve the speed range between 0.3 and 1 m, the frequency inverter will run in the range of 40 – 130 Hz which is within the normal operation dynamic range of the inverter.

Figure 3-7 shows the conveyor belt motor driving system.

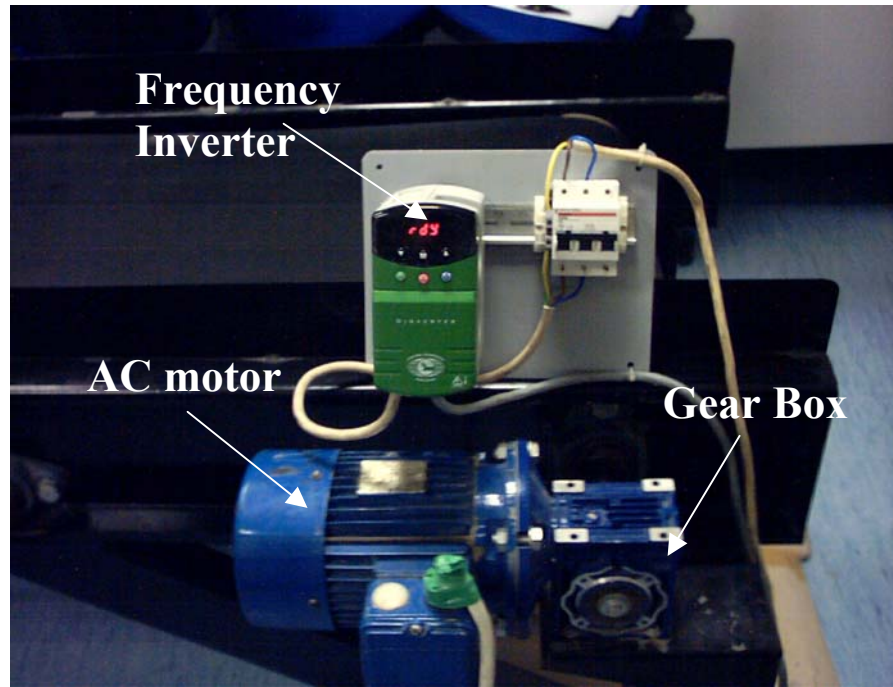


Figure 3-7 The Conveyor Belt Motor Driving System

3.2.2 Vision System

The fundamental task done by the vision system is grabbing frames via the CCD (Charged Coupled Device) camera interfaced to the host PC through the frame grabber to be processed and analyzed for color classification.

The hardware devices used in the vision systems are:

Computing Unit: Dell® personal computer Pentium 4 and 512 MB ram and uses Windows2000® operating system with service pack4. The acquisition and image processing analysis will be applied through Matlab® V.6.5 with the image processing and image acquisition toolbox to analyze the captured image.

Image acquisition setup: Composed of a Flashbus MV pro® frame grabber manufactured by Integral Technologies ® and Sony® XC999 CCD camera with a CMA999® RGB adapter.

Image acquisition toolbox in MATLAB was using Video for Windows (VFW) driver to communicate with the Flashbus frame grabber. The system was capable of capturing images at a maximum frame rate of 30 fps when the frame grabber is running at the on screen mode where the acquired image is transferred directly to the display memory directly without passing through the system memory. Capturing an image can be triggered by

- Timer
- Manual trigger through a single command.
- Hardware triggering by the falling or rising edge of the triggering signal.

In order to avoid extra hardware component in our system, we did not use the hardware triggering. Moreover, the bottles are not passing through the inspection chamber periodically therefore using a timer for triggering is meaningless. As a result, manual triggering method by a single command was implemented. To verify the capability of the image acquisition system, we measured the time period between each acquired frame for 100 consequential frames. As each frame is time stamped, Figure 3-8 illustrate the time stamp in terms of frame index.

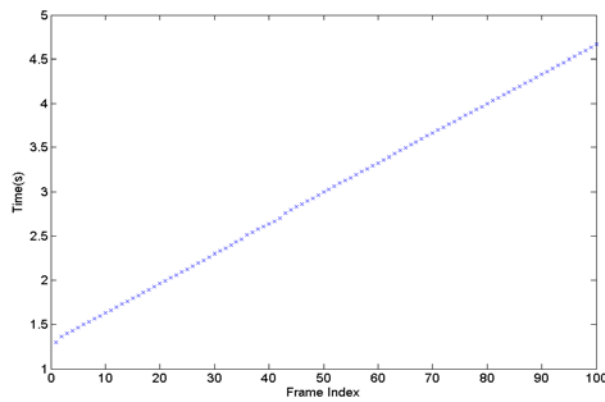


Figure 3-8 Frame Time Stamp in Terms of Frame Index

By calculating the difference time between two sequential frames we get the plot in Figure 3-9, and we found that the average period between the acquired frames over the 100 frames is: 0.0340 sec

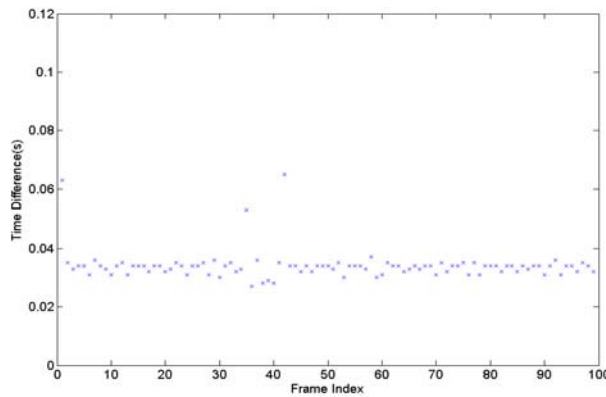


Figure 3-9 The Time Difference in Terms of Frame Index

Hence, the frame rate is: $1/0.0340 = 29.3943$ fps

The illumination system used for the prototype demonstration system consists of four 3U energy saving day light bulbs each of 11 watts. The bulbs are powered by 3-phase AC voltage at 230 Volts with respect to neutral. Each bulb is covered with a

layer of white paper to provide a uniform glare-free illumination. The lamps are angled downwards to avoid a direct light projection towards the CCD camera.

Plastic surface is extremely reflective and results in saturation of the CCD device in camera, reducing the information content in the image. To ensure uniform non-reflective illumination, an enclosure of steel sheets with black jute backing and black paint has been used. The illumination system helps in image acquisition by maintaining the proper level of brightness of the testing area. The illumination sources are placed by trial and error so as to minimize the reflection from the plastic bottle surface, which hampers the visual information of the digital image. Figure 3-10 is the photographic view of the conveyor.



Figure 3-10 A Photographic Image of the Automatic Color Sorting System

3.3 Preprocessing

Preprocessing operations are required to prepare the acquired imaged for performing the required measurements and data analysis required to extract the features and feed them to the classifiers. The preprocessing aims to reduce the noise and redundant data since acquiring an optimum-quality image is sometimes impractical due to imperfect detectors, inadequate illumination, illumination on irregular surface or other sources of noise.

However it is important to emphasize that these preprocessing operations are applied after the image has been digitized and stored, and therefore will be unable to deliver the optimum result that could have been achieved by applying some corrections in the acquisition process first.

In the context of designing preprocessing algorithms, it is important to list the potential difficulties and challenges in identifying the color of the plastic bottle to be addressed. One of the challenges is the detection of the plastic bottle, extracting it from the conveyor belt image and removing the blurring of a moving plastic bottle. Having different plastic bottle surfaces such as transparent or opaque will add more difficulties in the recognition of the plastic bottle. The color of the bottle can not be identified from an arbitrary area of the bottle image, since the existence of the label and the color of the cap should be ignored in the process of measuring the bottle color. The classification algorithm should be geometrically independent, which means that it can deal with the bottles coming in different orientations. The deformation of the plastic bottle surface causes some white dots to appear due to direct illumination, which reduce the accuracy of the direct color measurements. Also, for a waste recycling environment it is required by the machine vision software module to accommodate the possible environmental conditions such as light and conveyor belt contamination without affecting the performance of the classification. Although, for many of the problems listed above, there are several solutions which are available, but the real time constraints of this application and the throughput requirements add lots of restrictions on the algorithms used to address these problems. In the following sections, each of the listed problems above has been considered by one or more preprocessing steps.

3.3.1 Image Resizing

Interlacing is the process of sending the video data in two separate portions called fields. The odd numbered video lines are transferred first, followed by the even-numbered video lines, see Figure 3-11. Taking an image of a moving object using an interlaced video data will result in a blurred image since the two fields are not in alignment with each other. Since an interlaced camera (Sony XC999) has been used, running at a frame rate of 30 fps, there is a time difference of 20 milliseconds between the two fields that make up a complete interlaced frame (Provided that the speed of the shutter is 50 fps). During this time the conveyor moves by 20 millimeters (If the speed was 1m/sec), which is a considerable amount. This results in a blurred image, in order to remove the blur, the interlaced lines are removed. Thus odd lines will survive, while the even lines will be omitted from the acquired image.

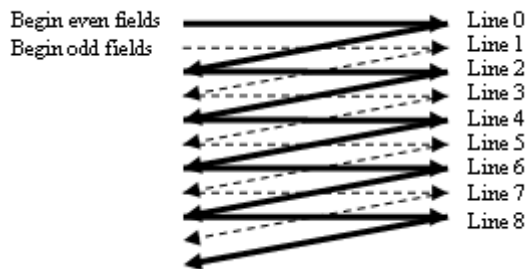


Figure 3-11 Interlaced Video Scanning

This procedure is applied also for the columns of the image in order to preserve the dimension ratios of the image. This procedure of minimizing the image by removing even lines and columns has two main benefits:

- Reducing the blurring effect of the acquired image of moving object.
- Minimize the computation load of the system. Since the deleted horizontal lines are redundant and can be removed.

Figure 3-12 shows the effect of blurring and some flickers on the acquired image of a moving bottle at the speed of 1m/sec and the image after removing even lines and columns.



Figure 3-12 The Effect of Interlaced Camera and Removing the Odd Lines and Columns of the Image

A white box appears at the right side of the image, this box was mounted on the wall of the inspection box, for two main reasons:

- Provide part of the image that is separated from the recycling process and can be used as a reference to monitor the illumination of the inspection area.
- To reduce the effect of the automatic white balancing function in the CCD image which scales the pixels value according to the overall brightness of the image and this can affect the color reading accuracy.

3.3.2 Background Foreground Segmentation

It is very important at the beginning of processing the acquired image to isolate the detected bottle from the background that is the conveyor belt. This operation will minimize the amount of pixels data to be processed. The accuracy of this operation is very critical for the results of the following processing operations. Many techniques have been examined, each has its advantages and disadvantages as we consider some of the challenges in this process such as light variation, belt contamination, real time process requirements... etc.

Region growing method

Since the background of the captured image tends to have a single color which is the black color, while the object (plastic bottle) has other colors, it is possible to perform the segmentation based on region growing method where the pixels of image are successively grouped together to form larger regions based on their intensity or other suitable properties such as color or saturation. Some rules should be provided

for not merging adjacent pixels that differ too much in intensity, while allowing for merging for which the intensity changes gradually because of the illumination variation over the background.

Obvious problems for such methods are noise and sharp edges and lines that form disconnected boundaries where it is difficult to formulate a criterion that can decide whether they form true region boundaries. In addition, region-growing algorithms usually operate iteratively and a pixel may be examined many times and as a result the process tends to be quite computationally intensive. For this reason it is not considered in real time applications.

Thresholding based Segmentation

Thresholding the image based on the intensity values is one of the easiest ways to perform the foreground – background segmentation, knowing that the dark pixels have low absolute values and the bright (white) pixels have high absolute values. In our application, non-uniformly distributed lighting or even potential contamination on the black conveyor belt can cause a real difficulty in applying a fixed thresholding technique based on a global threshold level. In the following text we will show this difficulty in the case of non-uniform lighting. Without loosing generality, the same result can be expected from contaminated belt.

The light spots appear in the background image, and they appear also in bottle images as shown in Figure 3-13. It is not possible to extract the bottle image from the background using global thresholding using the grey value histogram as shown in Figure 3-14, due to the overlap between the light spot pixel values and bottle pixel values in the intensity histogram.



Figure 3-13 Bottle Image before Processing

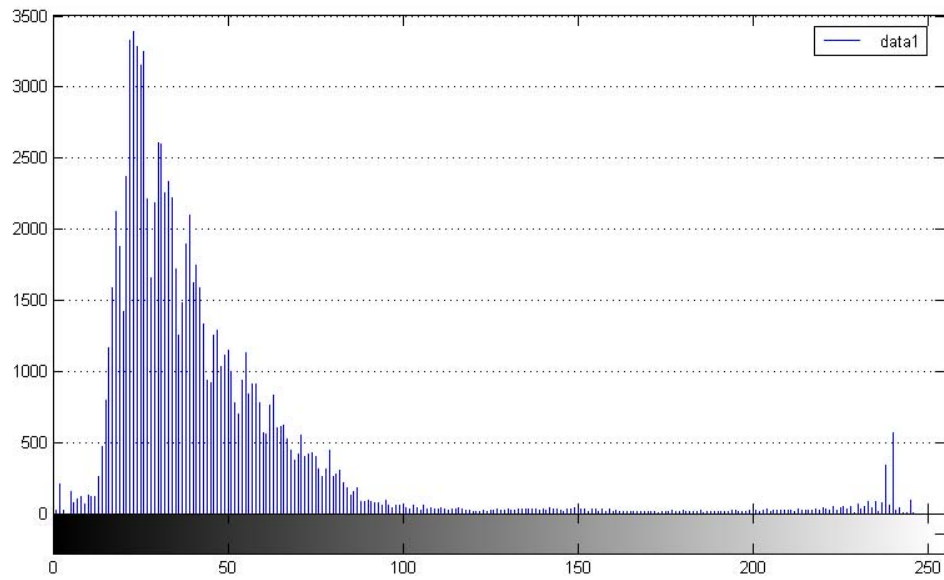


Figure 3-14 Gray Value Histogram

Figure 3-15 shows thresholding at 50, 75, 100 of the gray value image. It is clear that the normal thresholding is not successful and if the spots are left at the background it will be segmented in the segmentation level and will be recognized as an individual object.

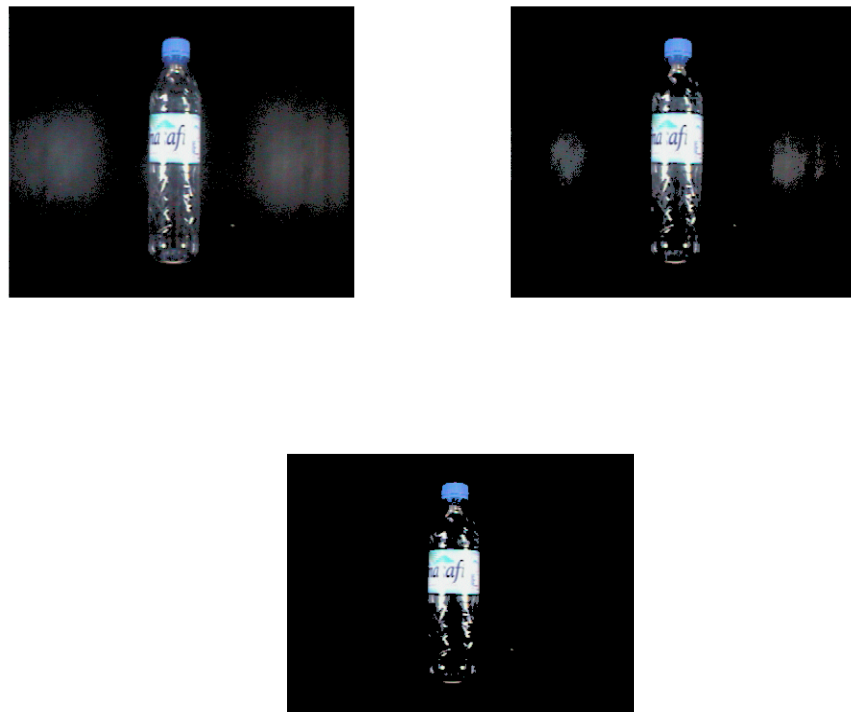


Figure 3-15 Threshold at Different Levels (a) Threshold at 50. (b) Threshold at 75.
(c) Threshold at 100

It is clear that using global thresholding alone is not efficient but it was found that using it after other segmenting operation is much more useful as can be found in the following methods.

Tophat Segmentation

The top hat transformation is used as a simple tool for segmenting objects in gray-scale images that differ in brightness from the background, even when the background is of uneven gray-scale. Therefore, trying this method is worthwhile. Assume a gray-level image I and a structuring element K . The residue of opening as compared to original image $I - (I \circ K)$ constitutes a new useful operation called a top hat transformation. The top hat transformation is a good tool for extracting light objects (or, conversely, dark ones, of course) on a dark (or light) but slowly changing background. Those parts of the image that cannot fit into structuring element K are removed by opening. Subtracting the opened image from the original provides an image where removed objects stand out clearly. The actual segmentation can be by simple thresholding. The origin of the name is from the fact that, an image were a hat, the transformation would extract only the top of it, provided that the structuring element is large than the hole in the hat.

Using the morphological operations on the bottle image Figure 3-16, the following steps illustrate the Tophat procedure:

- Transform the colored image to gray level image.
- Choose a structure element (Disk shape with radius = 5)
- Open the gray level image using the structure element.
- Subtract the result the original image. See Figure 3-17.
- Threshold the image at the same value (25). See Figure 3-18.

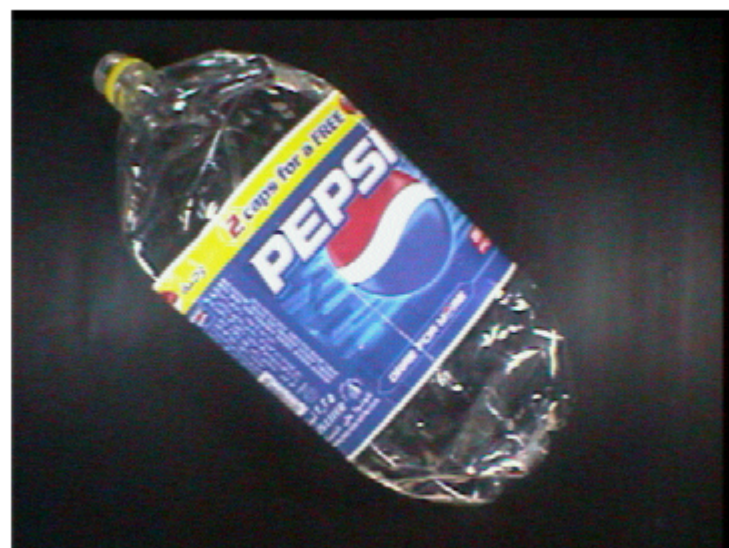


Figure 3-16 Captured Plastic Bottle Image

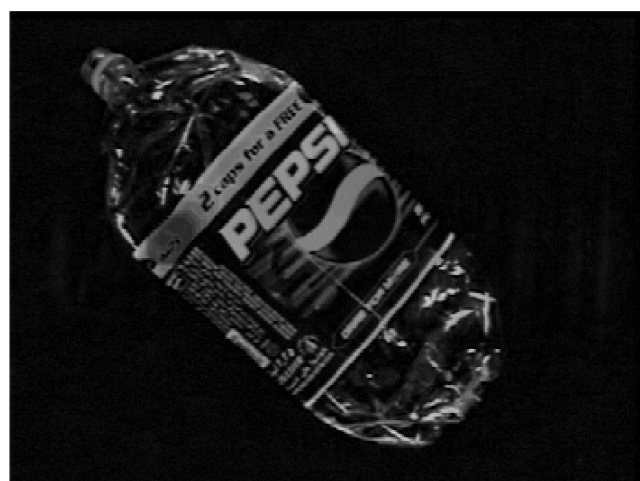


Figure 3-17 Gray Level Image after Tophat Transform



Figure 3-18 Thresholded Image after Tophat Transform

This method showed good results but it was a time consuming operation. The special advantage of this method that it does not require a reference image, and thus results in less memory needed to save this image, and it is robust in slight lighting variation and contamination on the conveyor belt.

Background Subtraction

Background subtraction is widely used as the basis for moving object extraction from stationary background in image sequences. This is done by comparing the captured image with an estimated reference (background) image by subtracting them and looking for large absolute values in the result. The estimated reference image can be fixed by using a reference image generated by averaging multiple samples of reference images or adaptive referencing as explained in Figure 3-19.

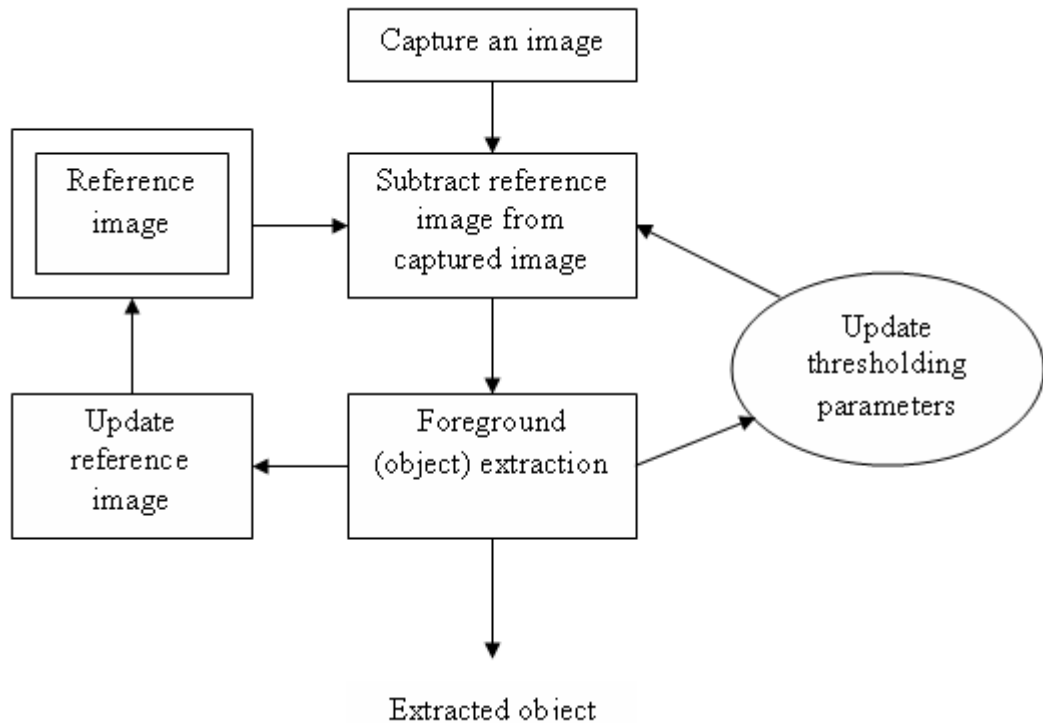


Figure 3-19 Background Subtraction Algorithm

In our application where the background is the conveyor belt, a single fixed reference image can be generated by averaging the conveyor belt images at different places along the conveyor belt that cover the whole length of it. In this case, the comparison between the captured image and the reference can be done at any place of the conveyor belt, while using an adaptive reference, multiple images of the conveyor belt will be taken and it requires the camera to work asynchronously using marks at different place of the conveyor belt. This method will be explained in details in section 3.4.2 since this method was used in our prototype system.

3.3.3 Object Orientation

Finding the orientation of the plastic bottle in order to rotate it to its vertical position can simplify the analysis process since the label for most of the plastic bottles can be found at the middle bottle body therefore the color at the bottom and upper part of the plastic bottle is most probably color of bottle itself. However, obtaining the bottle orientation can be done by several methods that are performed on the binary

image in order to minimize the computation load, some methods examined are listed below.

Morphological algorithms, thinning technique

Thinning operation is one of the morphological algorithms applied on a binary image A by hit or miss transform using a structural element B:

$$A \otimes B = A - (A \otimes B) = A \cap (A \otimes B)^c$$

For thinning A symmetrically, a sequence of rotated version of B is used:

$\{B\} = \{B^1, B^2, B^3, \dots, B^n\}$ where B^i is a rotated version of B^{i-1} . Using this concept, we now define thinning by a sequence of structuring elements as:

$A \otimes \{B\} = ((\dots((A \otimes B^1) \otimes B^2) \dots) \otimes B^n)$, this process is continued until no change occurs in any of the structural element sets.

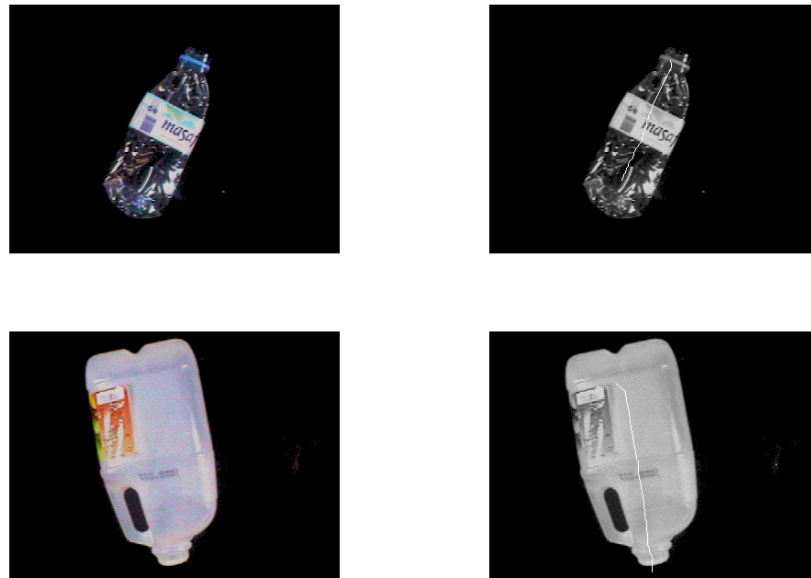


Figure 3-20 Examples of Using Thinning Algorithm to Find the Bottle Orientation

As we can see in Figure 3-20, a one pixel thin line is superimposed over the bottle image which is the result of the thinning process on the binary image of bottle. The direction of this line is approximately the direction of the bottle.

The problem of this algorithm is that it requires the binary image of the bottle to be filled without any holes, so it requires more filtering and filling stages before applying this algorithm.

Search for the least width of the bounding box

Another technique that was examined is to rotate the image searching for the minimum width of the box that is bounding the bottle. Of course this operation, as in the previous one, works on the binary image in order to save time and memory resources of the system. It is obvious that if we rotate the bottle by 180 degrees (1 degree at a time) the vertical position must exist at one of these 180 positions. If we tried to measure the width of the bounding box at each position we will end up with a signal that is similar to a sinusoidal signal as it is shown in Figure 3-21. However, this signal is bottle shape dependant and its maximum is corresponding to the horizontal position of the bottle while the minimum is corresponding to the vertical position.

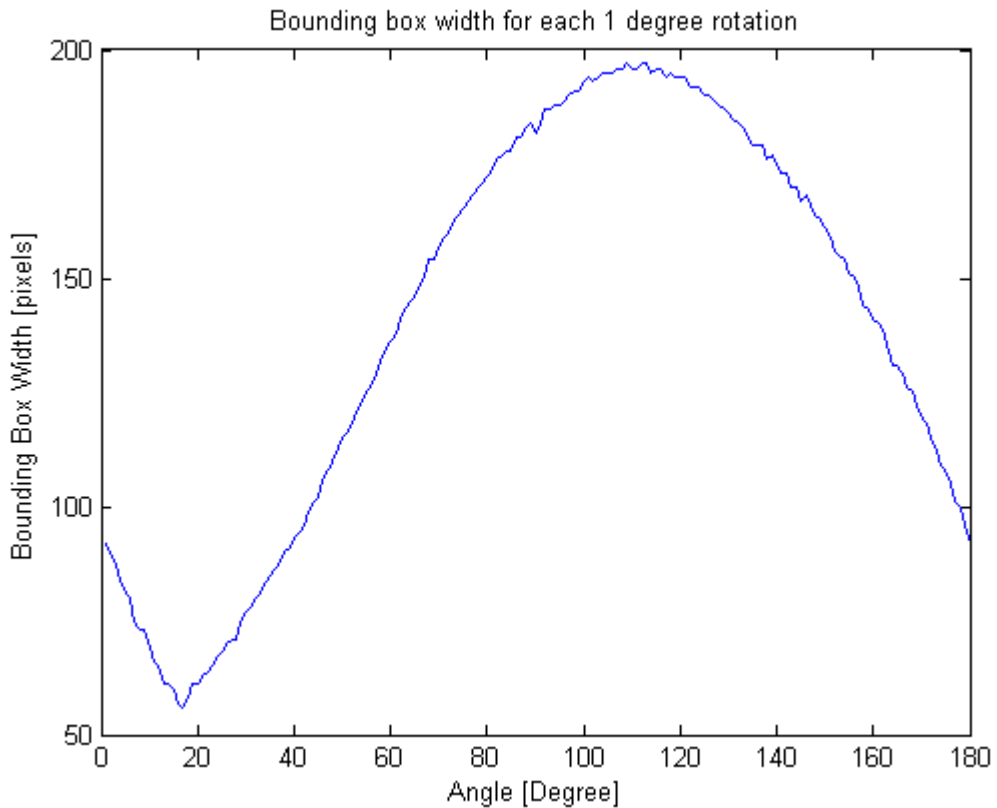


Figure 3-21 Bounding Box Width in Terms of Rotation Angle

As a result, the problem can be described as searching for a global minimum for a function. It is not practical to go through the whole 180 positions, recording the width at each position and then find the position at which the minimum width exists, this will be very time consuming. One way to address such a problem is similar to

gradient descent algorithm in the sense that it is measuring the slope of each position and jump adaptively.

First we measure the current width W of the bounding box, and then find an indication of the slope by measuring the width of the bounding box if the image were rotated by a step of 80 degree clockwise (WL) or counterclockwise (WR). If one of these two positions provided smaller width the image will be rotated to this position, otherwise the image position will not change. Then the next rotation step will be divided by 2 and the same procedure will be iterated until the updated step becomes less than 5 degrees which is the maximum acceptable error we chose. Figure 3-22 shows the algorithm stages to orient the plastic bottle image, and Figure 3-23 is the flowchart of this algorithm.

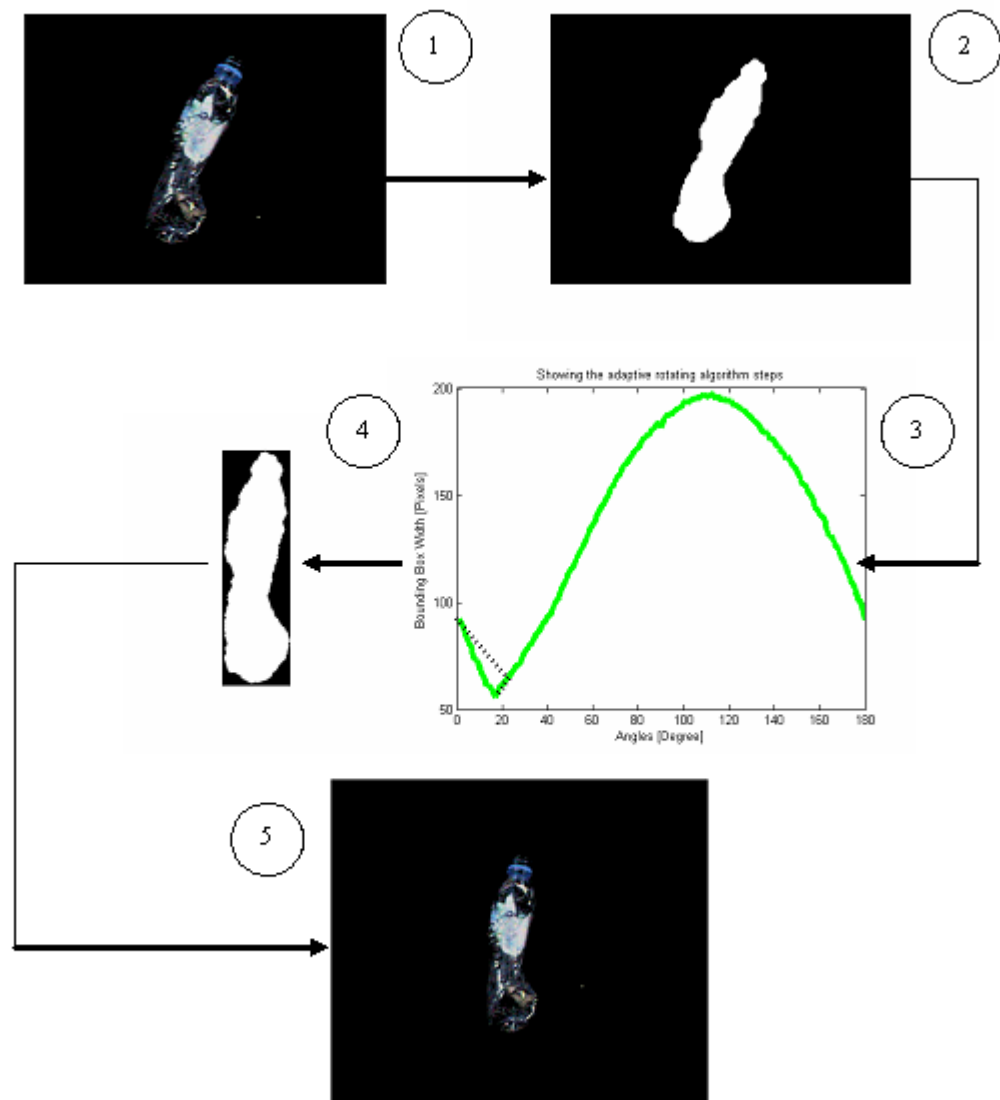


Figure 3-22 Bounding Box Algorithm to Determine the Bottle Orientation

- 1- The original image of a bottle after removing the background.
- 2- The binary image of the bottle after thresholding and preprocessing.
- 3- Applying adaptive rotation
- 4- The bounding box at the detected vertical position.
- 5- The bottle image after rotation.

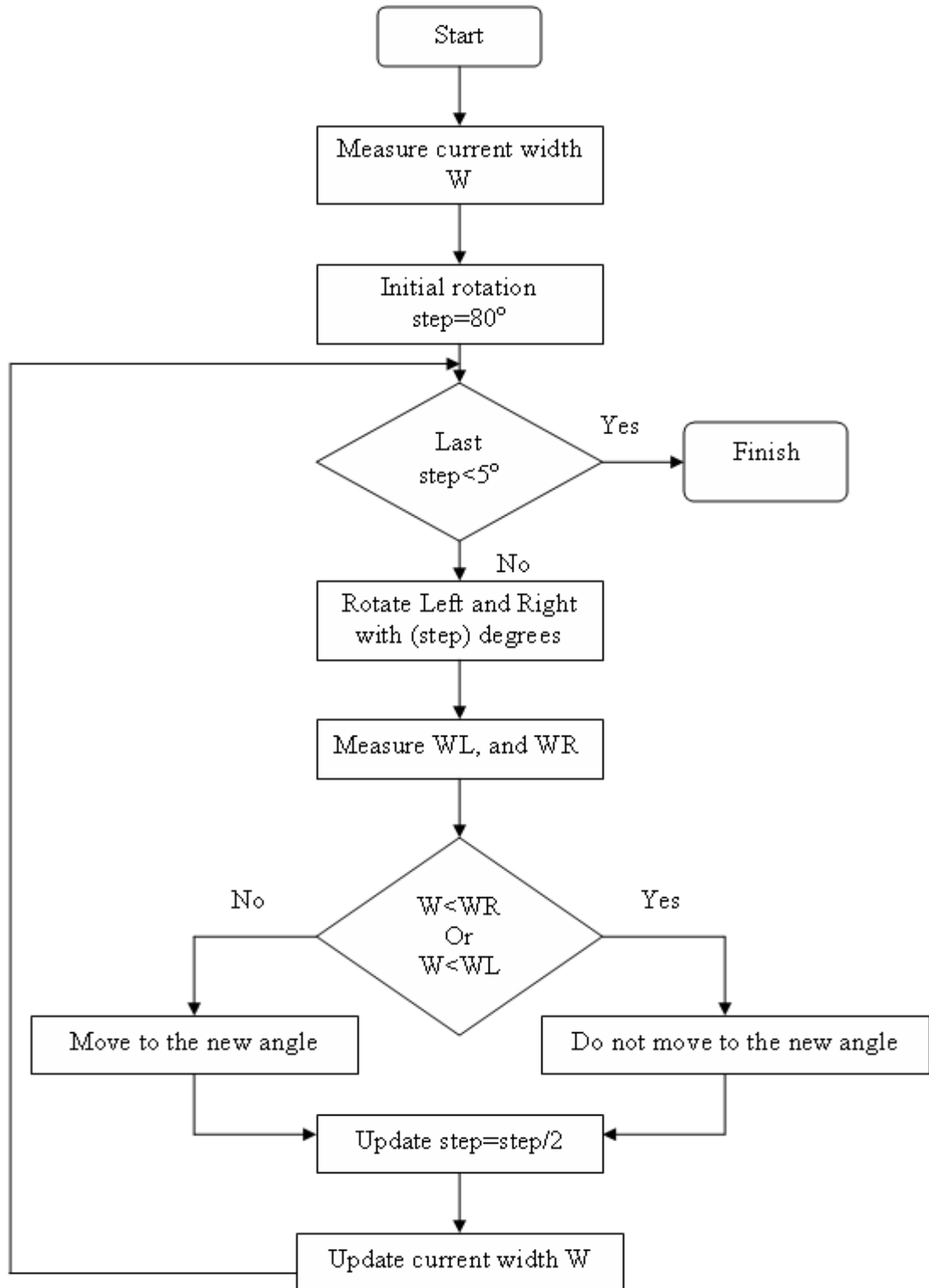


Figure 3-23 Flowchart of the Bounding Box Width Algorithm for Plastic Bottle Orientation
 Principal component analysis method

While the principal component analysis is widely used for dimensionality reduction and data compression, it is also used for principal axis detection of a set of data [54].

In PCA, a set S of N points or feature vectors in a two dimensional space represented by the XY coordinates of the white pixels (foreground pixels) in the binary image can be projected into an equivalent dimensional space, where the components of the transformed vectors are aimed to be uncorrelated, in other words, the scatter matrix of the vectors is diagonalized. The first of these components provide the greatest variance from the d components (which will be interpreted later as the orientation of the data in the feature space), and the second component provide the second greatest variance and it will be orthogonal on the first component.

As a result, principal component transformation can be considered as a translation and a pure rotation. In two dimensional space, let X be a set of points of an object in coordinate system x. Now first the origin of x is translated to the center of mass of the object and the coordinate system x is rotated by angle θ to a new coordinate system y, the transform matrix C is given by:

$$C = \begin{bmatrix} \cos \theta & \sin \theta \\ -\sin \theta & \cos \theta \end{bmatrix} = \begin{bmatrix} C_1 \\ C_2 \end{bmatrix} \quad (3.4)$$

Then, the new set Y of the points in coordinate system y is expressed by:

$$Y = C(X - \bar{X}) = \begin{bmatrix} C_1 \\ C_2 \end{bmatrix} [X - \bar{X}] = \begin{bmatrix} Y^1 \\ Y^2 \end{bmatrix} \quad (3.5)$$

So,

$$Y^i = C_i[X_1 - \bar{X} \quad X_2 - \bar{X} \quad \dots \quad X_N - \bar{X}] \quad (3.6)$$

We require that the first component Y^1 is the principal component of X, and the vector C_1 is the principal axis of X. If X is transformed to Y by the principal component transformation, the transform matrix C is:

$$C = \begin{bmatrix} c_{11} & c_{12} \\ c_{21} & c_{22} \end{bmatrix} = \begin{bmatrix} C_1 \\ C_2 \end{bmatrix} \quad (3.7)$$

Therefore, the two transformation matrices should be equal, which means:

$$\begin{bmatrix} \cos\theta & \sin\theta \\ -\sin\theta & \cos\theta \end{bmatrix} = \begin{bmatrix} c_{11} & c_{12} \\ c_{21} & c_{22} \end{bmatrix} \quad (3.8)$$

Thus, the angle θ of the principal axis is:

$$\theta = \arccos c_{11} \quad \text{or} \quad \theta = \arctan \left(\frac{c_{12}}{c_{11}} \right) \quad (3.9)$$

Because the length of the principal axis reflects the longest diagonal of the object, the direction θ of the principal axis is taken as the orientation of the object.

In order to optimize the time required for computing the angle using this method, it is sufficient to take the points of the boundary of the object rather than taking the points of all foreground pixels in the binary image. This will reduce drastically the execution time required for this method.

The procedures of orientation analysis by Principal Component transformation can be summarized as follows:

- Step1. Calculating the scatter matrix A of the set of the boundary points X of an object.
- Step2. Solving the characteristic equation of A to find the eigenvalues λ_i and arranging them in a descending order.
- Step3. Finding the eigenvectors C_i by equation (3.7), and pick up C_1 corresponding to λ_1 .
- Step4. Calculating the orientation θ of the object according to equations (3.9).
- Step5. Rotating the bottle image by an angle equal to $180 - \theta$.

Figure 3-24 shows some binary images of plastic bottles before and after applying the rotation algorithm.

Before Rotation



After Rotation



Figure 3-24 Examples of Bottle Binary Image Rotation

3.4 The Applied Methodology

The following is algorithm used in the automatic plastic bottle color sorting system. The main idea in this algorithm is to read the color from top and bottom parts of the plastic bottles since these parts are mostly not covered by labels and they have the real color of the plastic bottle. In order to extract these part from the bottle image easily, the bottle must be oriented into the vertical position and then a certain area from the top and bottom parts of the bounding box of the bottle image will be cropped. Using this method was found to be faster than other techniques such as morphological algorithms, and it is proper for such real time applications. Moreover, background subtraction was used to isolate the bottle from the conveyor belt image; therefore, a bank of conveyor belt images is created at the beginning of running the system to be used later in the program. This method will minimize the filtering operations and morphological algorithms used to clean up the image after background subtraction. In fact, a particular thresholding method was good enough to do the isolation in order to speed up the process at an acceptable cost of accuracy and the resulting binary image can be used later in other functions such as bottle orienting since dealing with binary values is much faster than integer values in the thresholded image. Another important advantage of using the background subtraction algorithm is that it provides a chance to have adaptive system to accommodate the variations in the lighting and conveyor belt contaminations. Figure 3-25 is the flowchart of the whole program with its sub functions. Using sub functions is preferable than writing a one complete program since it is consuming much smaller size of the memory for the program and the variables used in the program.

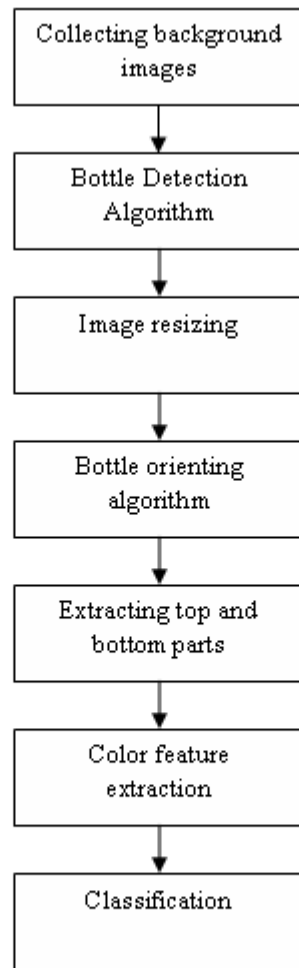


Figure 3-25 Flowchart of the Complete Software Classification Module

3.4.1 Collecting the Background Images

Background image collection is performed at multiple equally spaced places in the conveyor belt in order to cover the whole conveyor belt. These places must not be overlapped or disconnected and each is marked by a label pasted at the edge of the conveyor belt. While the conveyor is running, the program is acquiring images at the rate of 30 frame/sec and checking only a small area in the image. When the label passes by this area, the program will be triggered to save this acquired picture in the background image bank, this detection of the label is performed by calculating the summation of the pixel values at an area of 5x10 pixels only and comparing the result with a specified threshold. Triggering is performed at the falling edge of the signal or in other words, when the label leaves the inspection area in the image. Triggering at

the falling edge will enhance the accuracy of position taken for each part of conveyor belt. Each acquired background image in the bank is numbered as per the order at which the label passes by. After collecting all the required number of images the function will release the bank of stored images to be used by next function “Bottle detection algorithm” for background subtraction.

3.4.2 Bottle Detection Algorithm

The purpose of this function is to output a thresholded image of the detected plastic bottle. First, it will wait for a label in the conveyor belt. Once the label is detected, a background image subtraction and thresholding will be performed and the resulting image will be examined to verify the existence of a plastic bottle or not, this is done by checking 10 equally spaced horizontal lines in the image. There are three possible cases represented by a flag value in this function:

- Flag=0: No bottle exists in the image, and the function will return back waiting for the next label.
- Flag=1: A complete bottle appears in the image, and this thresholded image can be released to the next processing stages.
- Flag=2: Part of the plastic bottle appears at the top of the image, and this case can be verified by checking the top horizontal line in the thresholded image. In this case, the function will wait for the following image and combine the two images vertically and then crop the best image in the size of one image (270x360 pixels) that can fit the bottle.

The following flowchart in Figure 3-26 will explain the bottle detection function.

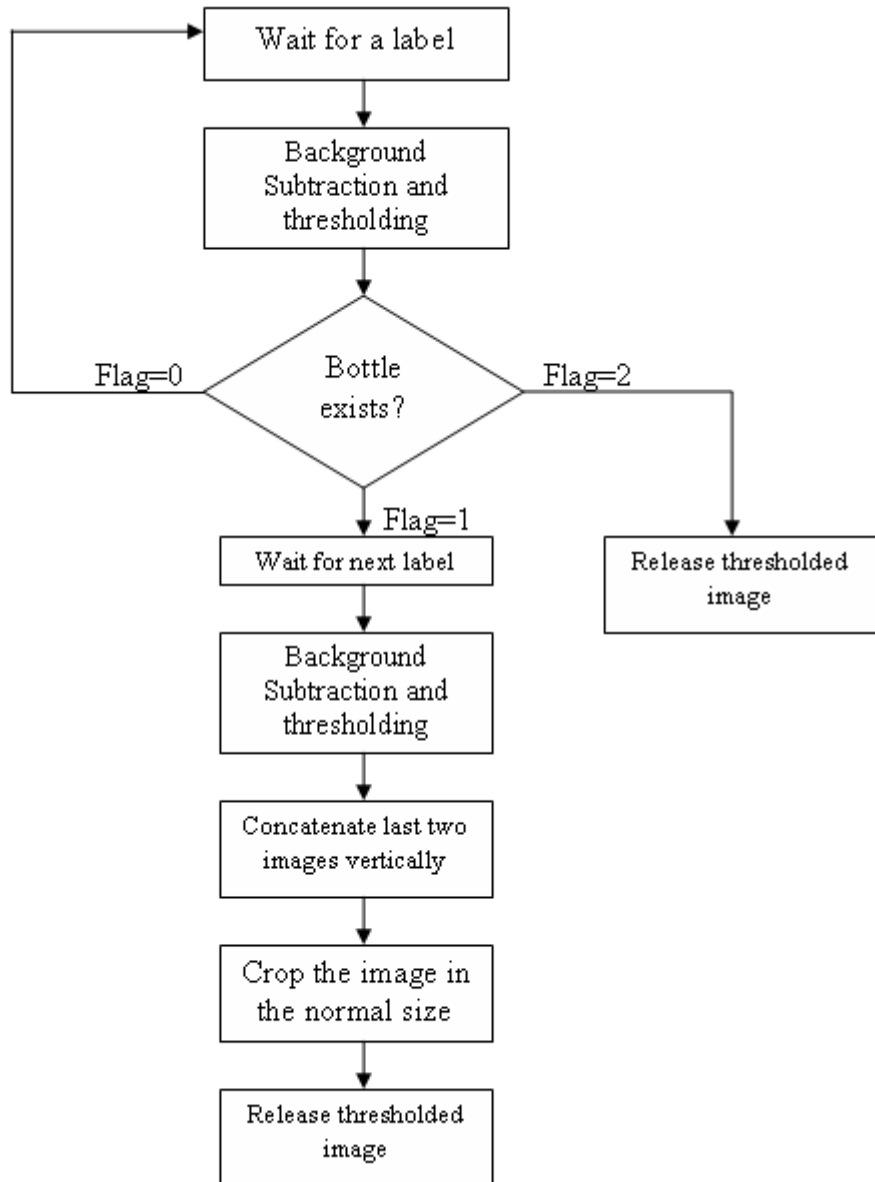


Figure 3-26 Flowchart of the Bottle Detection Algorithm

3.4.3 Image Resizing

As explained before, this step is performed by removing the odd numbered horizontal and vertical lines in order to remove the flickering and blurring effect in the image of moving plastic bottle. Moreover, this will reduce the amount of redundant information by 75% and therefore will reduce the computation time required in the following steps

3.4.4 Bottle Orientation Algorithm

This function will orient the plastic bottle image to its vertical position using principal component analysis method by finding the principal axes of the image as explained before. The following steps are performed in this function:

- 1- Creating a matrix $M=[X, Y]$, where X and Y are vectors which represent the coordinates of the boundary of the binary image.
- 2- Removing the mean from X and Y and find $Mm= [(X-\text{mean}(X)) , (Y-\text{mean}(Y))]$.
- 3- Finding A the scatter matrix of M. $A=\frac{1}{m-1}(Mm \times Mm^T)$
- 4- Finding the eigenvectors and values of A and sorting them in a descending order.
- 5- Finding the eigenvectors and picking up C_1 that corresponds to the maximum eigenvalue.
- 6- Calculating the orientation angle by equation (3.9).
- 7- Rotating the thresholded image by $180-\theta$.

3.4.5 Extracting the Top and Bottom Parts of the Bottle

Here the function will take the thresholded image after orienting and find the bounding box of the bottle then extract the top and bottom quarter of it. In order to distinguish which one is top part of the bottle since the orienting does not guarantee to bring the top part of the bottle upwards, the black pixels in both parts are counted. The top part is simply the one that has more black pixels, since the cap of the bottle will allow for more background pixels to appear, while the bottom part is flat and can have less background pixels in its neighborhood. Distinguishing the top from bottom parts is required since more weight is given for the bottom part color feature rather than the top part.

3.4.6 Color Features Extraction

This function receives the top and bottom parts and transforms them from RGB color space to HSV color space. Each part is divided into 5 equal parts of the same width of the original part, and division will provide the mean and standard

deviation of its Hue and saturation layers values. Therefore, the feature vector is of 4 dimensions, and since we have 5 divisions in both the top and bottom parts of the bottle (10 divisions in total) therefore we will get from the bottle a 10×4 feature matrix, each line will be classified individually and the resulting class will be the class that is voted more by the classifier. See Figure 3-27

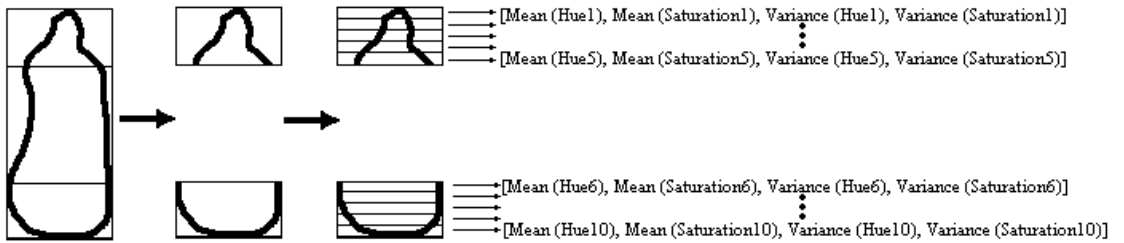


Figure 3-27 Color Feature Extraction for a Plastic Bottle Image

The following figures represent the feature space of Clear and Opaque bottle categories. Figure 3-28 shows the feature space using the hue mean value and saturation mean value, while Figure 3-29 shows the feature space using the hue standard deviation value and saturation standard deviation value. The wide spread of each color in this feature space that uses the standard deviation is due to some faulty colors obtained from some division lines due to the appearance of part of the label of the bottle at bottom image part or due to different cap color in the top image part where we can see that some faulty noisy lines.

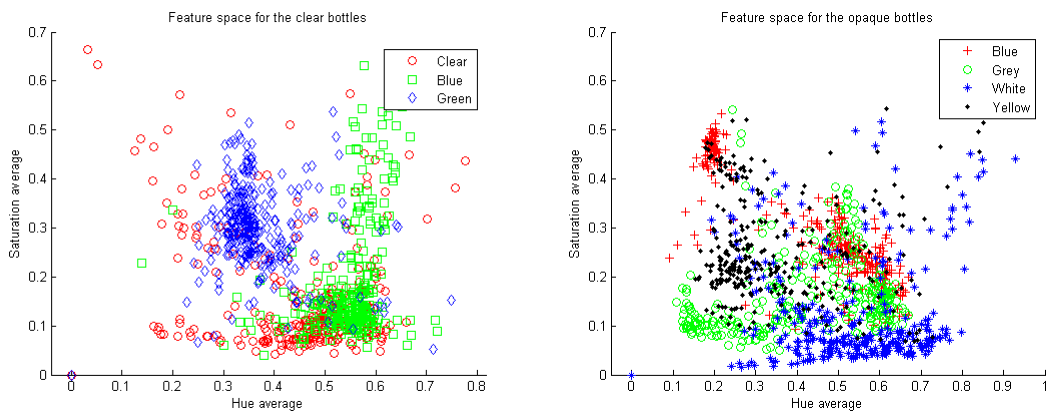


Figure 3-28 Feature Space Plotted for the Hue and Saturation Average

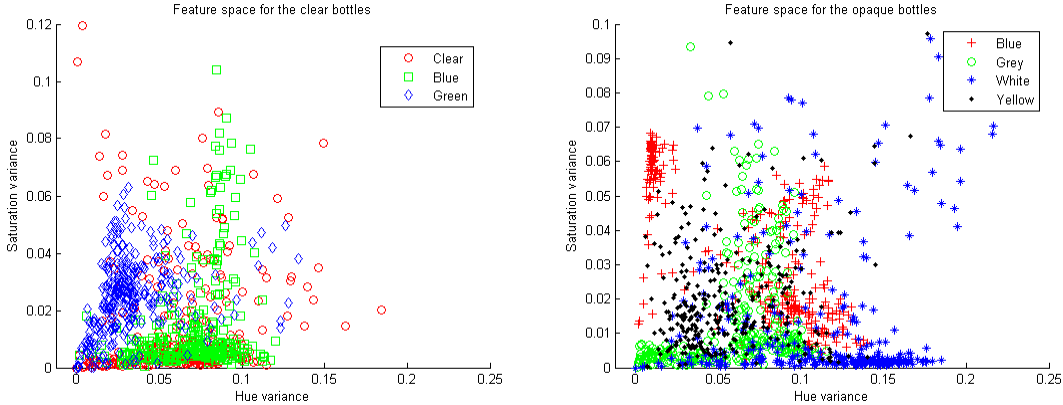


Figure 3-29 Feature Space Plotted for the Hue and Saturation Variance

3.4.7 Classification

By testing the five different classifiers, it has been found that the quadratic and tree classifiers were the only classifiers that provide acceptable results. However, the classifier performance differs from one color to the other. To go around this problem, a classifier fusion is proposed at which the decisions of both classifiers (Quadratic and Tree) are taken into consideration in order to come up with the classification result.

Since 10 feature vectors were extracted from the top and bottom part images. Each vector is classified individually by the classifier; therefore each bottle will have 10 possible classification results which are counted then to find the class that appeared the most. In other words, the classifier will vote 10 times for the possible classes (colors), the final class is the one that wins the maximum number of votes.

As mentioned before, quadratic and tree classifiers differ in their performances between different classes (colors). Therefore, the proposed methodology is to allow both of them to work in parallel then add the votes for each class coming from quadratic classifier with the votes for each class coming from tree classifier as shown in Figure 3-30. This will enhance the performance in two ways:

- The classifier that shows more confidence in its results by giving more than 8 (for example) votes out of 10 to a certain class will appear in the fusion output.
- If both classifiers did not show a confident result, the fusion output will be the common class that was voted with a fair number of votes from both classifiers.

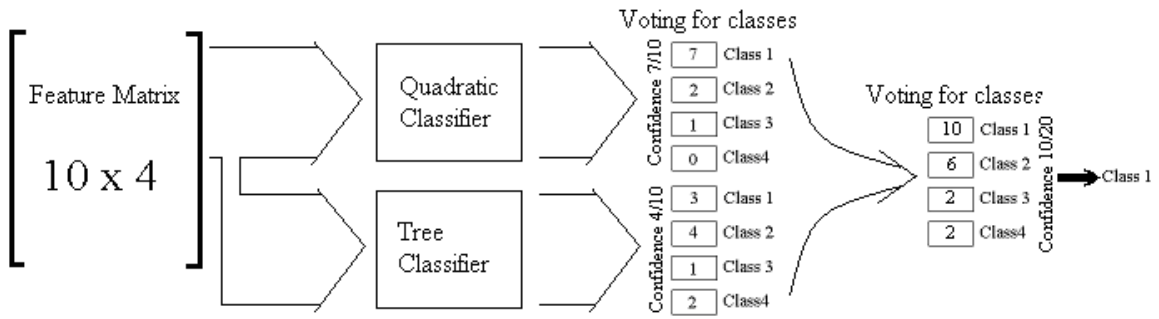


Figure 3-30 Classifier Fusion

Figure 3-30 illustrates that quadratic classifier showed more confidence about its classification than tree classifier. Assuming that class 1 is the correct classification. The fusion result will reflect the confidence of the quadratic classifier and overcome the misclassification in tree classifier.

The following Table 3-1 shows the results taken for 30 testing samples and 30 training samples for each class.

Table 3-1 The Color Classifier Accuracy for Clear Bottles

	Clear (no color)	Clear Blue	Clear Green	Total
Quadratic	83.33%	86.67%	93.33%	87.78%
Tree	86.67%	63.33%	100%	83.33%
Fusion	90.00%	86.67%	100%	92%

The results reflect the benefit of fusing the quadratic classifier and decision tree classifier to enhance the accuracy of system as in the case of the clear (no color) or at least scores the maximum accuracy obtained from one of the two fused classifiers. The low performance in the blue bottles using the decision tree can be related to the overtraining.

The decision boundaries can be shown in the Figures 3-31, 3-32.

Below are the decision boundaries of the quadratic and tree classifiers after training.

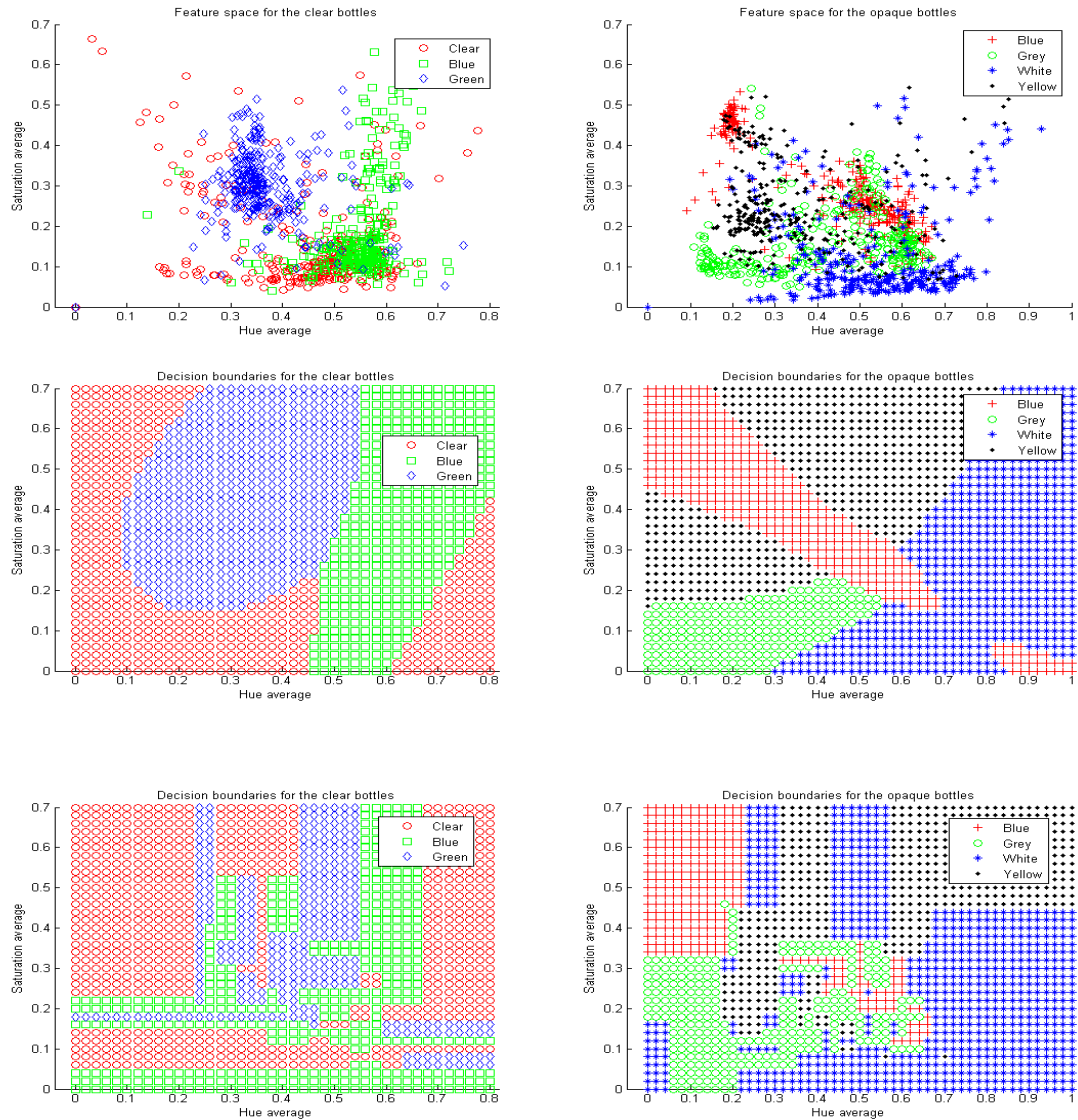


Figure 3-31 Decision Boundaries of the Quadratic and Tree Classifiers for Hue and Saturation Averages

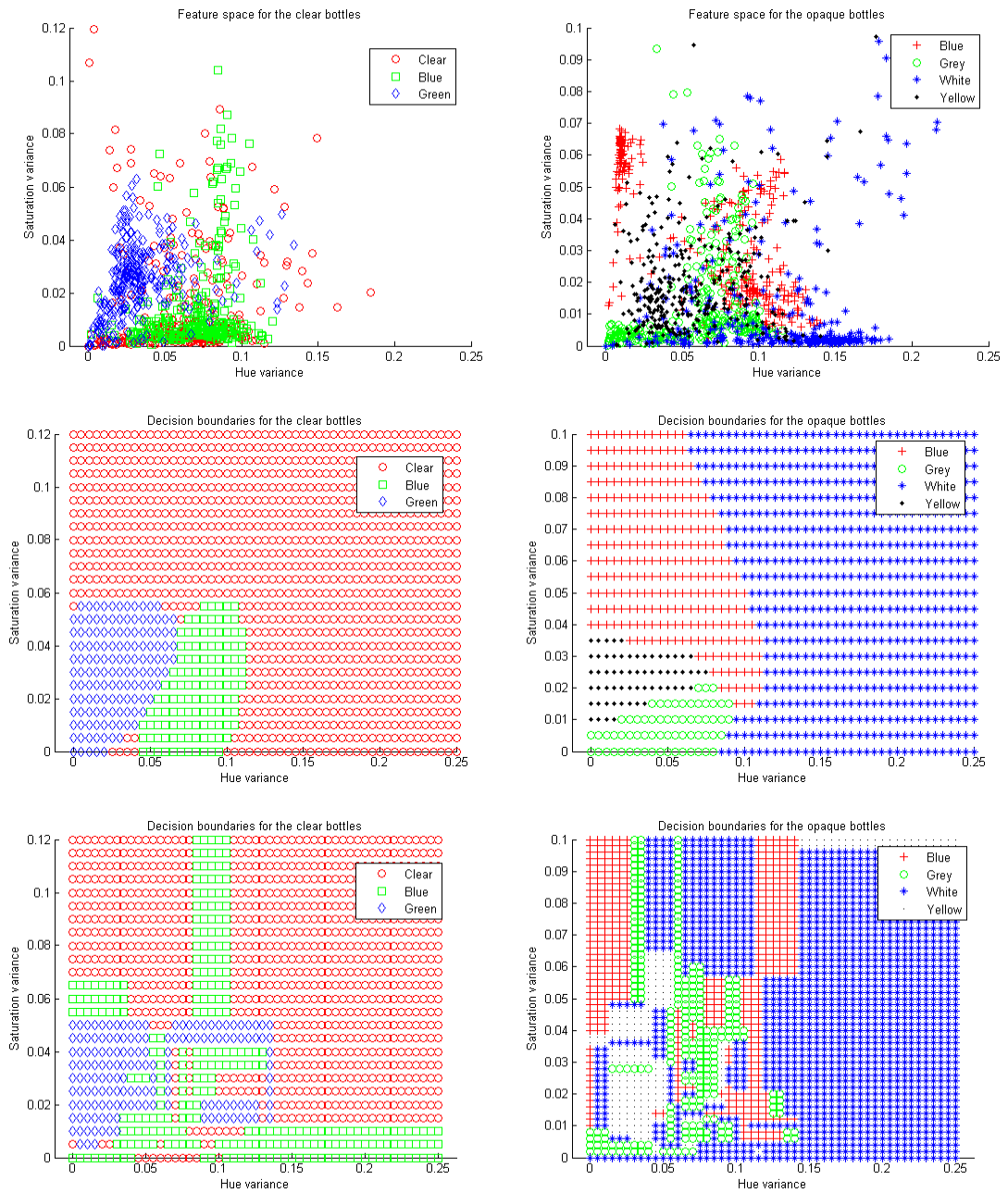


Figure 3-32 Decision Boundaries of the Quadratic and Tree Classifiers for Hue and Saturation Variance

However the fusion was successful in bringing the classification decision of the most confident classifier where the confidence is measured by the ratio of number of votes from the winning class over the total number of votes. Table 3-2 lists the classification accuracy for opaque bottles.

Table 3-2 The Color Classifier Accuracy for Opaque Bottles

	Blue	Grey	White	Yellow	Total
Quadratic	90.00%	100%	66.67%	80.00%	84.17%
Tree	86.67%	100%	96.67%	93.33%	94.17%
Fusion	93.33%	100%	96.67%	93.99%	96%

We had better performance in the opaque bottles because the standard deviation features are less noisy since the opaque bottles are less shiny and the appearance of white luminance dots is less than in the clear bottles. Hence the performance of the feature vector in providing better separability is increased.

Figure 3-33 shows some plastic bottle samples that have been fed to the color sorting system, and the consequent voting results.

	Opaque Sample	Clear Sample																																				
Thresholded Image																																						
Bottle image after Orientation																																						
Extracted top part																																						
Extracted bottom part																																						
Class voting Table	<table border="1"> <thead> <tr> <th></th> <th>Blue</th> <th>Grey</th> <th>White</th> <th>Yellow</th> </tr> </thead> <tbody> <tr> <td>Quadratic</td> <td>2</td> <td>0</td> <td>8</td> <td>0</td> </tr> <tr> <td>Tree</td> <td>1</td> <td>0</td> <td>9</td> <td>0</td> </tr> <tr> <td>Fusion</td> <td>3</td> <td>0</td> <td>17</td> <td>0</td> </tr> </tbody> </table>		Blue	Grey	White	Yellow	Quadratic	2	0	8	0	Tree	1	0	9	0	Fusion	3	0	17	0	<table border="1"> <thead> <tr> <th></th> <th>Clear</th> <th>Blue</th> <th>Green</th> </tr> </thead> <tbody> <tr> <td>Quadratic</td> <td>2</td> <td>7</td> <td>1</td> </tr> <tr> <td>Tree</td> <td>3</td> <td>4</td> <td>3</td> </tr> <tr> <td>Fusion</td> <td>5</td> <td>11</td> <td>4</td> </tr> </tbody> </table>		Clear	Blue	Green	Quadratic	2	7	1	Tree	3	4	3	Fusion	5	11	4
	Blue	Grey	White	Yellow																																		
Quadratic	2	0	8	0																																		
Tree	1	0	9	0																																		
Fusion	3	0	17	0																																		
	Clear	Blue	Green																																			
Quadratic	2	7	1																																			
Tree	3	4	3																																			
Fusion	5	11	4																																			

Figure 3-33 Image Processing Procedures for Bottles Fitted in a Single Frame

The low performance of the tree classifier to classify blue clear bottles is shown in this Table. The decision of the tree classifier has a confidence equivalent to only 4/10 which is much less than the confidence shown with the quadratic classifier 7/10. Hence, the fusion was able to bring out the correct decision of the quadratic classifier.

Also, from the results of the opaque bottle samples, it is seen that some votes have been given to the blue class and this is due to the green cap of the bottle. Since the classifier has not been trained on the green color, it sorted the color as blue which is the closest color to the green in the HSV color space.

Other examples are listed in Figure 3-34, where the bottles had to be in a position where two consequent images had to be combined, the black line that appears at the middle of the bottle is due to the imperfect label positions or more specifically, they are separated by a distance slightly bigger than required. So they may trigger the camera to take consequent images but a small part of the conveyor will be missed.

The quadratic classifier in the clear sample was wrong in classifying the clear bottle, but luckily the tree classifier showed the right classification with a higher confidence and therefore the output of the fusion classification was correct.

In the case of the blue opaque bottle, part of the white label with black writings appeared in the bottom part of the bottle and caused the classifier to vote in some division lines to the white (due to the color of the label) and grey classifier (due to the writing on the label). While the faulty yellow votes appear due to the edge effect at the boundaries of the bottle which causes a color distortion.

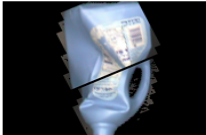
	Opaque Sample	Clear Sample																																				
The combination of thresholded images																																						
Cropped image to the size of 270x360 pixels																																						
Bottle image after Orientation																																						
Extracted top part																																						
Extracted bottom part	<table border="1"> <thead> <tr> <th></th> <th>Blue</th> <th>Grey</th> <th>White</th> <th>Yellow</th> </tr> </thead> <tbody> <tr> <td>Quadratic</td> <td>5</td> <td>2</td> <td>1</td> <td>2</td> </tr> <tr> <td>Tree</td> <td>6</td> <td>1</td> <td>2</td> <td>1</td> </tr> <tr> <td>Fusion</td> <td>11</td> <td>3</td> <td>3</td> <td>3</td> </tr> </tbody> </table>		Blue	Grey	White	Yellow	Quadratic	5	2	1	2	Tree	6	1	2	1	Fusion	11	3	3	3	<table border="1"> <thead> <tr> <th></th> <th>Clear</th> <th>Blue</th> <th>Green</th> </tr> </thead> <tbody> <tr> <td>Quadratic</td> <td>2</td> <td>8</td> <td>0</td> </tr> <tr> <td>Tree</td> <td>9</td> <td>1</td> <td>0</td> </tr> <tr> <td>Fusion</td> <td>11</td> <td>9</td> <td>0</td> </tr> </tbody> </table>		Clear	Blue	Green	Quadratic	2	8	0	Tree	9	1	0	Fusion	11	9	0
	Blue	Grey	White	Yellow																																		
Quadratic	5	2	1	2																																		
Tree	6	1	2	1																																		
Fusion	11	3	3	3																																		
	Clear	Blue	Green																																			
Quadratic	2	8	0																																			
Tree	9	1	0																																			
Fusion	11	9	0																																			
Class voting Table																																						

Figure 3-34 Image Processing Procedures for Bottles Fitted in Two Frames

3.5 The Integration of the Plastic and Color Classification Systems

From the results obtained in the previous chapters, we can summarize the choice of the plastic and color classifiers as follows:

- Plastic type classification

DiagQuadratic classifier with the spectrometer in the range 900-1700 nm and a four dimensional feature vector composed of the average power from the three readings of the spectrometer for each bottle and the global minimum points in each of the spectrums in the three readings.

- Color classification

The fusion of the tree and quadratic classifier.

Each of the previous classifiers showed different classification accuracies, as we integrate the two classifiers in one classification unit it is required to investigate the total accuracy of the system. The accuracy of the integrated system was examined on the 147 samples, and fall into the following categories.

- Clear bottles (no color) : 30 samples
- Clear bottles (light blue) : 30 samples
- Clear bottles (light green) : 30 samples
- Natural bottles (white): 30 samples
- Opaque (Different colors): 27 samples

The accuracy measured by counting the false classification of the bottles in either of the classification stages (Plastic type, or color) and considering them as a wrong classification. It can be noticed that the natural plastic bottles come in one color so the classification accuracy of this type is dependant on the accuracy of the plastic type classifier only. Appendix C lists the classification result details for all the bottles. The Table 3-3 contains the summary of the integration accuracy results.

Table 3-3 Total Classification Accuracy

	Color classifier accuracy [%]	Plastic type classifier accuracy [%]	Over all Accuracy [%]
Clear (no color)	86.67	96.67	83.33
Clear (light blue)	83.33	93.33	76.67
Clear (light green)	96.67	93.33	90
Natural	93.33	---	93.33
Opaque (different colors)	85.19	88.88	74.07
Total accuracy [%] →			83.67

As the color classifier parameters are adjusted (foreground extraction threshold values) according to the result of plastic type classifier, therefore the accuracy of the color classifier is affected heavily. This cascaded classification scheme as shown in Figure 3-35 can be improved by making the classifiers working in parallel individually. This requires adding more intelligence in the color classifier to adapt the thresholding parameter automatically for each bottle type (clear, natural or opaque) without receiving any feedback from the first classifier. The results represent the accuracy of the integrated system while each of the classifiers is working independently.

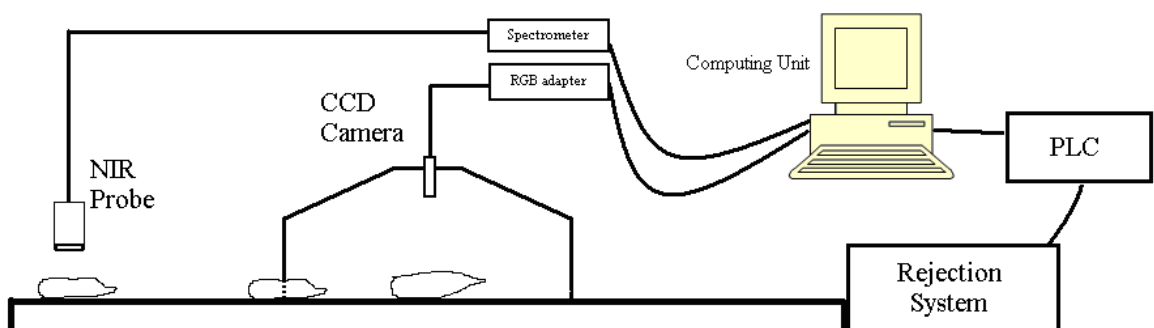


Figure 3-35 Integrated System Overview

CHAPTER

CONCLUSION AND FUTURE WORK

This thesis showed the design of a plastic bottles classification station that is capable of sorting the bottles based on their chemical resin (using near infrared spectrometer) and color (using CCD camera). We considered in the design a closed set identification. However, for practical implementation, it is required to integrate rejection capability to get rid of odd plastic bottles that do not belong to any of the classification categories. This chapter summarizes the contributions accomplished in this thesis. It also presents some techniques that can be implemented in the future work on the automatic plastic bottle sorting system.

4.1 Summary of the Contributions

4.1.1 Development and Implementation of a Plastic Bottle Sorting System

The main contribution that was accomplished in this thesis was the development, implementation, and testing of an automatic plastic bottle sorting system. The system is composed of two classification stages; each classification stage is composed of two main architectures: hardware and software architectures.

The first classification stage is the plastic type classification using near infrared spectroscopy, while the second stage is color classification using machine vision based on a CCD camera. The classification algorithms were developed to achieve the classification in real time. The system is able to learn new plastic bottle colors and extend the classification color categories by presenting new training sets of these new categories.

4.1.2 Implementing Classifier Fusion for Color Classification

Quadratic discriminant function based classifier and decision tree classifier were fused to achieve the task of color recognition of the plastic bottle. The combination was accomplished in multiple stages, and the classifiers combiner used is a static voting based combiner. Some results showed enhancements in the overall color classification accuracy since it differs from one classifier to another for each color.

4.1.3 Integration of Different Classifiers for Multilevel Classification

Sensor and classifier combination was accomplished to achieve the multistage classification process. The first classification stage is based on the transparency of the plastic bottle using near infrared Spectrometer while the second stage is based on the color using CCD camera. These classification stages are cascaded and the result of the first stage (Transparency) determines the classification categories for the second stage (color). In other words, the color classification categories for clear bottles are different from those for opaque bottles. The classification accuracy of this cascading (serial) combination was measured at each classification stage and the overall accuracy was 83.67 %.

4.1.4 Building a Low-Cost Classifier for Plastic Type Classification

For the chemical resin classification system, the near infrared spectroscopy was the technology chosen to identify the chemical characteristics of the plastic bottles. Different near infrared bandwidths have been examined. It was found that the range from 900-1700nm had more distinguishable signal characteristics between different plastic bottles type at that range. Different feature extraction methodologies were used, some of them was based on a new technique of measuring the plastic bottle type based on the power of the NIR signal as well as examining the chemical characteristic of the signal through the detection of the wavelength positions of the peaks and valleys in the plastic NIR spectrum.

4.2 Future Work

Some algorithms are presented in the following sections that can be applied in future work on the automatic sorting systems. These algorithms may provide additional intelligence to the system so it can handle more sophisticated plastic bottle classification tasks. Such as label detection, cap detections or other additive part detection. Also some of them can be applied in parallel with classification modules presented in this thesis to increase the accuracy of the classifiers by removing possible sources of noise in the image such as labels.

4.2.1 Morphological Algorithms

Morphological operations can be used to isolate labels from plastic bottles. However it is possible to get different results according to the transparency of the bottle. In other words, the algorithm will extract the paper label if it is applied on a clear labeled bottle image, while the same algorithm will remove paper label from a natural plastic bottle image. An example is provided using a structural element in the shape of disk with radius 15 pixel. This segmentation can be decomposed into four stages (see Figure 4-1).

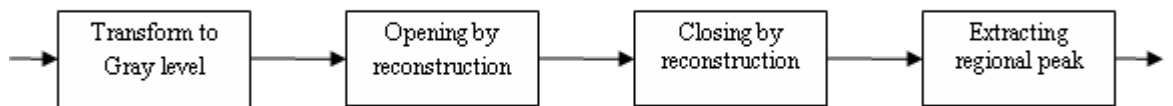


Figure 4-1 Segmentation Steps Using Morphological Algorithms

The followings are different samples and there image before and after extracting the regional maxima.



Figure 4-2 Segmenting Water Bottles Using Morphological Operations

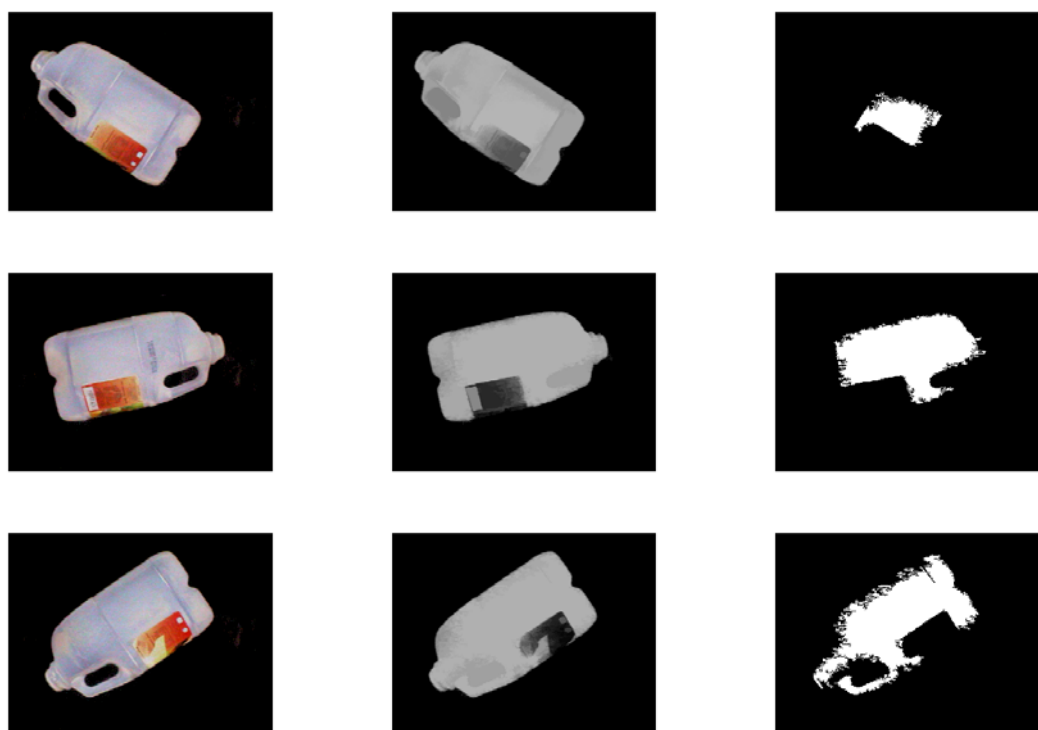


Figure 4-3 Segmenting HDPE Bottles Using Morphological Operations

We can see that this method was successful in segmenting labels for clear bottles, but for HDPE (natural bottles) this operation has an opposite effect by extracting the bottle instead of the label as shown in Figures 4-2 and 4-3.

A potential use of this algorithm is in the preprocessing stage, where it will remove the label from the image before presenting it to the classifier. This can enhance the classification performance since the paper label is a major source of misleading information to the classifiers.

4.2.2 K-Mean Clustering

Another possible algorithm for extracting labels and caps from the bottle image is by using K-mean clustering in the preprocessing stage. Different cap color and small parts of labels may appear at the extracted top and bottom parts of plastic bottle images. To improve the quality of the extracted feature, it is possible to find the common color clusters at the top and bottom parts using K-Mean clustering.

K-means clustering algorithm for finding the data clouds in a given data set can be described as follows:

Let us consider the problem of distributing M feature vectors into K clusters in N dimensional feature space. Let, X_{ij} denote the j'th component of the i'th vector.

Here, we label each vector to be belonging to a definite cluster, according to the minimum distance classification algorithm. The distances (eg. Euclidean distance) of each vector from the K cluster centers are computed, and the vector is assigned to the cluster having its centre at a minimum distance. The K-means clustering algorithm in Figure 4-4 is thus an iterative procedure of vector labeling, till a stable cluster assignment [55].

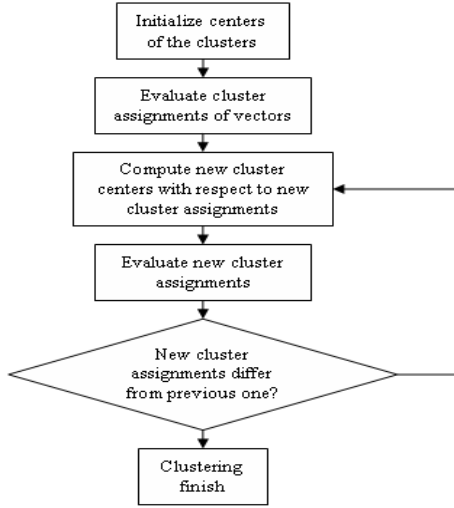


Figure 4-4 K-Mean Clustering Algorithm Flowchart

Generally, the components of the K initial centers are computed as K arithmetic means between the vector components. To start with, we find a cluster assignment based on the initial cluster centers. The cluster centers are updated from the newly obtained cluster assignment by computing the centroids of the cluster members. The vectors are again labeled according to the updated cluster centers. This procedure of cluster centre updating and vector labeling continues till the cluster assignment becomes a stable structure and does not change any more.

In Figure 4-5 we can see the functionality of the K-mean clustering in different plastic bottle types. The first example shows the ability to extract labels and caps, the second one shows excellent results in extracting paper label.

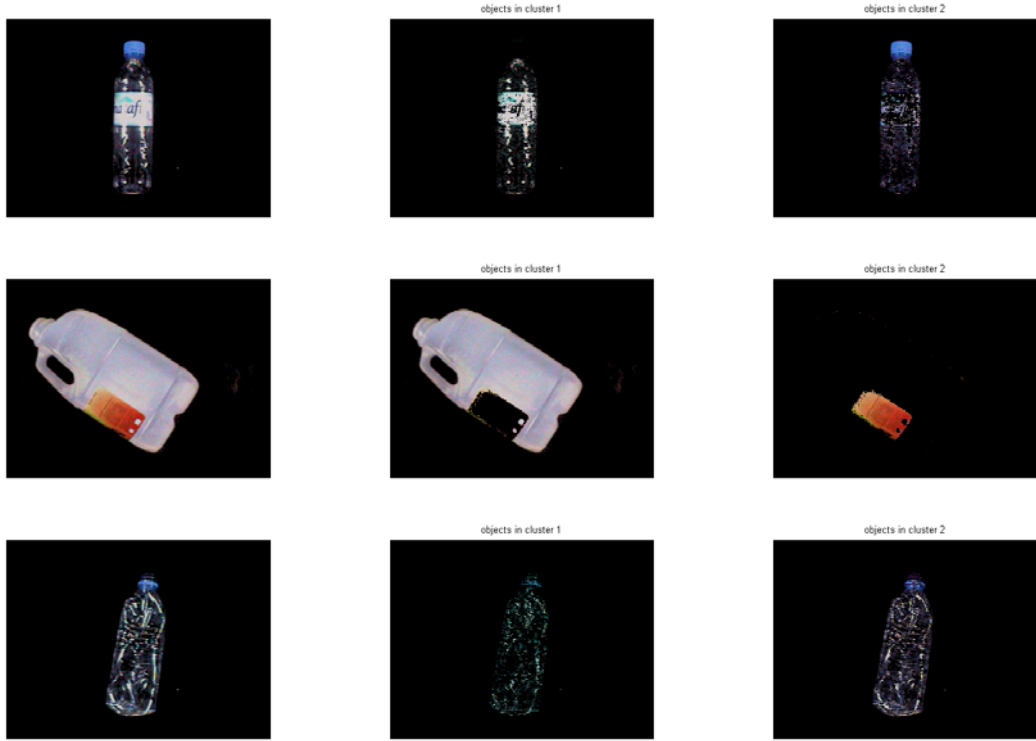


Figure 4-5 Segmenting Plastic Bottles Colors Using K-Means Clustering

4.2.3 Tracing Ring

One possible way to extract the color of the plastic bottle is by extracting a ring from the plastic bottle image which is the result of XOR the original binary image and the eroded version of it. The thickness of the ring is related to the size and shape of the structural element. This ring can be opened and analyzed; it is possible to distinguish the label color from the original color of the plastic bottle. Figure 4-6 shows the result of extracting the ring out of a thresholded bottle image.



Figure 4-6 Extracting Tracing Ring from Plastic Bottle Images

4.2.4 Nonlinear Filtering

A traditional averaging may not be adequate for transparent bottles since the chance for merging some parts with the background will be high. In order to perform a low pass filtering taking into consideration the edge information, KUWAHARA nonlinear filter is used [56], which is based on taking the mean of the least variance calculated in 4 subwindows of a window that is scanning the image. It can be seen from the images below that this filter can smooth out some unwanted details such as the printing on the labels while preserving the edges in the picture. Although this filter provided good results for transparent and opaque bottles but the cost of computational power for this filter for real time application is relatively high. A prototype program to simulate the filter was written as the Figure 4-7 illustrates the promising results of KUWAHARA filter.

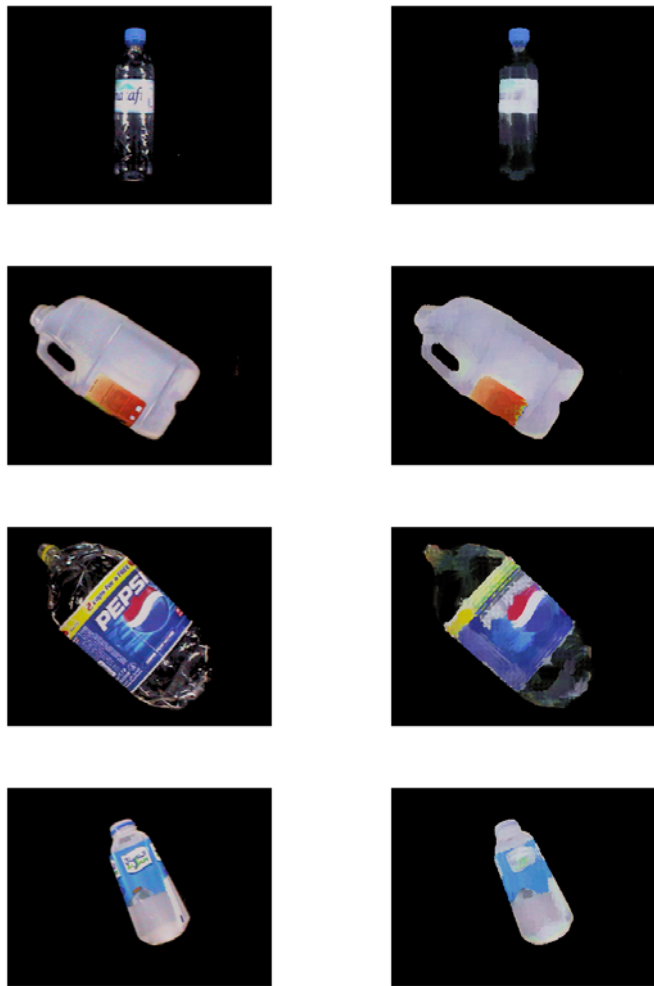


Figure 4-7 The Result of the Kuwahara Filtering on the Plastic Bottle Images

4.2.5 Adaptive Monitoring System

In order to accommodate the variation in the lighting and color changes in the conveyor due to possible contaminations that may appear or objects stick on the conveyor during the sorting process, an adaptation algorithm is used to modify the bank of the background images stored in the memory according to the variations mentioned before.

The main idea in this algorithm to assign two additional pieces of information to each pixel in the stored background image I_{bg} which are:

- Last pixel color values in the recent image taken from this belt position are contained in the update image I_u .
- The number of times this color has been consequently seen at this pixel place is saved in a counter array C.

Obviously, if this color was observed for a certain number of times, this means that a new color has appeared in the background and this color should be the new background color at this position.

In Figure 4-8, a flow chart of the adaptation algorithm of the background images is provided. The initial values for the counter array $C(x,y)=0$ for all the (x,y) values.

For updating the images I_u or I_{bg} , the new updated image is an average assigned by a ratio $w \in [0\dots 1]$ as follows:

$$(1) I_u(x,y) = (1-w).I_u(x,y) + w .I(x,y)$$

$$(2) I_{bg}(x,y) = (1-w).I_{bg}(x,y) + w .I(x,y)$$

Actually the function of the update image I_u is to modify the background images by assigning its values to the background image at the corresponding conveyor position. However, this assignment is conditioned by the counter crossing a certain counter threshold which indicates at this case that the new color contained in the update image I_u has appeared for more than the threshold number of times and it can be a new member of the background image at that particular position of the conveyor belt.

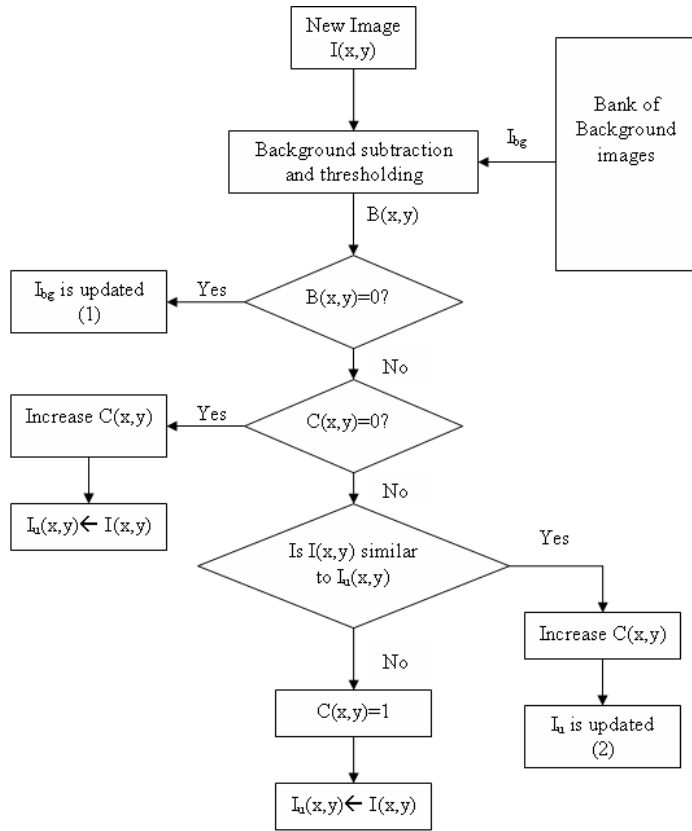


Figure 4-8 Background Updating Algorithm

REFERENCES

- [1] Hammaad, S (2005) “*7.25 Million AED is the Cost of Waste Recycling*” Al-Bayan newspaper, 11/03/2005
- [2] Dubanowitz, A J.(2000) “*Design of a Material Recovery Facility MRF for Processing in Recyclable Material of New York City’s Municipal Solid Waste*” Master thesis in Earth resources engineering, Columbia University.
- [3] Stevens, A (2003) ”*Expanding Plastic Bottle Recycling in Essex & Cambridgeshire*”,WasteWISE Overview Report 1
- [4] EnviroS RIS (2001) “*Plastic Waste Management Strategy for Ontario*” Environment and Plastic Industry Council
- [5] ITDG technical paper ”*Recycling plastics*”
Website:
www.itdg.org/docs/technical_information_service/recycling_plastics.pdf
- [6] Kowol,F., Oleimeulen, M., Freitag, H., and Huth-Fehre, T. (1998) “*Mid Infrared Acousto-Optical Tunable Filter-Spectrometer for Rapid Identification of Black Plastics from Automobile Construction*”. Institut für Chemo- und Biosensorik e.V., Mendelstraße 7, D-48149 Münster, Germany. A149–A151
- [7] Huth-Fehre, T., Feldhoff, R., Kowol, F., Freitag, H., Kuttler, S., Lohwasser B., and Oleimeulen, M. (1998) ”*Remote Sensor Systems for the Automated Identification of Plastics*” Institute of Chemical and Biochemical Sensor Research, Mendelstr. 7, D-48149 Münster, Germany. A7–A11
- [8] Biddle, M.B., Dinger, P., Fisher, M.M. (1999) “*An Overview of Recycling Plastics from Durable Goods: Challenges and Opportunities*” Identiplast II, Brussels, Belgium.
- [9] Stchur, P.; Cleveland, D.; Zhou, J.; Michel, R.G. (2002) ”*A Review of Recent Applications of Near Infrared Spectroscopy, and of the Characteristics of a Novel PbS CCD Array-Based Near-Infrared Spectrometer*” Appl. Spectrosc. Rev. 37(4), 383-428
- [10] Great Lakes Institute for Recycling Markets (1998) “*Auto Recycling Demonstration Project*” The Michigan DEQ, P2 Section, Environmental Assistance Division.

- [11] Hendrix, J., Massey, K.A., Whitham, E. and Bras, B. (1996) “*Technologies for identification, Separation and recycling of automotive plastics*” International Journal of Environmentally Conscious Design and Manufacturing vol5, pp. 35-47
- [12] Shutov, F. (1999) “*Effective Energy and Gas Emission Savings Using Plastics Waste Recycling Technologies*” Expert Group Meeting On Industrial Energy Efficiency, Cogeneration and Climate Change, Vienna International Center, Vienna, Austria.
- [13] Enviro RIS, “*Plastic Waste Management Strategy for Ontario*” ,September 2001
- [14] Dubanowitz, A.J. (2000) “*Design of a Material Recovery Facility MRF for Processing in Recyclable Materials of New York City’s Municipal Solid Waste*”
- [15] Stevens, A. (2003) , ”*Expanding Plastic Bottle Recycling in Essex & Cambridgeshire* ” ,WasteWISE Overview Report 1
- [16] NFESC Environmental Department (1993) “*Solid Waste Management Plan (SWMP) Guide*” Naval Energy and Environmental Website: <http://enviro.nfesc.navy.mil/ps/swmp/append-g.pdf>
- [17] American plastics council, “*Resin Identification Codes - Plastic Recycling Codes*” Website: www.americanplasticscouncil.org
- [18] Lancaster County, Solid Waste Management Authority. Website: www.lcsdma.org/faq.asp
- [19] Hurd, D.J. (1997) “*Best Practices and Industry Standards in PET Plastic Recycling*”, Washington state department of community, trade and economic development’s clean Washington center. Website: www.napcor.com/Master.pdf
- [20] Bruno, E.A. (2000) “*Automated Sorting of Plastic for Recycling*” North Carolina Department of Environment and natural resources. Website:www.p2pays.org/ref/09/08620.pdf
- [21] Fisher, M.M. (2004) “*Plastics and Environment*” ISBN0471095206 John Wiley & Sons Inc

- [22] Child, J.,(2002), “*Vision-Based Sorting System Helps Recyclers Distinguish a Spectrum of Plastic-Bottle Colors using Custom Image-Processing Software*” Vision System Design, Web Article.
 Website:
http://vsd.pennnet.com/Articles/Article_Display.cfm?Section=Archives&Subsection=Display&ARTICLE_ID=133298&KEYWORD=DALSA
- [23] Crank, M. L., Kern, J. M., Lindquist, J.L., Spitz, A. H., Wolf, A. A., and A. Závodská (2000) “*Low Cost Optical Sorter for Recyclable Materials*” Final Report submitted for ADEQ Grant WRA-99-0047AD.
- [24] Stchur, P.; Cleveland, D.; Zhou, J.; Michel, R.G.(2002) “*A Review of Recent Applications of Near Infrared Spectroscopy, and of the Characteristics of a Novel PbS CCD Array-Based Near-Infrared Spectrometer*” Appl. Spectrosc., 37(4), 383-428
- [25] Broek, V.D., Wienke, D., Melssen, W.J., and Buydens, L.M.C. (1998) “*Plastic Material Identification with Spectroscopic Near Infrared Imaging and Artificial Neural Networks*”. Anal. Chim. Acta, 361 161-176
- [26] Sabatto, Z., Bodruzzaman, M. (1993) “*A Neural Network Classifier for Recycling Process*” Southeastcon '93, Proceedings., IEEE 4-7 April Page(s):4 p
- [27] Groot, P. d. Postma, G. Melsen, W. and Buydens, L. M. (1999) “*Selecting a Representative Training Set for the Classification of Demolition Waste using Remote NIR Sensing*” Analytica Chimica Acta 392, pp. 67–75,
- [28] Barcala, J.M. (2004 “*Identification of Plastics using Wavelets and Quaternion Numbers*”, Meas. Sci. Technol. 371-376 doi:10.1088/0957-0233/15/2/009
- [29] Kowol, F. Oleimeulen, M. Freitag, H. and Huth-Fehre, T. (1998) “*Mid Infrared Acousto-Optical Tunable Filter Spectrometer for Rapid Identification of Black Plastics from Automobile Construction*”, Proceedings of NIR 97, NIR Publications, edt. A.M.C. Davies and Phil Williams, A149-A151.
- [30] Paschos, G. (2001, June) “*Perceptually Uniform Color Spaces for Color Texture Analysis: An Empirical Evaluation*” IEEE transactions on image processing, VOL 10, NO.6
- [31] Wan, X. and Kuo, C.-C.J. (1998, September) “*A New Approach to Image Retrieval with Hierarchical Color Clustering*” IEEE Trans. Circuits Syst. Video Technol., vol.8, no.5, pp.628–643.

- [32] Zhang, L., Dehghani, A., Su, Z., King, T., Greenwood, B., Levesley, M., (2005, August) “*Real-Time Automated Visual Inspection System for Contaminant Removal from Wool*”, RealTimeImg (11), No. 4, pp. 257-269
- [33] Gao, H. ,Siu, W.C, Hou, C.H. (2001) “*Improved Techniques for Automatic Image Segmentation*”. IEEE Trans. Circuits Syst. Video Techn. 11(12): 1273-1280
- [34] Zöller, T., and Buhmann, J.M. (2002) “*Self-Organized Clustering of Mixture Models for Combined Color and Texture Segmentation*” , in: Proceedings of Texture 2002, The 2nd international workshop on texture analysis and segmentation, pp:163-167.
- [35] Boskovitz, V. and Guterman, H. (2002)"*An Adaptive Neuro-Fuzzy System for Automatic Image Segmentation and Edge Detection,*" IEEE Transactions on Fuzzy Systems, Vol. 10, No. 2, pp. 247-262.
- [36] Neumann, A. (2003) “*Graphical Gaussian Shape Models and Their Application to Image Segmentation*” IEEE Trans. Pattern Anal. Mach. Intell. 25(3): 316-329
- [37] Huang Q et al. (1995, October) “*Foreground/Background Segmentation of Color Images by Integration of Multiple Cues*”. In: IEEE Int. Conf. on Image Processing, Vol. 1 , Washington, DC, pp 246—249
- [38] Li,L., Huang, W., & Gu, I.Y., & Tian, Q. (2004) “*Statistical Modeling of Complex Backgrounds for Foreground Object Detection*”. IEEE Transactions on Image Progressing 13(11): 1459-1472.
- [39] Chan, F.H.Y., Lam, F.K. and Zhu, H. (1998) “*Adaptive Thresholding by Variational Method*”, IEEE Transactions on Image Progressing pp. 468-473 volume 7, number 3
- [40] Papamarkos, N., Strouthopoulos, C., and Andreadis, I., (2000) “*Multithresholding of Color and Grey-Level Images through a Neural Network Technique*”. Image and Vision Computing.,18: 213-222
- [41] Tsai, C.M and Lee, H.J (2002) “*Binarization of Color Document Images via Luminance and Saturation Color Features*”, IEEE Transactions on Image Processing, pp. 434-451 volume 11, number 4
- [42] Balthasar, D. and Erdmann, T. and Pellenz, J. and Rehrmann, V., and Zeppen, J., and Priese, L., (2001) “*Real-Time Detection of Arbitrary Objects in*

- Alternating Industrial Environment". In Proceedings Scandinavian Conference on Image Analysis. 321-328*
- [43] Statistics Toolbox User's Guide (2003), The Mathworks, Inc
 - [44] Webb, A. (2002) "Statistical Pattern Recognition" , Second Edition, Wiley. ISBN: 0-470-84514-70
 - [45] Robert Schalkoff, "Pattern Recognition, statistical, structural, and neural approaches", Willey, ISBN 0-471-52974-5 Copyright 1992
 - [46] Duda, R.O., Hart, P.E., Stork, D.G., (2001) "Pattern classification" (2nd edition), Wiley, New York, ISBN 0471056693.
 - [47] S.K. J Al-Ani and J.Beynon "The refractive index of thin solid films" Phys.Educ 20 1995
 - [48] Kraft, M. (2004) "Vibrational Spectroscopic Sensors. Fundamentals, Instrumentation and Applications" Carinthian Tech Research AG, Villach Austria
 - [49] JETI Technische Instrumente GmbH (2005, May) "Basics of Spectral Measurement"
 - [50] Website: www.mathworks.com
 - [51] Davies, E.R., (2005) "Machine Vision : Theory, Algorithms, Practicalities" ISBN 0122060938 Amsterdam ; Boston : Elsevier
 - [52] Gonzalez R.C, Woods, R.E. (2002) "Digital Image Processing" ISBN 0-201-18075-8, Second Edition Prentice Hall
 - [53] Image Acquisition Tutorial, Developer Zone, National Instruments.
Website:
<http://zone.ni.com/devzone/conceptd.nsf/webmain/a49b1d8d7fe14f1a86256b250077210c?OpenDocument>
 - [54] Luo, D., (1998) "Pattern Recognition and Image Processing" ISBN 1898563527 Chichester Horwood.
 - [55] Guha, P. (2001 ,April) "Automated Visual Inspection of Steel Surface, Texture Segmentation and Development of a Perceptual Similarity Measure" Master thesis, INDIAN INSTITUTE OF TECHNOLOGY, KANPUR
 - [56] Ridder, D.de., Dulin, R.P.W., Verbeek, P.W. and Vliet, L.J.van (1999) "The Applicability of Neural Networks to Non-Linear Image Processing", Pattern Analysis and Application, vol.2, no. 2, , 111-128

APPENDIX A
CHARACTERISTICS OF PLASTIC BOTTLE SAMPLES

Table A-1 Clear Bottles Identity List

bottle number	Label exist	Recycle code	Remarks
1	yes	1	dirty with oil, compressed
2	yes	1	compressed, clear, cola
3	no	2	compressed, clear, cola
4	yes	3	small cocacola good clean
5	yes	1	clean, thick
6	no	2	clean compressed water big
7	yes	2	dirty, miranda
8	yes	1	clean,
9	yes	1	compress thick oil
10	yes	x	pepsi, compressed, clean
11	yes	1	too compressed, some dirty
12	yes	x	clean
13	yes	1	compressed clean
14	yes	1	ketchup, drops
15	no	1	compressed, contaminated with milk
16	yes	1	with plastic label, clean and thick
17	yes	1	good condition, cllear
18	yes	1	compressed, some drops
19	yes	1	thick clean
20	yes	1	clean, compressed
21	yes	1	big clean thick oil bottle
22	yes	1	thick container cracker small dirts
23	yes	6	small drops
24	yes	1	clean, compressed
25	yes	1	wet with water
26	yes	x	clear
27	yes	1	wet
28	yes	1	clean, good, small
29	yes	1	clean, good condition
30	yes	x	compressed clear
31	yes	1	clean
32	yes	1	good, blurred dirty

Table A-2 Natural Bottles Identity List

bottle number	Label exist	Recycle code	Remarks
1	no	2	clear, compressed
2	yes	2	clear, milk
3	yes	2	contaminated, compressed
4	yes	no code	juice
5	yes	2	juice, compressed with some water
6	yes	no code	juice, clear
7	yes	2	milk, wet, good shape
8	no	2	contaminated, compressed, burned
9	no	2	juice, clean
10	yes	2	not clear, milk
11	no	2	clear and clean
12	yes	no code	juice, clear
13	no	2	clear, very small
14	yes	no code	milk, clear
15	yes	2	milk, clear
16	yes	2	clear, milk, good (not pressed)
17	yes	2	milk, clear
18	yes	2	compressed, water inside
19	yes	2	contaminated, juice
20	no	2	compressed
21	yes	7	clear milk
22	yes	7	clear milk
23	yes	2	not clear, milk
24	yes	6	clean juice
25	yes	6	milk,
26	yes	2	not clear, compressed
27	yes	2	milk, clear
28	no	2	clear, compressed
29	yes	2	good shape, juice, little bit dirty
30	yes	8	milk, little drops

Table A-3 Opaque Bottles Identity List

bottle number	Label exist	Recycle code	Remarks
1	yes	2	orange good clean
2	yes	2	white
3	yes	3	white yellow break
4	yes	pe	blue compressed
5	yes	2	white good
6	yes	2	yellow good
7	yes	1	off yellow plastic label
8	yes	2	yellow good
9	yes	2	green clean
10	no	1	only writing exists, yellow
11	yes	2	yellow good
12	no	x	yellow compressed
13	no	2	red good thick
14	yes	2	gray, good , clean
15	yes	2	gray, good , dirty
16	yes	pe	white , dirty
17	yes	x	white, milk
18	yes	2	white, milk
19	yes	2	white dirty with ink
20	yes	pe	off yellow compressed
21	no	pe	yellow
22	yes	1	white with big plastic cover
23	yes	1	white good clean with some liquid inside
24	no	2	white compressed
25	no	2	yellow, writing exists
26	yes	5pp	yoghurt basket
27	yes	pe	blue compressed
28	yes	2	white totally covered by plastic label, good
29	yes	2	white totally covered by plastic label, good

Colored clear bottles identity list:

Table A-4 Colored Clear Bottles Identity List: Light Blue

bottle number	Label exist	Recycle code	Remarks
1	yes	1	clean
2	yes	1	good
3	no	1	compressed big
4	yes	1	water and vapor
5	no	1	with caves
6	yes	1	good
7	yes	1	light blue big compressed
8	yes	1	compressed max
9	no	1	water drops
10	yes	1	clean
11	yes	1	big compressed with drops
12	yes	1	compressed max
13	no	1	half a bottle
14	yes	1	caves
15	yes	1	compressed

Table A-5 Colored Clear Bottles Identity List: Light Green

bottle number	Label exist	Recycle code	Remarks
1	no	x	compressed
2	no	x	compressed
3	yes	x	good with water inside
4	no	x	compressed
5	yes	4	compressed and with water drops
6	yes	x	good
7	no	x	compressed
8	no	x	compressed
9	yes	x	good with water inside
10	no	x	compressed
11	yes	4	compressed and with water drops
12	yes	x	good
13	no	x	compressed
14	no	x	compressed
15	yes	x	good with water inside

APPENDIX B
CONVEYOR SYSTEM DRAWING

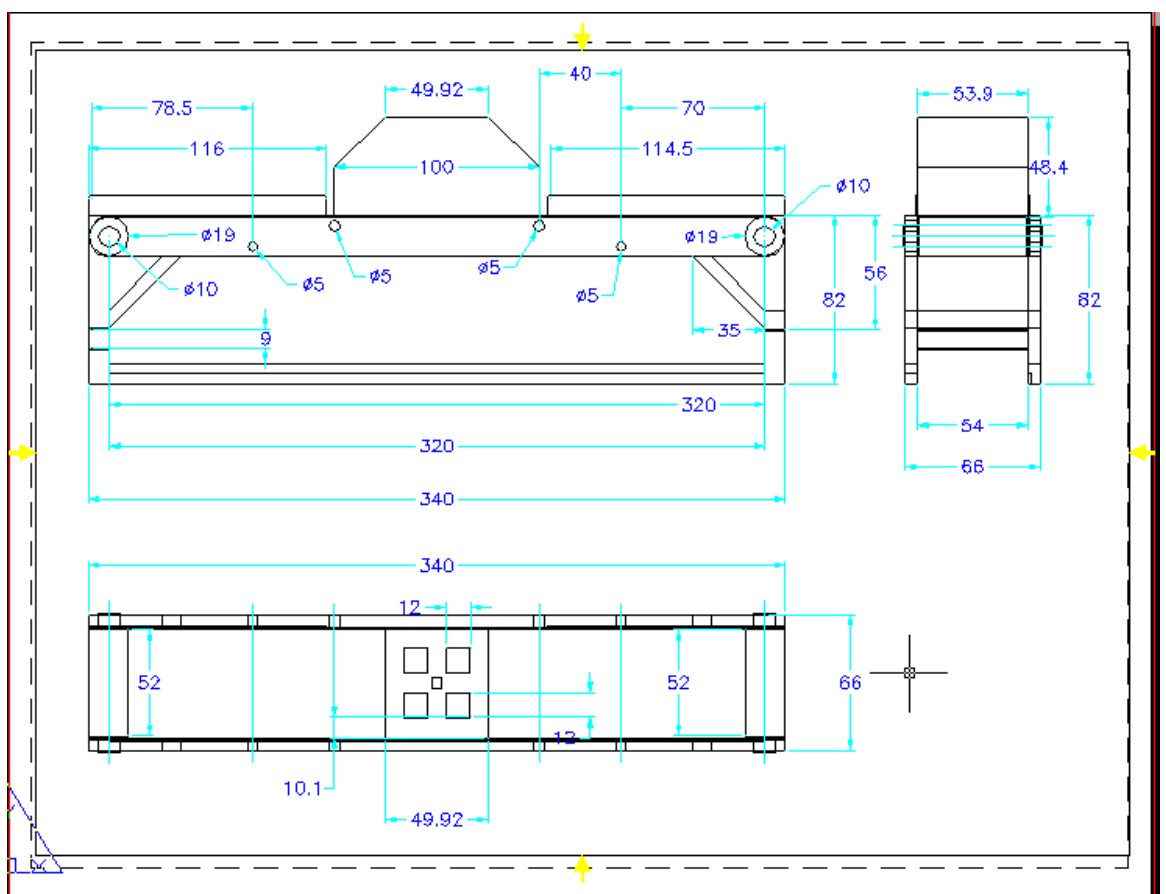


Figure B-1 Conveyor System Drawing

APPENDIX C
NIR BASED CLASSIFICATION RESULTS

Classification error rate at 900-1700 nm

Extracted Features: Spectrum Characteristics

Training data ratio = 60%

Table C-1 Error Rates at 900-1700 nm for 60% Training Ratio (PV)
Feature Dimension

	P1V1	P1V3	P3V1	P3V3
Linear	0.1352	0.1487	0.1487	0.1802
Quadratic	0.0901	0.1622	0.0991	0.1757
Tree	0.1351	0.1622	0.1262	0.1441
Mahalanobis	0.1036	0.1982	0.2162	0.2748
DiagQuadratic	0.0946	0.1351	0.0586	0.1306

min= 0.0585833

Training data ratio = 50%

Table C-2 Error Rates at 900-1700 nm for 50% Training Ratio (PV)
Feature Dimension

	P1V1	P1V3	P3V1	P3V3
Linear	0.1268	0.1304	0.1341	0.1522
Quadratic	0.0870	0.1522	0.1196	0.1775
Tree	0.1486	0.1449	0.1486	0.1812
Mahalanobis	0.1087	0.1848	0.2210	0.2754
DiagQuadratic	0.0978	0.1196	0.0761	0.1087

min= 0.0760833

Training data ratio = 40%

Table C-3 Error Rates at 900-1700 nm for 40% Training Ratio (PV)
Feature Dimension

	P1V1	P1V3	P3V1	P3V3
Linear	0.1250	0.1369	0.1369	0.1607
Quadratic	0.0893	0.1637	0.1280	0.1845
Tree	0.1488	0.1369	0.1637	0.1756
Mahalanobis	0.1220	0.2054	0.2441	0.2619
DiagQuadratic	0.0923	0.1221	0.0863	0.1280

min= 0.0863167

Classification error rate at 1100-2200 nm

Extracted Features: Spectrum Characteristics

Training data ratio = 60%

Table C-4 Error Rates at 1100-2200 nm for 60% Training Ratio (PV)

Feature Dimension

	P1V1	P1V3	P3V1	P3V3
Linear	0.4414	0.4370	0.4280	0.4099
Quadratic	0.5315	0.4775	0.4730	0.4730
Tree	0.6306	0.6171	0.7072	0.6622
Mahalanobis	0.5631	0.4595	0.4504	0.3919
DiagQuadratic	0.5360	0.5406	0.4775	0.4910

min= 0.391917

Training data ratio = 50%

Table C-5 Error Rates at 1100-2200 nm for 50% Training Ratio (PV)

Feature Dimension

	P1V1	P1V3	P3V1	P3V3
Linear	0.4239	0.4094	0.3804	0.3986
Quadratic	0.5000	0.4638	0.4420	0.4891
Tree	0.6196	0.5870	0.6232	0.6305
Mahalanobis	0.4928	0.4058	0.4239	0.3949
DiagQuadratic	0.5145	0.5580	0.4928	0.4964

min= 0.380433

Training data ratio = 40%

Table C-6 Error Rates at 1100-2200 nm for 40% Training Ratio (PV)

Feature Dimension

	P1V1	P1V3	P3V1	P3V3
Linear	0.4167	0.4315	0.3899	0.3721
Quadratic	0.5298	0.5209	0.4673	0.4941
Tree	0.6488	0.6339	0.6578	0.6875
Mahalanobis	0.4940	0.4464	0.4435	0.4048
DiagQuadratic	0.5208	0.5506	0.4732	0.5179

min= 0.37205

Classification accuracy at 900-1700 nm

Extracted Features: Principal Components

Training data ratio = 60%

Table C-7 Classification Accuracy at 900-1700 nm for 60% Training Ratio (PCA)

	Principal Components			
	1	2	5	10
Linear	0.66215	0.75675	0.86938	0.84685
Quadratic	0.67115	0.8018	0.86037	0.86937
Tree	0.54503	0.6937	0.81982	0.75675
Mahalanobis	0.68015	0.77928	0.73875	0.7793
DiagQuadratic	0.67115	0.77027	0.9054	0.93692

min= 0.93692

Training data ratio = 50%

Table C-8 Classification Accuracy at 900-1700 nm for 50% Training Ratio (PCA)

	Principal Components			
	1	2	5	10
Linear	0.66667	0.80797	0.88407	0.8732
Quadratic	0.67755	0.83693	0.86232	0.87318
Tree	0.56885	0.75	0.85143	0.78985
Mahalanobis	0.66668	0.78263	0.7174	0.80433
DiagQuadratic	0.67755	0.77537	0.90578	0.91667

min= 0.91667

Training data ratio = 40%

Table C-9 Classification Accuracy at 900-1700 nm for 40% Training Ratio (PCA)

	Principal Components			
	1	2	5	10
Linear	0.61905	0.81843	0.83632	0.83628
Quadratic	0.62203	0.79762	0.81548	0.81252
Tree	0.57438	0.74403	0.81847	0.8125
Mahalanobis	0.65178	0.72917	0.71133	0.79465
DiagQuadratic	0.62203	0.75892	0.90478	0.88693

min= 0.90478

Classification accuracy at 1100-2200 nm

Extracted Features: Principal Components

Training data ratio = 60%

Table C-10 Classification Accuracy at 1100-2200 nm for 60% Training Ratio (PCA)

	Principal Components			
	1	2	5	10
Linear	0.45047	0.68017	0.76127	0.77477
Quadratic	0.44145	0.7117	0.79728	0.84235
Tree	0.33335	0.68017	0.72522	0.70272
Mahalanobis	0.4189	0.66668	0.72073	0.7928
DiagQuadratic	0.44145	0.67568	0.69822	0.67567

min= 0.84235

Training data ratio = 50%

Table C-11 Classification Accuracy at 1100-2200 nm for 50% Training Ratio (PCA)

	Principal Components			
	1	2	5	10
Linear	0.43477	0.67755	0.7355	0.77173
Quadratic	0.41305	0.71377	0.82968	0.80433
Tree	0.39493	0.63772	0.66667	0.65942
Mahalanobis	0.39853	0.62682	0.73913	0.76448
DiagQuadratic	0.41305	0.6703	0.7029	0.66303

min= 0.829683

Training data ratio = 40%

Table C-12 Classification Accuracy at 1100-2200 nm for 40% Training Ratio (PCA)

	Principal Components			
	1	2	5	10
Linear	0.42558	0.6756	0.74703	0.79762
Quadratic	0.43157	0.69345	0.78868	0.71428
Tree	0.3631	0.63988	0.71725	0.67857
Mahalanobis	0.38988	0.62202	0.73213	0.70833
DiagQuadratic	0.43157	0.68155	0.69345	0.6637

min= 0.797617

Classifier error rate at 900-1700 nm for different feature vectors:

Extracted Features: Spectrum Characteristics

Training data ratio = 60%

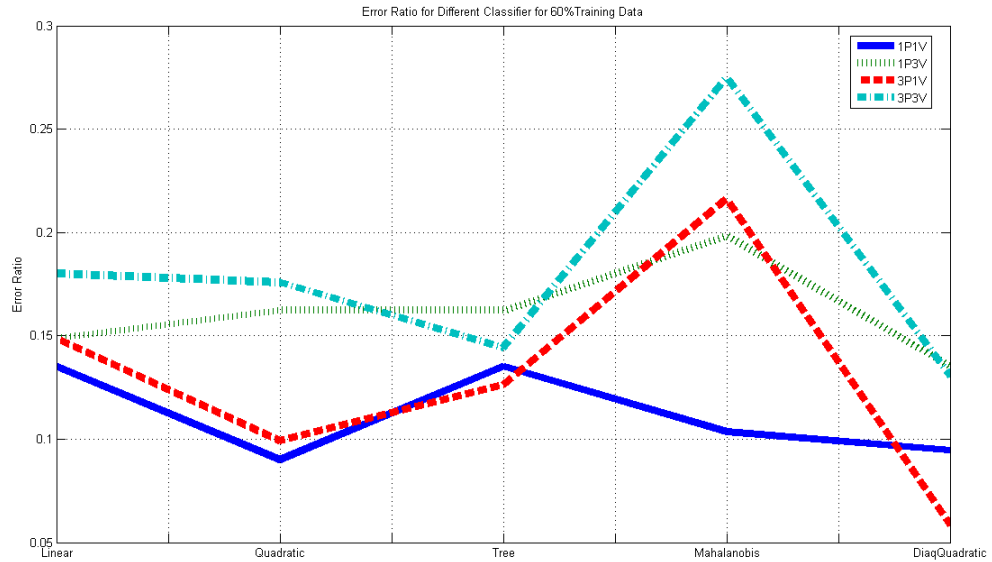


Figure C-1 Error Rate Using 60% Training Ratio

Training data ratio = 50%

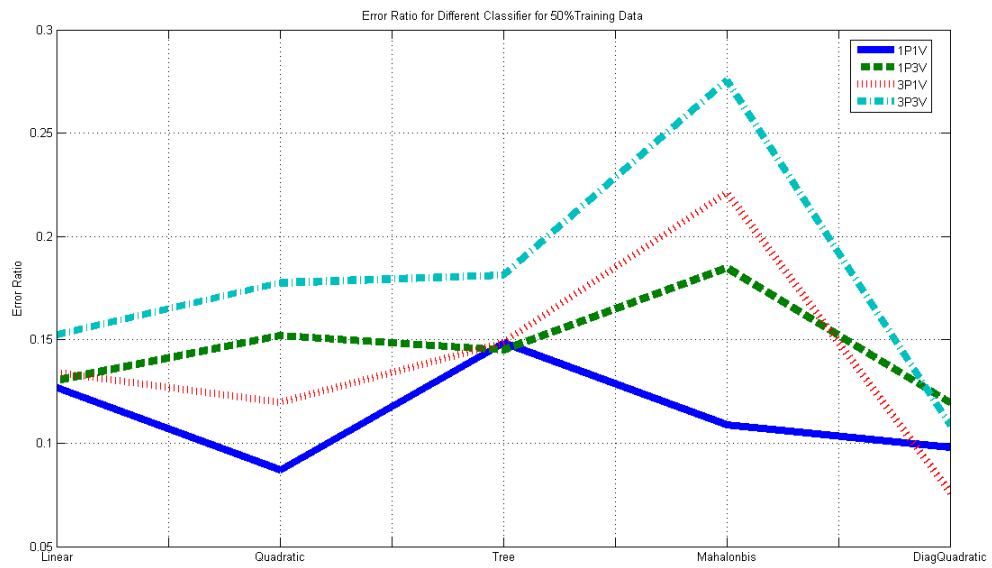


Figure C-2 Error Rate Using 50% Training Ratio

Training data ratio = 40%

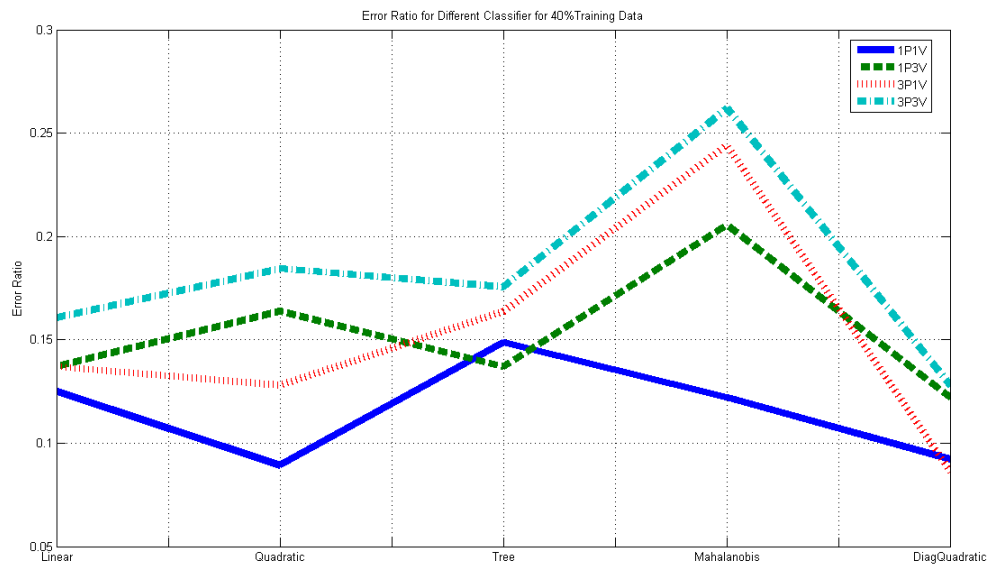


Figure C-3 Error Rate Using 40% Training Ratio

Classification accuracy as a function to training data ratio

Spectrum Range: 900-1700 nm

Extracted Features: Spectrum Chrematistics

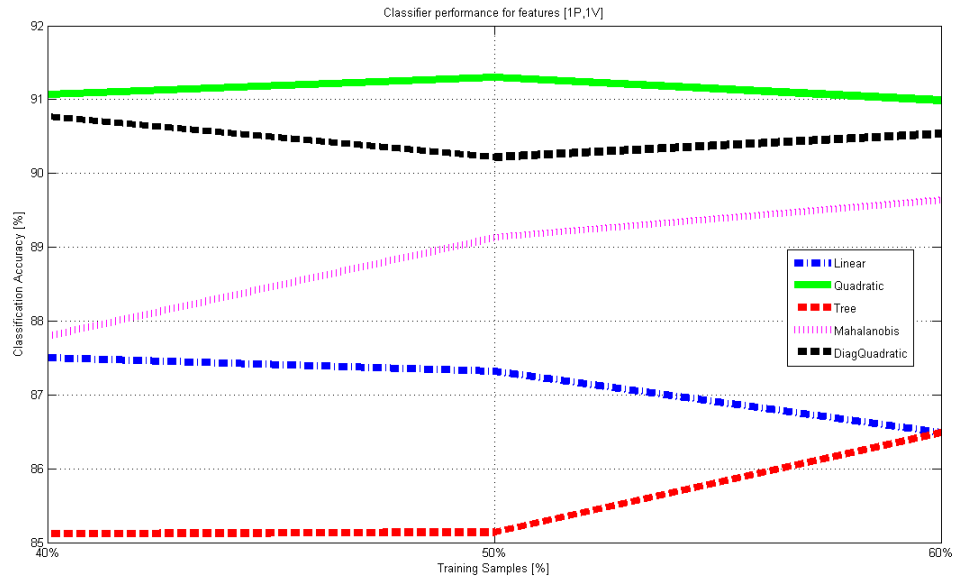


Figure C-4 Accuracy as a Function to Training Data Ratio for [1P1V]

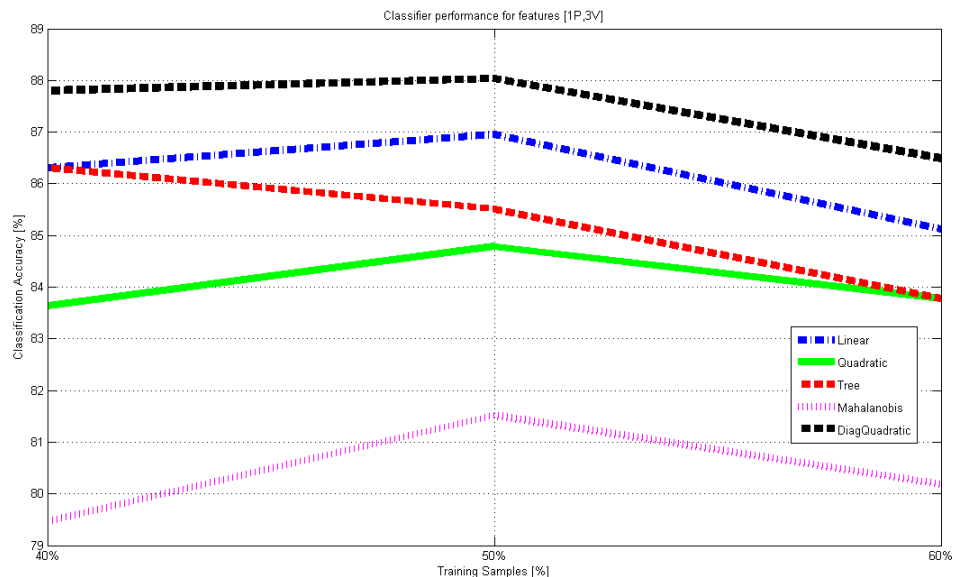


Figure C-5 Accuracy as a Function to Training Data Ratio for [1P3V]

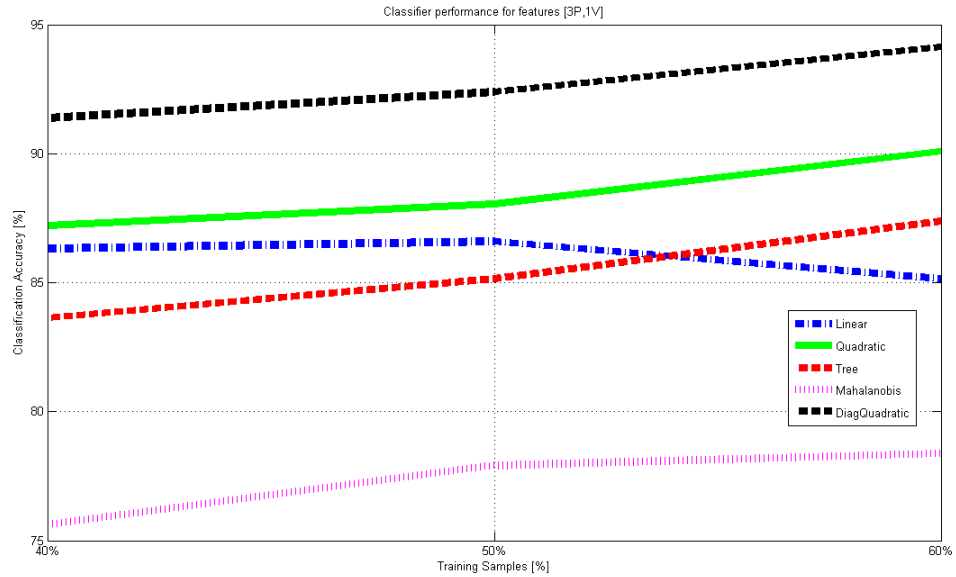


Figure C-6 Accuracy as a Function to Training Data Ratio for [3P1V]

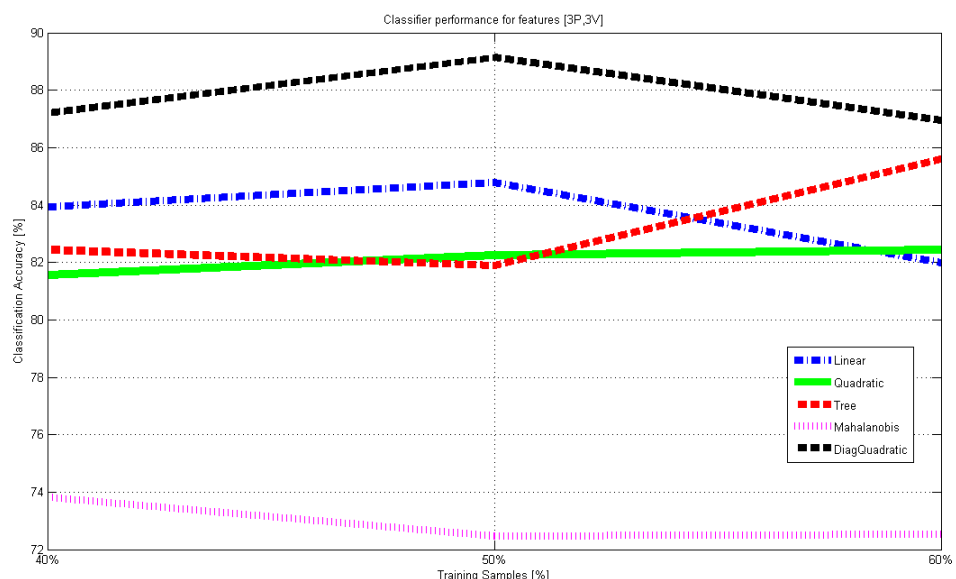


Figure C-7 Accuracy as a Function to Training Data Ratio for [3P3V]

APPENDIX D
NIR TEST FINAL REPORT IN DRESDEN, GERMANY

Subject : Final Report on Tests and Measurements Using NIR
Spectrometer for Automatic Plastic Bottles Sorting.
Date : 28/10/2005

Abstract

This report describes the testing and measurements procedures performed by Mr.Yahia Tachwali from American University during his visit to Sentronic GmbH in Dresden between 25th and 31st of October 2005. These tests were performed to evaluate the proper NIR spectrometer hardware setup for the automatic plastic bottles sorting project.

Performed by :

Mr.Yahia Tachwali

[Tachwali@ieee.org]

American University of Sharjah

Sharjah,UAE

Supervised by :

Mrs.Katrin Glatzer

[K.Glatzer@getSpec.de]

Sentronic GmbH

Dresden, Germany

Tuesday [25th of October 2005]

Overview

This day was mainly assigned to check the hardware setup, getting familiar with the hardware and software settings, make some initial measurements with plastic bottles from the different categories to check the functionality of the system over a sample of the conveyor belt sample and determine the best settings for the measurements of next day.

Procedure

- Check the hardware setup, and its main components :
 - The Spectrometer : Polytec PSS NIR2.1
 - The Probe or head : 1-Sentrohead [NIR100]
2-Reflection probe with 6 illumination fibers
and one reading fiber
 - The Interface software: Polytec, PSS Device Driver ActiveX Demo.
- Learning the interface software utilization :
 - Installation.
 - Parameters settings. [Measurement Types- Calibration settings- Online scanning- Single scanning- Save and read the spectrum measurement text files].
 - Brief introduction on GramsAE.
- Learning the calibration procedure:
 - Recording the dark signal (Internal instrument noise).
 - Determining the Reference of the Spectrum level using Sentrohead White Standard.
 - Assigning the proper integration time.
 - Determining the proper head height from the background (Conveyor Belt)
- Acquire the NIR spectrum [1100-2200 nm] of different plastic bottles type to find the spectrum region of interest.
- Verifying the effect of the conveyor belt effect on the measurements and taking its reflectance NIR spectrum.

Wednesday 26th of October 2005

Overview

NIR spectrum acquisition was performed for all the plastic bottles samples from different categories using one of the best spectrometer products which has a wide spectrum range [1100-2200 nm], the acquisition was performed from 3 different places of the bottle [top - near the label (if exist) - bottom].

Initial settings

- Hardware: Polytec PSS NIR2.1+ Sentohead [NIR100]
- Software: Polytech: PSS Device Driver ActiveX Demo.
- Reference: Sentohead White Standard placed over the conveyor.
- Head height level: 135 mm between the head and the conveyor belt sample.
- Integration time: 30msec
- Number of integration: 10
- Dark Setup: Dark Spectrum Subtraction in manual mode.
- Sample Setup: Measurement type is Reflection in percentage and for the reference in counts.

Procedure

Spectrum acquisition was performed and referencing was taken periodically in around 30 minutes bases.

Overview

NIR spectrum acquisition was performed for all the plastic bottles samples from different categories using the hardware setup offered to the American University of Sharjah, the acquisition was performed from 3 different places of the bottle [top - near the label (if exist) - bottom].

Initial settings

- Hardware: GetSpec NIR1.7-128TTS + Sentohead 50/35
- Software: Spec32 [SNAB0030 (Serial Number of the Spectrometer)].
- Reference: Sentohead White Standard placed over the conveyor.
- Head height level: 80 mm between the head and the conveyor belt sample.
- Integration time: 450 msec – 100 msec.
- Number of integration: 1
- Dark Setup: Dark Spectrum Subtraction in manual mode.
- Sample Setup: Measurement type is Reflection in percentage and for the reference in counts.

Procedure

Spectrum acquisition was performed for 450 msec integration time and referencing was taken periodically in around 30 minutes bases. Then the acquisition was repeated for 100 msec integration time due to the saturation occurred in some spectrum measurements.

Overview

To Test the acquisition speed and take 10 readings of each bottle along its major axis using SentroProc 2.2 NIR spectrometer which is an integration of a PC and a spectrometer and the interface software was installed inside.

Initial settings

- Hardware: SentroProc 2.2 NIR spectrometer + SentroHead 100
- Software: Spec32 [SNIR0500 (Serial Number of the Spectrometer)].
- Reference: Sentohead White Standard placed over the conveyor.
- Head height level: 100 mm between the head and the conveyor belt sample.
- Integration time: 40msec
- Number of integration: 1
- Dark Setup: Dark Spectrum Subtraction in manual mode.
- Sample Setup: Measurement type is Reflection in percentage and for the reference in counts.
- Detector temperature control set point was -20°C.

Speed Test

To verify the effect of the integration time on the acquisition speed.

- Procedure:
 - Initially the sampling time was 40 msec which is the optimum setting for the hardware setup available.
 - Trace logging was performed for 2 minutes with zero sampling time interval using the system clock to generate the time interval between logged files.
 - After 2 minutes time period elapsed, the data files (18KB each) stored in the hard disk along one complete minute were counted.
 - Determining the number of readings possible for one average size bottle.
 - Repeat the procedure for an integration time of 25 msec.

- Results:
 - For 40 msec:
 - Number of files found along one minute: 531 files.
 - Approximately 3 different spectrum readings can be achieved for an average bottle length of 30 cm moving in a speed of 1m/sec.
 - For 25 msec:
 - Number of files found along one minute: 652 files.
 - Complete 3 different spectrum readings can be achieved for an average bottle length of 30 cm moving in a speed of 1m/sec.

Vertical multiple bottle scan test

To acquire 10 sequential readings along the major axis of the bottle. 5 bottles were taken from each category; therefore 150 readings were acquired in total.

VITA

Yahia Tachwali was born on June 15, 1980, in Aleppo, Syria. He graduated from Almaamon High school in 1998 and from Aleppo University with a Bachelor of Science degree in Electronic Engineering in 2003. He ranked first in his batch and received multiple academic distinction awards during his undergraduate study.

He worked as an instrumentation and control engineer with RENTEC L.L.C in Dubai, UAE, between 2003 and 2004. Then he worked as a teacher assistant in the Mechatronics Program in American University of Sharjah (AUS), between 2004 and 2005. He received his Master degree from American University of Sharjah in Mechatronics Engineering in 2006. He decided to complete his education in Machine Vision.

His research interests include pattern recognition, adaptive system design and image processing using artificial intelligent techniques.

Mr. Yahia enjoys reading, swimming, touring and listening to classical music.